786

THE MOTION OF GRANULES AND THEIR TIME OF PASSAGE THROUGH ROTARY KILNS AND DRYERS.

A thesis submitted to the
University of London
for the Degree of
Doctor of Philosophy

by

SHABBIR AHMAD QURESHI

M.Sc. (Hons.) Tech.

Department of Chemical Engineering,
Imperial College of Science & Technology,
London, S.W.7.

December, 1960.

E R R A T A

No.	Page	Line	Read	For
1.	24	8	Volume	Value
2.	47	14	$-V^2/g$	$-g/V^2$
3.	48	13	$y = V^2/g\ [------]+C'$	
4.	49	21	F×r	F×R
5.	56	3	(47)	(35)
6.	68	16	μ	u
7.	72	14	d_s	D_s
8.	92	4	μ	u
9.	101	13	Sin β	Sin

ABSTRACT.

The effect of the speed of rotation on the surface profile in a rotating cylinder of free flowing materials has been studied and a modified version of Gow's equation, which takes into account the contact of the granules is presented. The effect of particle size and bulk density on the surface profile has been determined.

The flow of granular material from feed hoppers through circular orifices has been studied and a relationship between the rate of discharge and more important variables of the system has been derived.

Finally, in the case of an inclined rotary cylinder, the effect of cylinder variables such as length, diameter, slope and speed have been investigated for a wide range of materials. A theoretical analysis based on the cyclic motion of the granular bed is presented.

ACKNOWLEDGEMENT.

The author wishes to express his gratitude to Professor D.M. Newitt F.R.S., for the supervision and the invaluable advice given to him in the course of the present investigation.

Thanks are also due to Mr. A.C.V. Sweetings and the members of the workshop for their help in the construction of the apparatus.

NOMENCLATURE.

Symbol.		Dimensions.
A_o	Cross-section of the circular-aperture. Sq. Ft.	L^2
α	Static Angle of Repose. Degrees.	-
β	Surface Dynamic Angle of Repose. Deg.	-
C_1	Chord-length at feed-end. Ft.	L
C_n	Chord-length at exit-end. Ft.	L
γ	Internal dynamic angle of repose. Deg.	-
d_a	Mean sieve diameter. Ft.	L
D	Internal diameter of the rotating cylinder. Ft.	L
ϵ	Voids.	-
f	Surface shape factor.	-
F	Frictional Forces.	$ML/_{T^2}$
g	Acceleration due to gravity.	$L/_{T^2}$
H	Granular material head in feed-hopper. Ft.	L
k	Volume shape factor.	-
k_e	Volume shape factor of equidimensional particle.	-
L	Length.	-
m	Flatness ratio.	-
n	Elongation ratio.	-
N	Revolutions per minute.	-
N_c	Critical revolutions per minute.	-

ρ_a	Bulk-density. lbs/C.Ft.	$M/_{L^3}$
ρ_t	True-density. lbs/C.Ft.	$M/_{L^3}$
ρ_r	Relative-density.	-
μ	Coefficient of Friction.	-
Q	Discharge-rate. lbs/sec.	$M/_T$
S	Cylinder inclination Deg.	-
$t_{emp.}$	Average time of passage through rotary-cylinder. (Empirical).	T
$t_{theo.}$	" " " (Theoretical).	
ψ	The angle showing the difference between the slope of the bed and the slope of cylinder. Deg.	-
ϕ	Slope of the bed in rotary cylinder.Deg.	-
V	Peripherical speed.	$L/_T$
W_a	Apparent Weight.	M.
$\dot{\theta}$	Angular Velocity Radius/sec.	$1/_T$
$\ddot{x}_c$	Acceleration along x-axis	$L/_{T^2}$
$\ddot{y}_c$	" " y-axis	$L/_{T^2}$
I_c	Moment of inertia of a rolling body round its centre of gravity c.	ML^2

CONTENTS.

Page

Section I.

Motion of Granules in Rotary-Cylinder.

Chapter 1.

1. Introduction. 1

2. Angle of Repose, Bulk-density, Particle Size and Shape-factor. 3

Chapter 2.

1. Description of Apparatus and the experimental procedure for studying cascading. 29

2. Variation of Surface-Profile of the Cascading-Mass with speed. 31

Chapter 3.

1. Free Curved-Surface. 42

2. Theory of Free Flight. 42

3. Gow's Equation and Pushing-Effect. 46

4. Modified Gow's Equation. 49

5. Effect of Apparent Change in Weight of particles on their trajectories. 57

6. The Proposed Construction. 61

Section II.

Flow of Granules Through Circular Apertures.

Chapter 4.

1. Introduction. 67

2. Literature Survey. 68

Page.

3. Description of the Proposed Feed Hopper and testing its output. 75

4. Experimental results. 77

5. Dimensional Analysis and Correlation. 90

Section III.

Time of Passage of Granule Through Rotary-Cylinders.

Chapter 5.

1. Introduction. 95

2. Literature Survey. 96

3. Comparative Study of the Proposed and Existing Correlations. 105

Chapter 6.

1. Description of Apparatus. 110

2. Experimental Procedure. 114

3. Path of Granules through the Inclined-cylinder. 114

4. Experimental. 123

5. Empirical Equations. 153

6. Effect of Feed-rate on Hold-up, the Bed-Depth and the Time of Passage. 156

7. Bed Slope vs Cylinder Slope. 161

Page

Chapter 7.

Theory.

1. Angle of Slide/Descent vis Angle of Inclination of Cylinder. 164

2. Number of cycles over the cylinder length. 170

3. Time of Passage Through Rotary-cylinder. 177

4. Discussion. 180

Appendix.

Tables. 184

Bibliography. 229

SECTION I.

CHAPTER 1.

1. Introduction.

When a cylinder partly filled with a free flowing granular material is rotated on a horizontal axis at low speeds, the granules begin to rise in circular paths, concentric with the circle of reference of the cylinder and finally having emerged out of the bed slide down the inclined plane which constitutes the surface of the bed. The bed may therefore be considered to be in two parts, the one rotating with the cylinder and the other sliding as a thin layer over the rotating portion. In this state the bed is said to be cascading.

When the peripheral speed is gradually increased, the surface profile of the sliding-mass begins to change and to develop a hump. This is due to the material being projected from the wall of the cylinder towards its centre, the motion being described as cataracting.

Still further increase in speed results in the entire charge adhering to the walls by centrifugal action. The speed at which this occurs is termed the critical or centrifuging speed and may be calculated from the equation:

$$N_c = 76.6\sqrt{1/D} \qquad (1)$$

where N_c = Revs. per minute (critical)
D = Internal diameter of the cylinder (ft.)

The present study of the behaviour of granular material in a cylinder rotating at low speeds, relates to cascading motion only. A considerable amount of work has been carried out by Davis [1], von Steiger [2], Gow, Campbell and Coghill [3], White [4], Conner [5] and Rose and Sullivan [6], on the theoretical aspects of cataracting and centrifuging but relatively little attention appears to have been given to cascading.

The object of the present work was to concentrate on that aspect of the granular motion which has so far been little explored. Attention has been focussed on the nature of the surface profile of the granular charge in the case of two materials e.g. coal, felspar, sand, limestone and magnesite, having a specific grvity range of from 1.42 to 3.5 g./cc. The effect of particle size (as defined later) which plays an important role, has also been included in the study.

2. Angle of Repose, Bulk Density, Particle Size and Shape Factor.

Before considering in detail the movement of a granular mass in a rotary cylinder, it is necessary to take account of properties of particulate material which may be expected to influence its movement. Of these the angle of repose, the bulk density and the shape-factor are the most important.

Angle of Repose. (Definition).

This property is connected with the frictional forces operative when the particles of a granular mass move relative to one another. If we consider first a single particle B (Fig.1), resting on an inclined plane PQ, the weight of the particle mg acting vertically downwards may be resolved into two components, namely mg cos θ, acting normally to the plane and mg sin θ, acting tangentially to the plane, where the angle θ gives the slope of the plane. The latter force tends to cause the particle to move down the plane but as long as the particle is at rest, it is resisted by an equal and opposite force known as the tangential friction force. As the slope of the plane is gradually increased, a point is reached at which the

FIG. 1

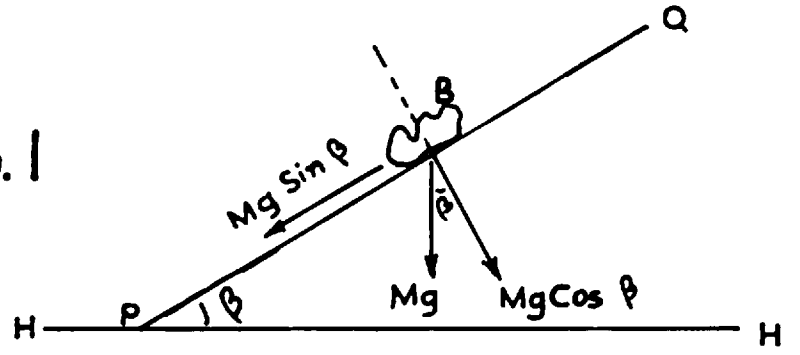
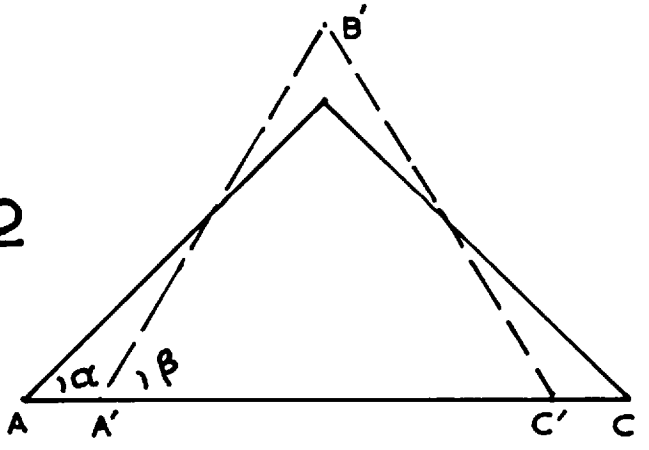


FIG. 2



tangential force just balances the frictional force and any further increase causes the particle to move downwards. If β represents the angle of the plane at this time, then:

$$\frac{\text{Frictional Force}}{\text{Normal Force}} = \tan \beta = \mu \qquad (2)$$

and μ is called the Dyn. Coefficient of Friction. The angle β may also be called the Surface Dynamic Angle of Repose.

It may be noted that once the particle is in motion, it will continue to move down the plane even if the angle β is somewhat reduced. This lesser angle defines the Sliding Coefficient of Friction.

A considerable amount of work has been done by Wilson [7], Crossthwaite [8] and Cain [9] on the effects of earth pressure on the angle of repose, in an attempt to verify the earlier theory of Rankine [10] on stability of loose earths. Richter [11] measured the static coefficient of friction for straw, hay, corn, etc. to provide data for chute design. Later Holbrook and Fraser [12] showed that for a given size distribution the coefficient of friction depends upon the particle shape and for given shape upon the size distribution.

Fowler and Chodzeisner [13] have proposed a

general correlation for the coefficient of friction, the roughness of the surface, the partcle size and shape and its relative density.

$$\mu = \tan \beta = \frac{0.2110}{S_f^2} + 0.3436(E/d_a)^{0.5} + 0.0171\,\rho_r + 0.1834 \qquad (3)$$

where μ = coefficient of friction of the material
β = surface dynamic angle of repose
E = roughness index of surface in cms.
S_f = surface shape factor
ρ_r = relative density
d_a = particle diameter, cm.

Angle of Repose.

According to the methods of measurement [14-22], three values of the angle of repose of any given material may be obtained. These are designated as the static angle of repose, the surface dynamic angle of repose and the internal dynamic angle of repose.

Static and Surface Dynamic Angle of Repose.

When a powder flows from an orifice on to a horizontal plate it forms a cone and if the distance between the orifice and the apex of the cone is kept constant so that the distance of the free fall is at all times constant, then whilst flow continues the cone will be found to have

a base angle β (see Fig.2) which is defined as the surface dynamic angle of repose. When flow ceases the cone settles to a more stable configuration with a base angle α, which is defined as the static angle of repose.

The static angles of repose for coal, felspar, sand, limestone and magnesite, for fine ranges of particle sizes, are given in Table 1.

Table 1.

Surface Static Angle of Repose as Functions of Particle Size.

No.	Material	Sp.Gr.	Static Angles of Repose (Degrees) (Particle Size Mesh B.S.S.)			
			(22-30)	(30-36)	(36-52)	(52-60)
1	Coal	1.420	40	39	37.5	36.
			(18-36)	(36-60)	(60-85)	(85-100)
2	Felspar	2.070	39	37.5	37	36.5
3	Sand	2.620	36.5	35	34.9	35
4	Limestone	2.660	40.5	38.5	37	36.6
5	Magnesite	3.332	38	37	35.5	35.5

It will be noted that the static angle of repose in all cases tends to diminish with the decrease in particle size but there is no obvious relationship connecting the angle with the specific gravity of the material.

Internal Dynamic Angle of Repose.

Visual observation of the movement of granules in a slowly rotating cylinder indicates that the granules follow approximately circular paths as shown in Fig.3. When the granules reach the surface of the mass which is inclined at angle β, it slides down the surface under the action of gravity. This may be seen in the photographs in Plates 1 and 2, which relate to the speed of 2,5,10,20, 40 and 60 r.p.m. A close examination of the photographs indicates that there is in fact a sliding wedge of material shown in Fig.3 by ABB'. The angle γ made by AB' with the horizontal, is called the internal dynamic angle of repose.

Bearing in mind the nature of the movement in a rotary drum, it is proposed to use the surface dynamic angle of repose as a measure of frictional force operative in a rotary drum (see also Chapter 2).

FIG.3

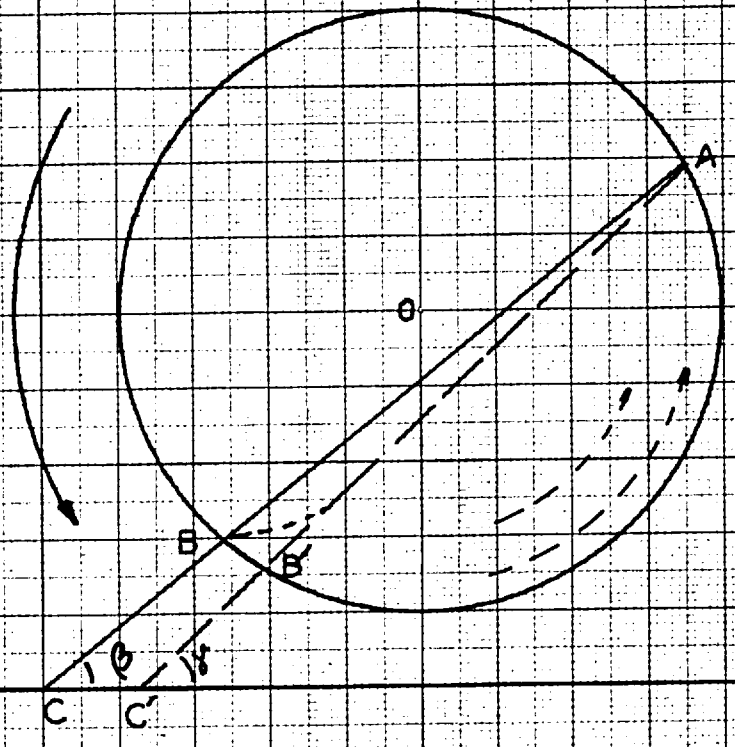


Plate 1.

Motion of Granules in a Rotating Cylinder
Coal (-18+36) Mesh B.S.S.



R.P.M
2

R.P.M. =



R.P.M
5

R.P.M 2

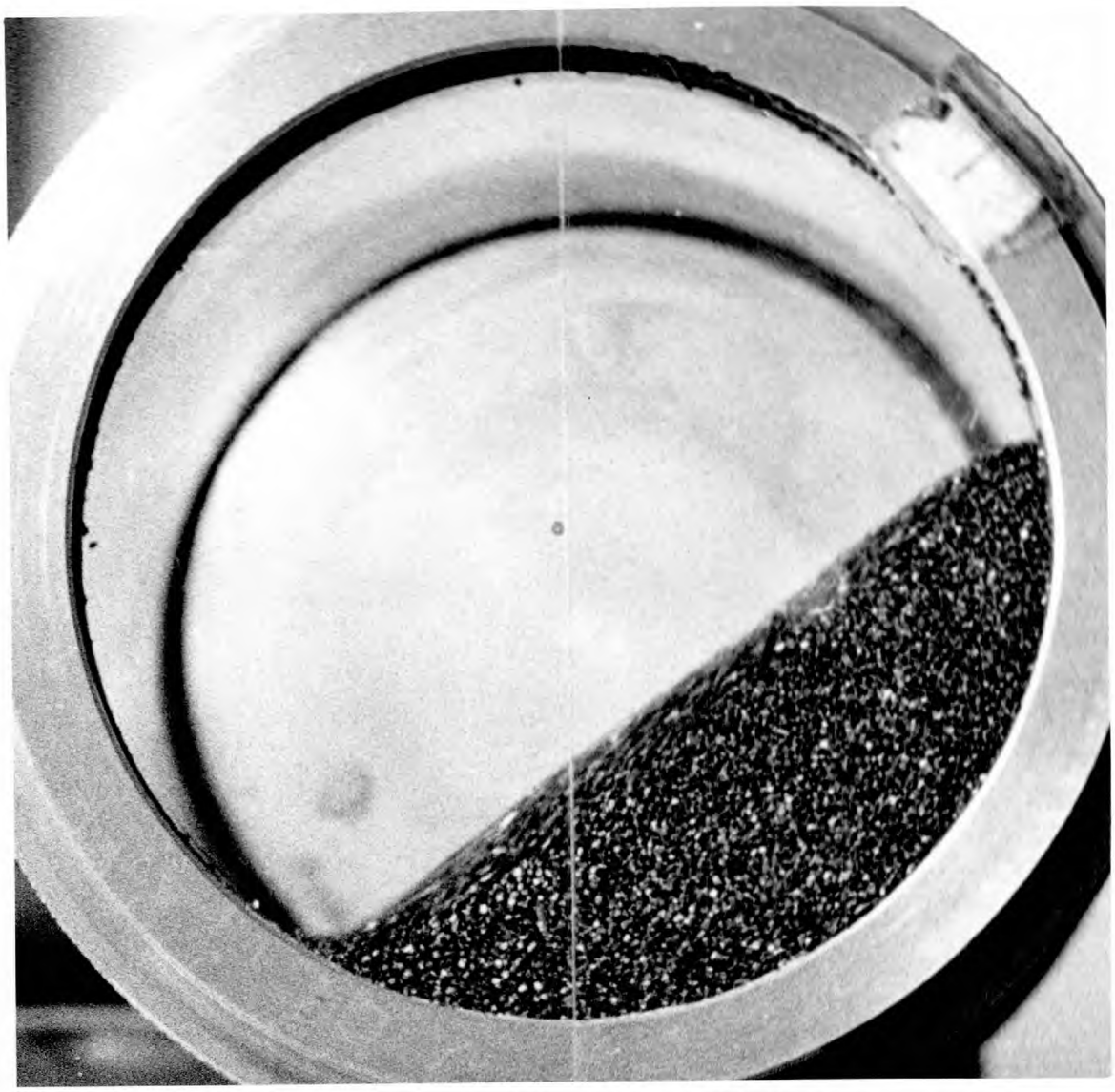
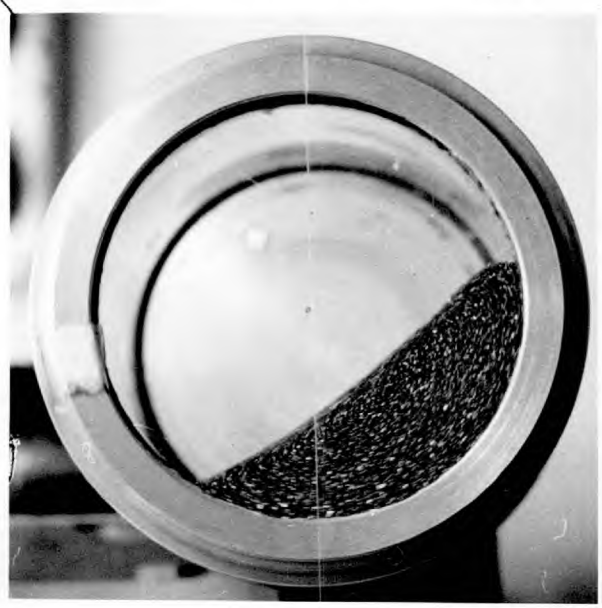


Plate 1.

Motion of Granules in a Rotating Cylinder
Coal (-18+36) Mesh B.S.S.



R.P.M
10

R.P.M =



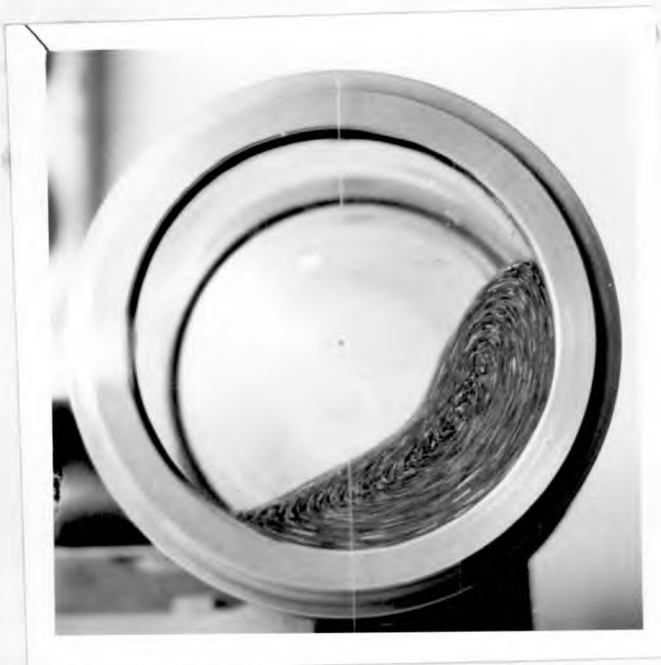
R.P.M
20

Plate 1.

Motion of Granules in a Rotating Cylinder
Coal (-18+36) Mesh B.S.S.



R.P.M
40

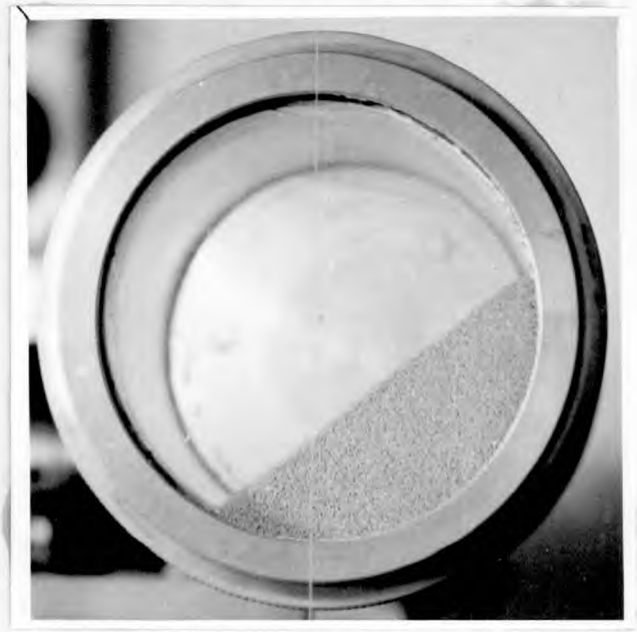


R.P.M
60

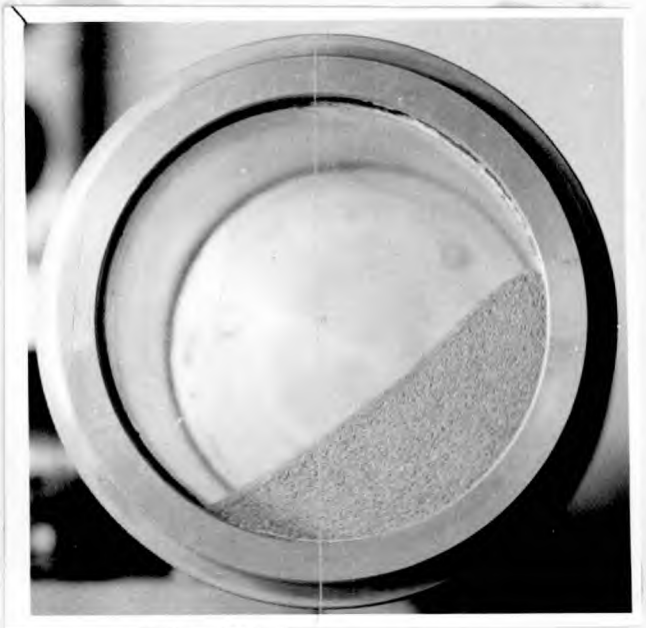
Plate 2.

Motion of Granules in a Rotating Cylinder

Magnesite (-18+36) Mesh B.S.S.



R.P.M.= 2

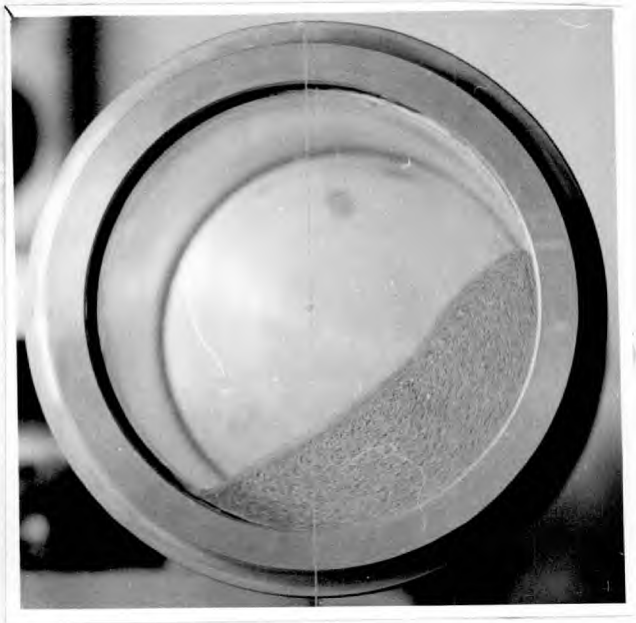


R.P.M.= 5

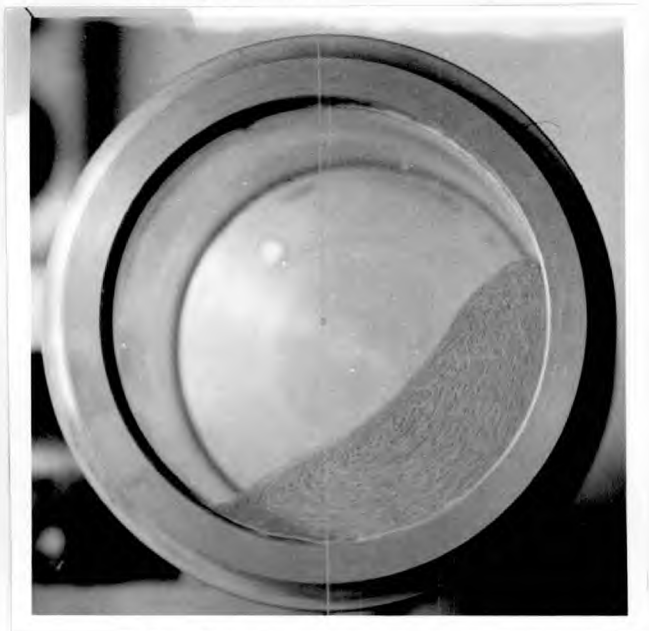
Plate 2.

Motion of Granules in a Rotating Cylinder

Magnesite (-18+36) Mesh B.S.S.



R.P.M.= 10



R.P.M.= 20

Plate 2.

Motion of Granules in a Rotating Cylinder

Magnesite (-18+36) Mesh B.S.S.



R.P.M.= 40



R.P.M.= 60

The Bulk Density.

The bulk density of a granular material is governed by the method of packing of the granules, their size distribution and shape. It gives the measure of voids ϵ, in the mass and hence is related to porosity by :

$$\epsilon = (1 - \rho_a/\rho_t) \qquad (4)$$

where ϵ = voids, ρ_a = bulk density (lbs/c.ft.)
and ρ_t = true density (lbs./c.ft.).

There are several methods for determining the bulk density, all of which, however, depend on filling a container of known dimensions under carefully specified conditions. The method employed in this work was to pour the material into a glass cylinder of 1.25 cm. diameter and 100 cc. capacity from a funnel, the end of the funnel resting against the cylinder wall until the cylinder was half-full. Its contents were then weighed.

Measurements were made for five materials over a range of particle sizes, the results being summarised in Table 1 (see Appendix). In the table the column headed "Particle size" refers to the arithmetic mean of the sieve-range (B.S.S.) and gives the average diameter for non-spherical particles [23-25].

The results in the form of bulk density ρ_a vs.

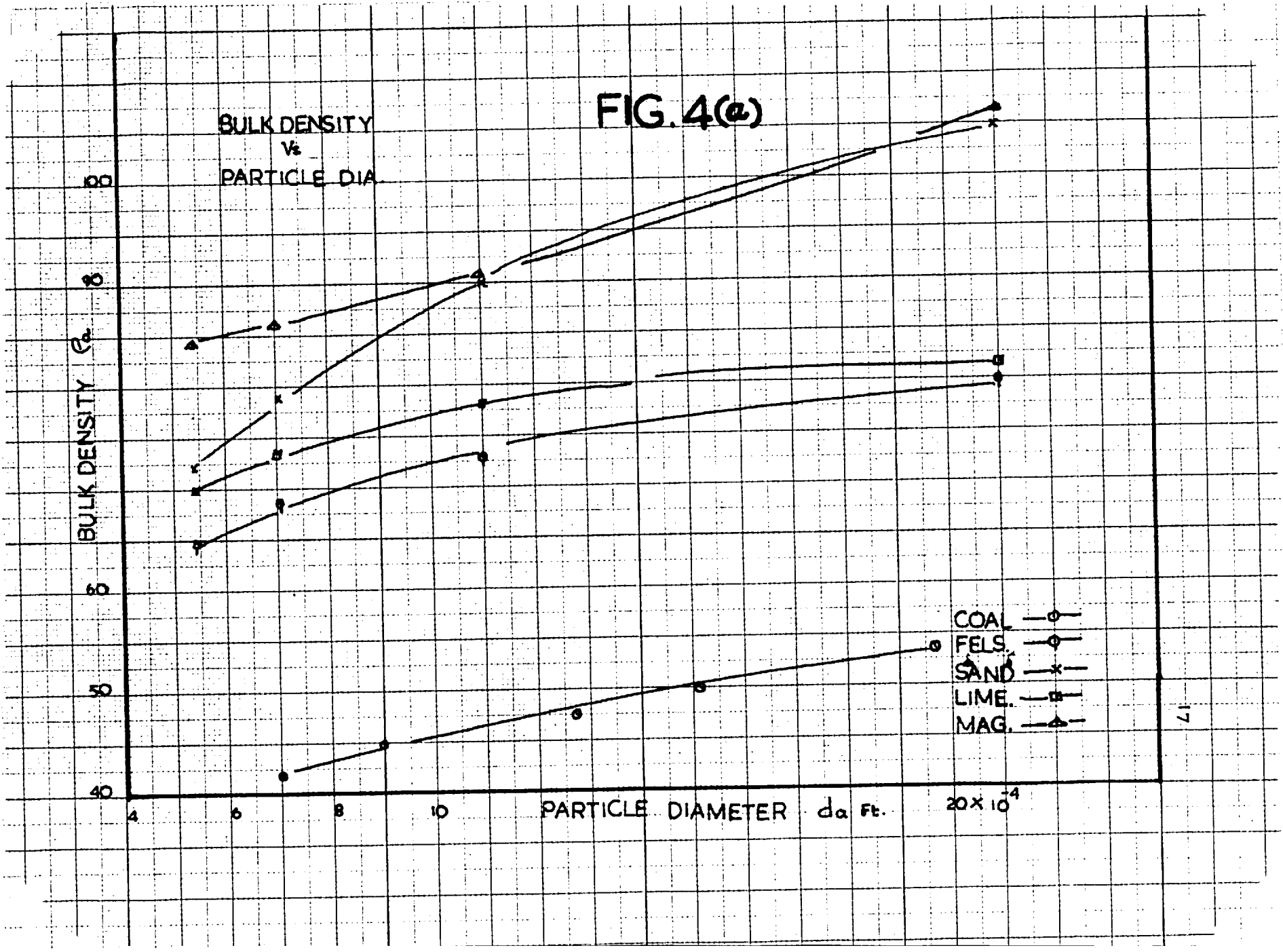
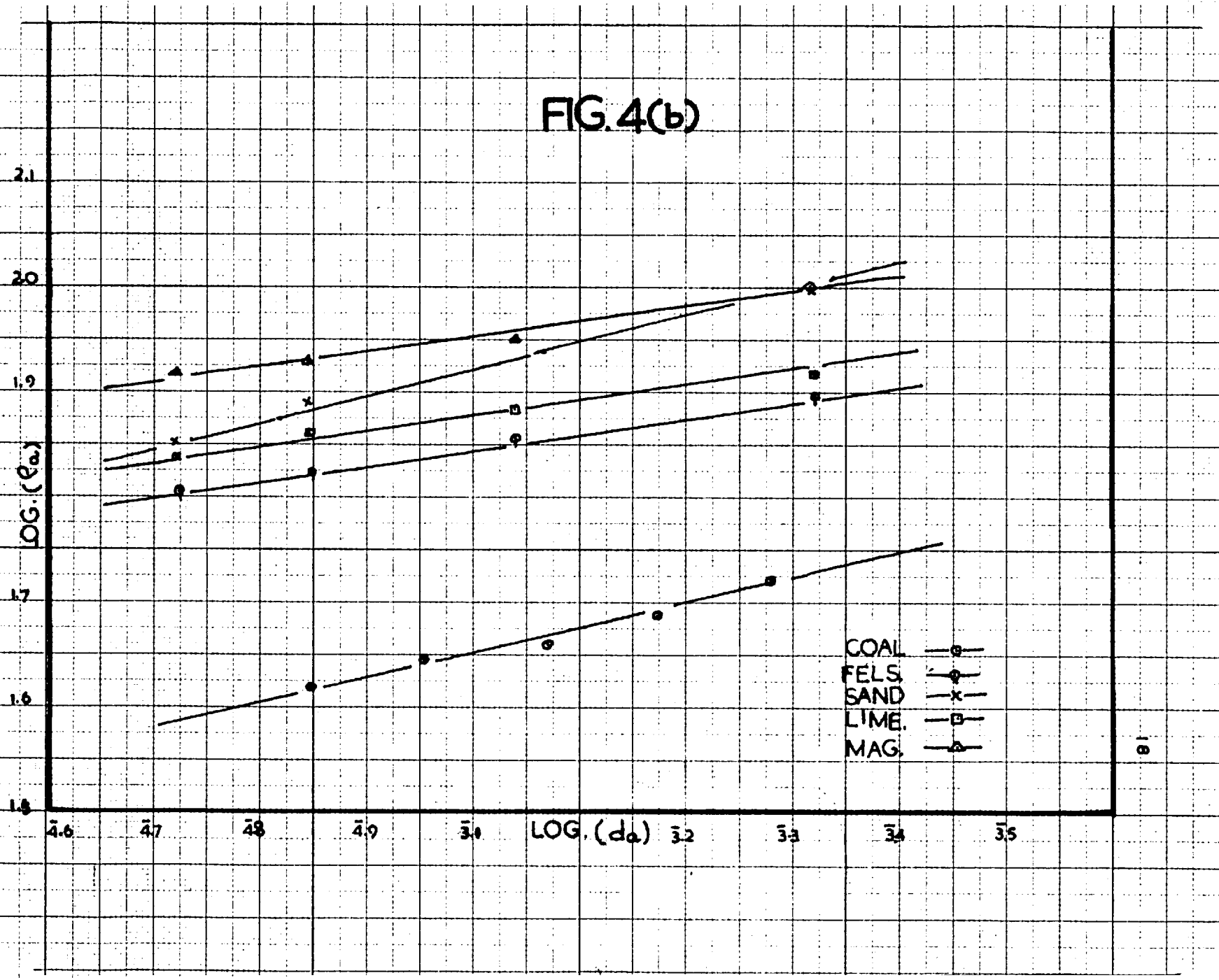

FIG. 4(a)
BULK DENSITY
Vs
PARTICLE DIA.
BULK DENSITY ρa
100
90
80
70
60
50
40
4
6
8
10
PARTICLE DIAMETER da Ft.
20 × 10⁻⁴
COAL
FELS.
SAND
LIME.
MAG.
17

FIG. 4(b)


2.1
2.0
1.9
1.7
1.6
LOG. (Qa)
COAL
FELS.
SAND
LIME.
MAG.
$\bar{4}.6$
$\bar{4}.7$
$\bar{4}.8$
$\bar{4}.9$
$\bar{3}.0$
LOG. (d_a)
$\bar{3}.2$
$\bar{3}.3$
$\bar{3}.4$
$\bar{3}.5$

particle size d_a and log (ρ_a) vs. log (d_a) are shown in Figure 4 (a) and (b).

It will be seen that the bulk density increases with the particle size but bears no obvious relationship to the density of the material. The slope of the lines for sand and coal are steeper than that of felspar, limestone and magnesite.

The relationship between the bulk density and the particle size for the materials examined may be represented by the equation :

$$\rho_a = K (d_a)^n \qquad (5)$$

where ρ_a = bulk density (lbs./c.ft.)
d_a = mean sieve diameter (ft.)
K, n = constants for a given material.

Values of K and n are given in Table 2.

Table 2.

No.	Material	K	n
1	Coal	2.381×10^2	0.2401
2	Felspar	1.868×10^2	0.1405
3	Sand	4.93×10^2	0.2401
4	Limestone	1.587×10^2	0.1405
5	Magnesite	2.456×10^2	0.1405

Cocking [26] and Roller [27] have studied the density as a function of particle size and the latter has

represented his results by the equation :

$$\epsilon = K\,(1/d)^n \qquad (6)$$

where d = diameter of the particle,
K,n = constants for a given material
and ϵ = the same as defined before.

Shape Factor.

The study of the effect of particles on bulk density would be incomplete without referring to the shape of the particles.

Methods of expressing shape by means of linear dimensions of a particle have been discussed by Heywood [28,29]. The theoretical relationship derived by him for geometric shapes and subsequently modified for irregular shaped particles, are explained in brief in the following paragraphs.

The two important shape-coefficients, frequently mentioned in literature, are the volume coefficient, k, and the surface coefficient, f, as defined by the following equations:

$$V = k \cdot d_p^{\,3} \qquad (7)$$

$$\text{and} \quad S = f \cdot d_p^{\,2} \qquad (8)$$

where V = volume of the particle; S = surface of the particle; d_p = projected diameter; k = coefficient based on volume; f = coefficient based on surface area.

According to Heywood, the mean projected diameter of the particle, d_p, is the diameter of the circle when the particle is viewed from the direction vertical to the plane of greatest stability (area of the circle being equal to the projected area of the particle). If L, B and T represent the length, breadth and the thickness of the particle, in decreasing order, then L/B (=n) is called Elongation Ratio, while B/T (=m) has been termed the Flatness Ratio. Both m and n may also be referred to as the 'proportions' of the particle. Thus, if a particle is to be completely defined, its geometric shape (approx.) and proportions must be considered together.

In order to correlate the coefficients f and k (see equations 7 and 8), Heywood considered three simple geometric shapes, e.g. rectangular-prisms, tetrahedra and ellipsoids. Since the mathematical approach is comparatively simple for rectangular prisms, he developed his theory on the following lines.

Consider a cube with each side equal to unity, then its volume is 1 cubic ~~inch~~ unit (i.e. $L^3 = 1$), surface 6 sq. units and projected area is 1 sq. unit. Since the projected area for the cube is given, the projected diameter may be worked out on the following lines:

$$\frac{\pi (d_p)^2}{4} = L^2 = 1 \text{ sq. unit}$$

whence $$d_p = \sqrt{\frac{4}{\pi}} \qquad (9)$$

For an equidimensional particle (i.e. cube), equation (7) can be rewritten in the form

$$V = ke \cdot (d_p)^3 \qquad (10)$$

where ke is the coefficient based on an equidimensional particle

V and d_p have their usual significance.

Substituting the value of d_p (equation 9) and V in equation 10, we can get the value of ke :

$$ke = \frac{V}{(d_p)^3} = \frac{V}{8(\sqrt{1/\pi})^3}$$

$$= 0.696 \qquad (11)$$

Similarly, substituting the value of (d_p) in equation 8, and solving for 'f', we get

$$f = \frac{\text{surface area of cube}}{(d_p)^2}$$

$$= \frac{6}{2\ (1/\pi)^2} = 4.72 \qquad (12)$$

Thus for a cube ke = 0.696 and f = 4.72.

Next, cut a slice of thickness 't' from the above cube, parallel to the horizontal plane, to give a so called 'flattened' particle. It will be seen that d_p remains

the same but the volume will be reduced say by a factor 'm' (m is the same as defined before) and so will be the surface but by a different factor. The volume, surface area and the projected diameter of the slice may be expressed as :

$$\text{Volume} = L^2 \times t \quad \text{cubic units}$$

$$\text{Surface} = 2L^2 + 4Lt \quad \text{sq. units}$$

$$\text{Projected area} = L^2 \quad \text{and} \quad d_p = L\sqrt{4/\pi}.$$

Since the value is reduced by a factor 'm', the volume coefficient may be expressed as :

$$k = \frac{\text{original volume}}{(d_p)^3} \cdot \frac{1}{m}$$

$$\text{i.e.} \quad k = ke/m \qquad (13)$$

The surface coefficient for the slice may be calculated, by first calculating the surface coefficient for the 'remaining cube' and then subtracting this value from the value of 'f' for the cube.

Thus f (for remaining cube)

$$= \frac{\text{surface area of the remaining cube}}{(d_p)^2}$$

$$= \frac{\text{Total surface area} - \text{surface area of slice}}{(d_p)^2}$$

$$= \frac{6L^2 - 2L^2 - 4Lt}{L^2 \times 4/\pi} = \frac{4L^2 - 4Lt}{L^2} \cdot \frac{\pi}{4}$$

$$= (1 - t/L)\,\pi = \pi\,(1 - 1/m)$$

$$(L/t = B/T = m).$$

The surface shape coefficient for the slice 'f' is given by :

$$f = 4.71 - (3.14 - \frac{3.14}{m})$$

$$= 1.57\ (1 + 2/m) \qquad (14)$$

Now, elongate the cube into a square prism of length 'n' (n is the same as defined before) such that $n > 1$ and let the particle rest in its plane of maximum stability. Its value will then become n cubic units, surface (2 + 4n) sq.units, projected area = n sq.units and the projected diameter $d_p = \sqrt{4/\pi.n}$. Then the volume coefficient is given by the expression

$$k = \frac{\text{volume}}{(d_p)^3} = \frac{n}{(\sqrt{4/\pi.n})^3}$$

$$= \frac{1}{\sqrt{n}} \times \frac{1}{(d_p)^3}$$

i.e. $$k = \frac{ke}{\sqrt{n}} \qquad (\because \text{for cube } 1/(d_p)^3 = ke) \qquad (15)$$

Also, $$f = \frac{\text{Surface area}}{(d_p)^2}$$

$$= \frac{2 + 4n}{n(\sqrt{4/\pi})^2}$$

$$= \frac{2 + 4n}{6 \times n} \cdot \frac{6}{(\sqrt{4/\pi})^2}$$

$$= \frac{1 + 2n}{3n} \times 4.71 \quad (\because \text{for cube, } f = \frac{6}{(\sqrt{4/\pi})^2} = 4.71)$$

or $$f = 1.57\ (\frac{2n + 1}{n}) \qquad (16)$$

Finally, in the case of a rectangular prism with dimensions n.a, a and a/m (where a is a constant) when n.a, a and a/m are in order of decreasing magnitude, the volume of such a prism is given by $\frac{n}{m}.a^3$ cubic units, surface as $2a^2\ (\frac{1 + n + mn}{m})$ sq. units and projected diameter $d_p = \sqrt{n}.a\ \sqrt{(4/\pi)}$.

Both the volume and surface coefficients k and f may be worked out as follows:

$$k = \frac{\text{volume}}{(d_p)^3} = \frac{n.a^3}{m} \times \frac{1}{n^{1.5} \times a^3 \times (\sqrt{4/\pi})^3}$$

$$= \frac{1}{m\ n^{0.5}} \times \frac{1}{(\sqrt{4/\pi})^3}$$

$$\text{i.e. } k = \frac{ke}{m\sqrt{n}} \qquad (\because \frac{1}{(\sqrt{4/\pi})^3} = ke) \qquad (17)$$

and

$$f = \frac{\text{surface area}}{(d_p)^2}$$

$$= \frac{2a^2\ (1 + n + mn)}{\frac{m}{n.a^2\ (\sqrt{4/\pi})^2}}$$

$$= \frac{2\ [\frac{1 + n + mn}{m}]}{6\ n} \times \frac{6}{(\sqrt{4/\pi})^2}$$

Since $6/(\sqrt{4/\pi})^2 = 4.71$ for a cube, the above equation reduces to :

$$f = \frac{2}{3} \times \frac{1 + n + mn}{m.n} \times 4.71$$

$$= 1.57\ (1 + \frac{(n + 1)}{m.n}) \qquad (18)$$

In equation (18), by introducing a constant C' and raising the flatness-ratio m to the power b, i.e. $(m)^b$, Heywood proposed a general form of the type:

$$f = 1.57 \left[1 + \frac{C'}{(m)^b} \cdot \left(\frac{n+1}{n}\right) \right] \qquad (19)$$

The equation (19) has been simplified further in view of the fact that the rectangular prism are rare and as such a constant value of 1.333 for b was considered to fit in the above equation without introducing much error. Equation (19) may now be rewritten as :

$$f = 1.57 \left[1 + \frac{C'}{m^{1.333}} \left(\frac{n+1}{n}\right) \right]$$

$$= 1.57 + 1.57 \frac{C'}{m^{1.333}} \cdot \frac{n+1}{n} \qquad (20)$$

Since

$$ke = k.\ m.\ n^{0.5} \qquad (17)$$

which gives

$$m^{1.333} = (ke/k)^{1.333} \cdot 1/n^{0.669}$$

Substituting the value of $m^{1.333}$ in equation (20), we get:

$$f = 1.57 + 1.57\ C'\ (k/ke)^{1.333} \cdot \frac{n+1}{n^{.333}} \qquad (21)$$

The factor $\left(1.57\ C' \cdot \frac{1}{ke^{1.333}}\right)$ in equation (21), may be expressed by the coefficient C, to give the final equation :

$$f = 1.57 \cdot C.\ k^{1.333} \times \frac{(n+1)}{n^{.333}}$$

$$= 1.57 + C \left(\frac{ke}{m}\right)^{1.333} \times \frac{n+1}{n} \qquad (22)$$

where f = surface shape factor of an irregular shaped particle,

m = flatness ratio, B/T,

n = elongation ratio, L/B,

and ke and C are constants depending on the shape of particles.

Table 3.

Values of ke and C for various geometric shapes.

No.	Geometric Shape	ke	C
1.	Angular		
	Tetrahedra	0.38	3.3
	Prismoidal	0.47	3.0
2.	Sub-Angular	0.51	2.6
3.	Rounded	0.54	2.1

In the present work, about twenty-five granules were picked out at random from samples of coal, felspar, sand, limestone and magnesite (-18 +36 mesh, B.S.S.) and their length L, breadth B, and thickness T, determined by measurement with a travelling microscope according to Heywood's method and the approximate geometrical appearance noted. The corresponding values of both the volume coefficient ke and C, were read from Table 3 and substituted in equation (22) to obtain the values of the surface coefficient, f, which appear in Table 4(a)

Table 4(a)

No.	Material	Surface Shape Coefficient (f)
1	Coal	2.70
2	Felspar	2.57
3	Sand	2.713
4	Limestone	2.487
5	Magnesite	2.780

Assuming that the roughness index E is equal to the diameter of the particle, d_a, the values of the surface shape coefficient from Table 4(a), when substituted in equation (3), give the coefficient of friction and consequently the surface dynamic angle of repose of the corresponding materials. These values have been compared with those obtained experimentally, as shown in Table 4(b):

Table 4(b)

No.	Material	Coeff. of friction (calculated)	Surface Dyn. Angle of Repose β (Calculated) Degrees (approx)	β (observed) Degrees
1	Coal	0.5806	30.25	34.5
2	Felspar	0.5885	30.50	35.5
3	Sand	0.6009	31.0	34.0
4	Limestone	0.6069	31.0	37.5
5	Magnesite	0.6114	31.75	36.0

From the above table, it will be seen that the calculated values of the surface dynamic angle of repose based on equation (3) for different materials, are lower as compared with the experimental values.

CHAPTER 2.

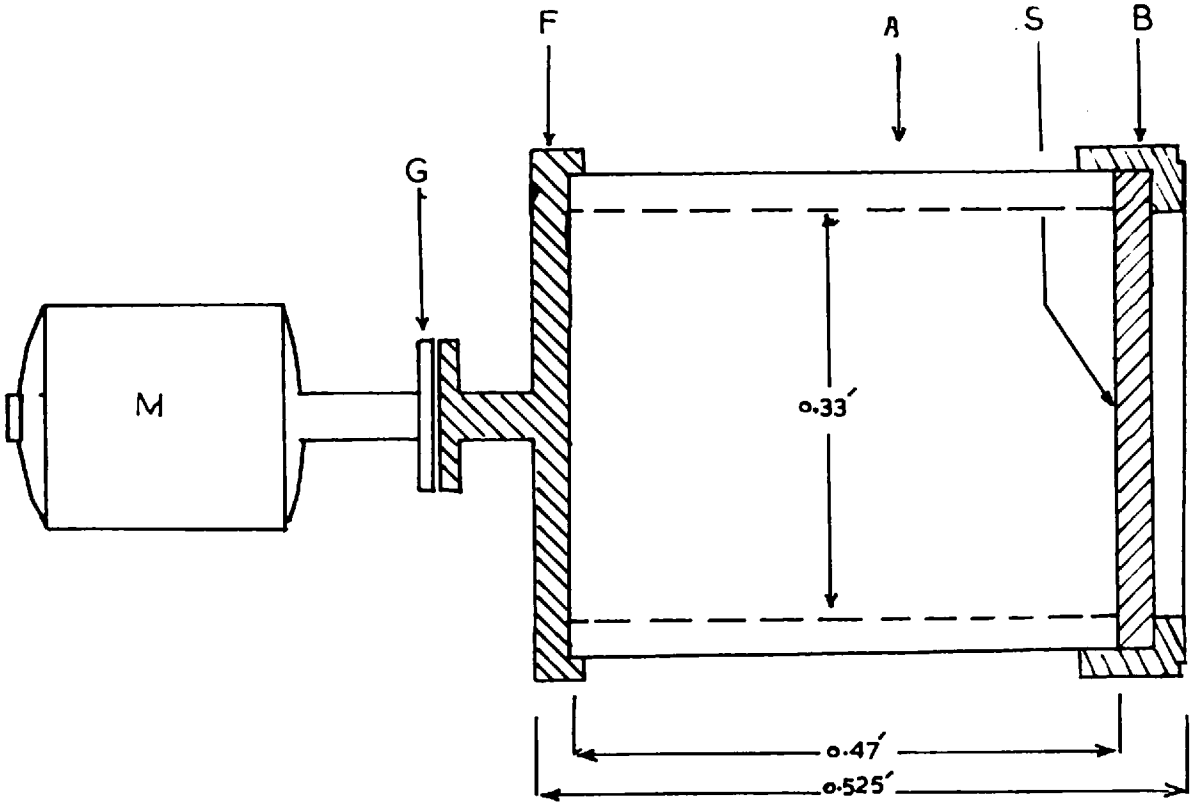
1. Description of Apparatus and the Experimental Procedure for Studying Cascading.

The apparatus used for the study of cascading in a rotary cylinder is comparatively simple. A line drawing is shown in Figure 5.

It consists of a pyrex glass cylinder A, about 0.5 feet in length and 0.33 ft. in internal diameter which is mounted on a Blind-Flange F, welded onto a horizontal shaft passing through a ring-bearing and coupled to a 0.25 H.P. (A.C.) motor M, through a small gear-box G. The motor is connected to the mains via a rheostat, which affords a means of controlling the speed. The whole arrangement is assembled on 6-inch channel iron mounted on a wooden base 2.5 ft. x 0.75 ft. The free end of the cylinder is fitted with a flat glass plate, held in position by a brass ring B. The solid charge usually represents 25% of the cylinder capacity.

Before carrying out an experiment, it is important to set the cylinder in a horizontal position since slight changes in level will modify the profile of the moving charge. The cylinder is set in motion and its speed adjusted with thehelp of a rheostat and a stopwatch.

FIG. 5



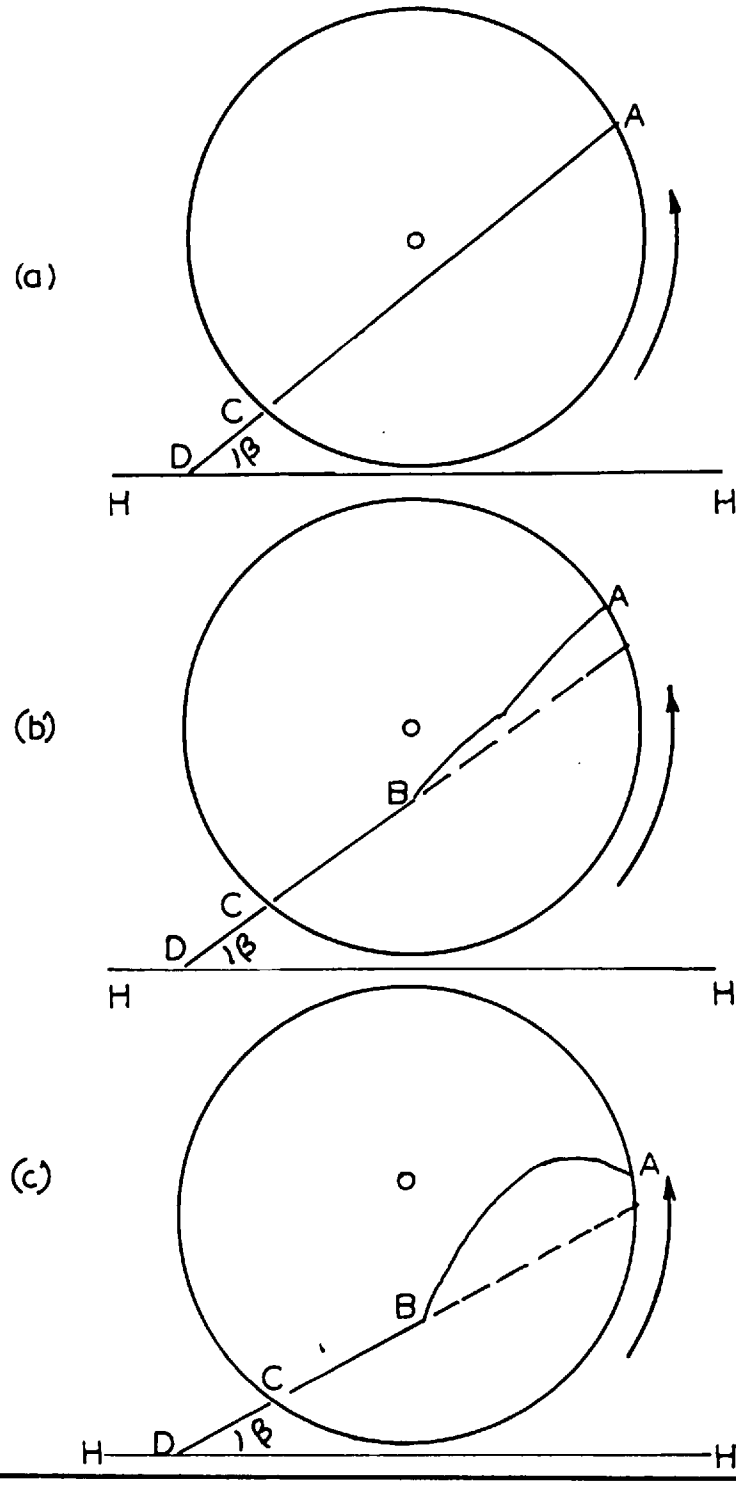
While the cylinder is in motion, the angle of the surface of the charge with the horizontal is measured with the help of a circular protractor, held against the glass plate S, in a vertical position such that the centre of the protractor is in alignment with the foot of the charge. To check whether or not the protractor is in a horizontal position a plumb-line is used.

2. Variation of Surface Profile of the Cascading Mass with Speed.

It has already been mentioned that when granular material in a rotating cylinder is cascading at low speeds (1.032 to 2.064 ft./min.), the granules slide smoothly down the inclined plane of the surface and the surface profile remains practically plane. The angle of this plane to the horizontal gives the surface dynamic angle of repose, as shown in Figure 6(a) and photographs No.1 in Plates 1 and 2.

When the cylinder speed exceeds about 2 ft/min. (2 r.p.m.), the upper part of the free surface first becomes irregular as shown in Figure 6(b) and at speeds above 5 r.p.m. a distinct hump AB develops, imposed on the plane surface (Figure 6(c)). Further increase in

FIG. 6



speeds does not produce any appreciable change although the hump becomes more pronounced and the angle of the plane section of the surface diminishes. This makes it possible to study the effect of speed on the surface dynamic angle of repose (β) and this has been done using coal, felspar, sand, limestone and magnesite in size ranges, -18+36, -36+60, -60+85, and -85+100 mesh B.S.S. [23]. In all the experiments the charge was maintained constant at 25% of the cylinder volume and the range of speed covered was from 2 to 70 r.p.m. (i.e. from 2 ft/min. to 70 ft/min approx.). The angles were measured while the cylinder was in motion, by means of a protractor. It will be seen from Table 2 (see Appendix) and from the curve in Figure 7(a) that the value of β diminishes with the speed of rotation for all sizes and that save at the lowest speed β diminishes with particle sizes.

Similar results obtained for sand, felspar, limestone and magnesite are summarised in Tables 3, 4, 5 and 6 (see Appendix) and plotted in Figures 8(a), 9(a), 10(a) and 11(a).

On plotting speed vs. $1/\beta$, a linear relationship is found to exist in all cases. (See Figures 7(b), 8(b), 9(b), 10(b) and 11(b)). We can therefore write:

$$\frac{N}{N_c} = \frac{B}{\beta} - A \qquad (23)$$

where N = speed of the cylinder in r.p.m.

N_c = critical speed of the cylinder

β = surface dynamic angle of repose (deg.)

A and B = constants depending upon the nature of the material and the particle size.

Values of A and B are given in Table 5.

It has not been found possible to relate either A or B to any specific physical properties of the material but it may be noted that B/A is approximately constant for all the materials studied and that B increases with particle size as shown in Figure 12 (a) and (b) (See also Table 7, Appendix).

FIG. 7

EFFECT OF R.P.M ON SURFACE DYN. ANGLE OF REPOSE 'β'

COAL

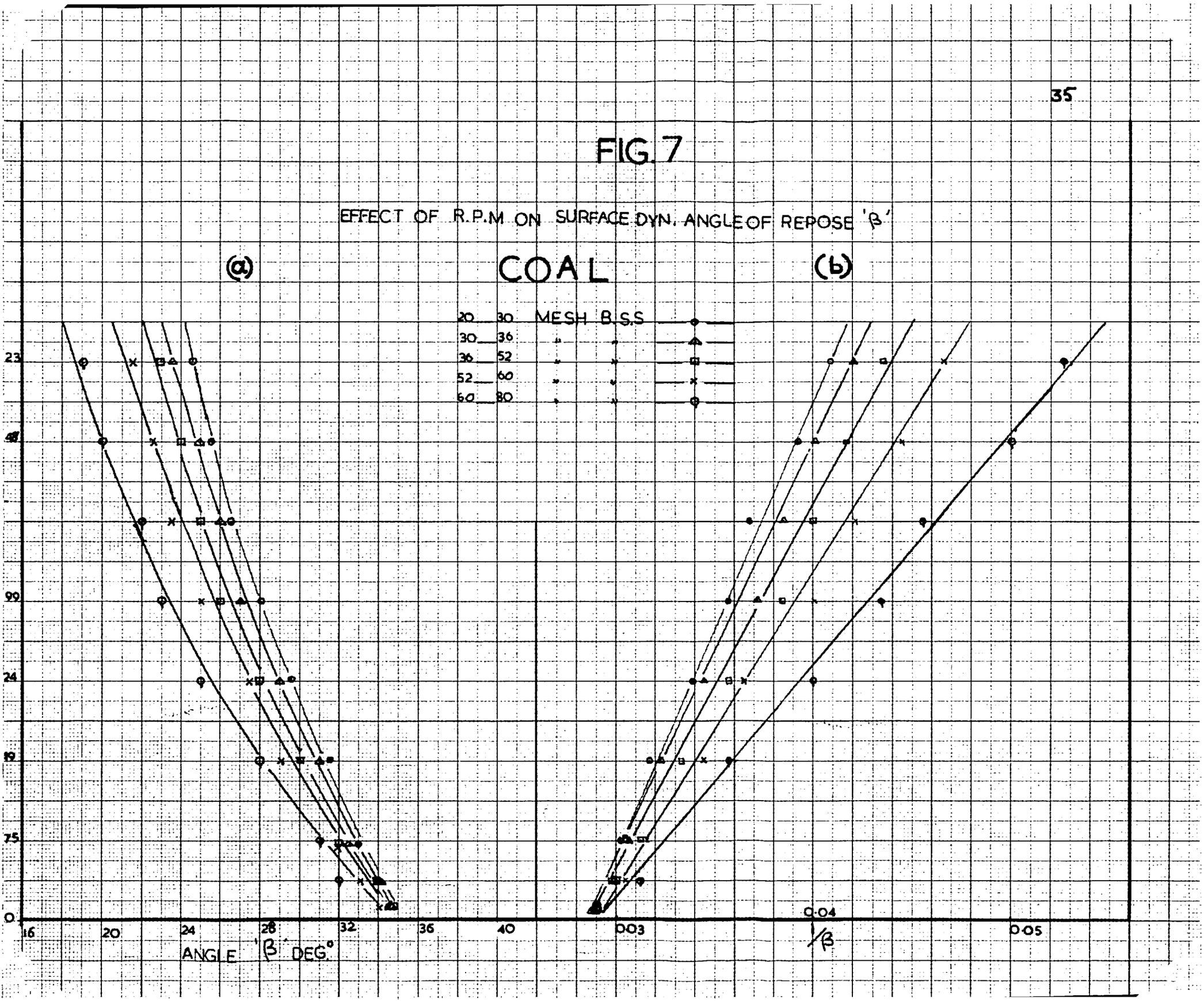


FIG. 8

EFFECT OF R.P.M ON SURFACE DYN. ANGLE OF REPOSE

FELSPAR

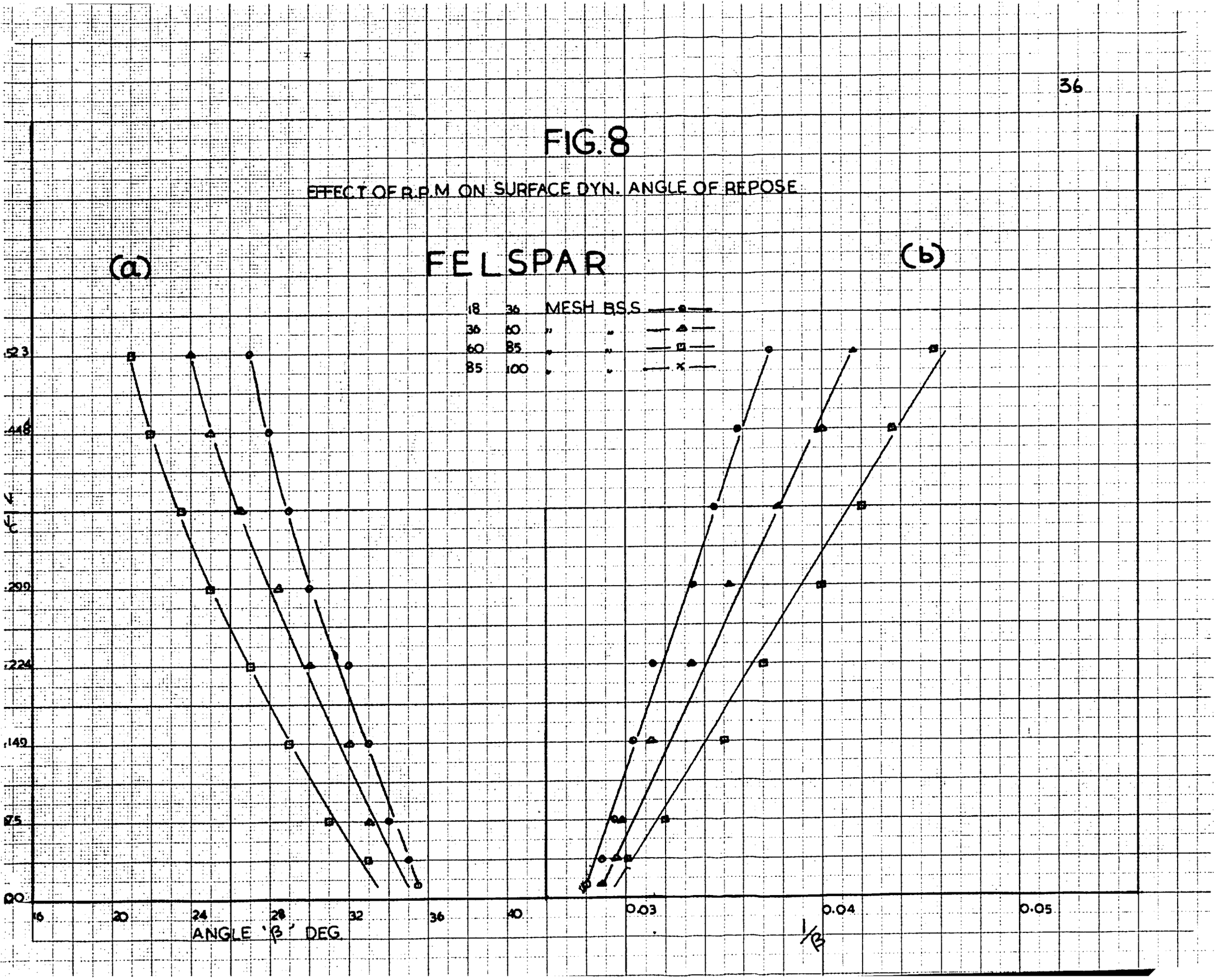


FIG. 9

EFFECT OF R.P.M. ON SURFACE DYN. ANGLE OF REPOSE

SAND

(a)

(b)

18 36 MESH B.S.S —o—
36 60 " " —Δ—
60 85 " " —□—
85 100 " " —×—

.523
.448
.299
.224
.149
.075
.00

12 16 20 24 28 32 36
ANGLE 'β' DEG.

0.03 0.04 0.05
1/β

FIG. 10

EFFECT OF R.P.M. ON SURFACE DYN. ANGLE OF REPOSE

LIMESTONE

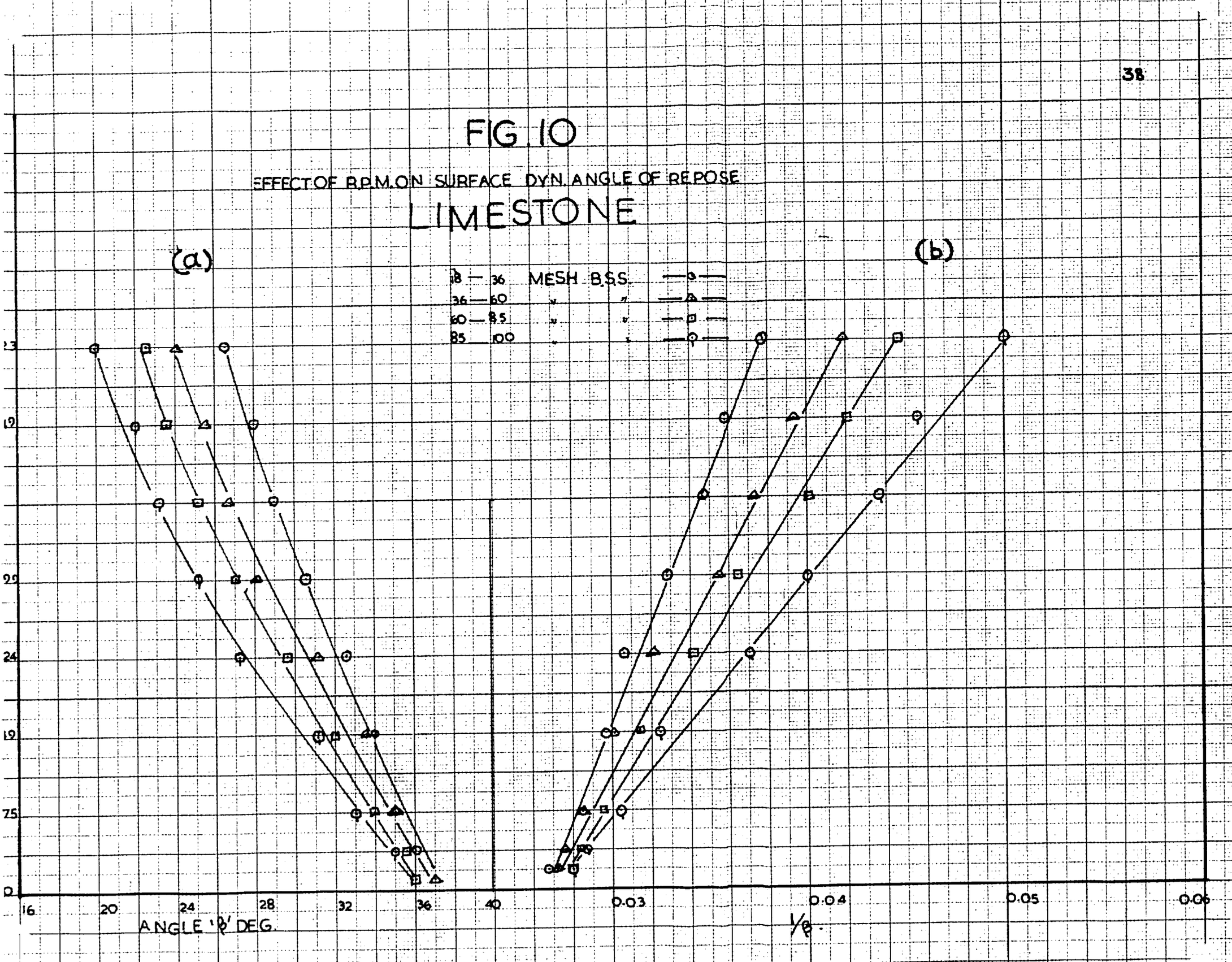


FIG. 11

EFFECT OF R.P.M. ON SURFACE DYN. ANGLE OF REPOSE

MAGNESITE

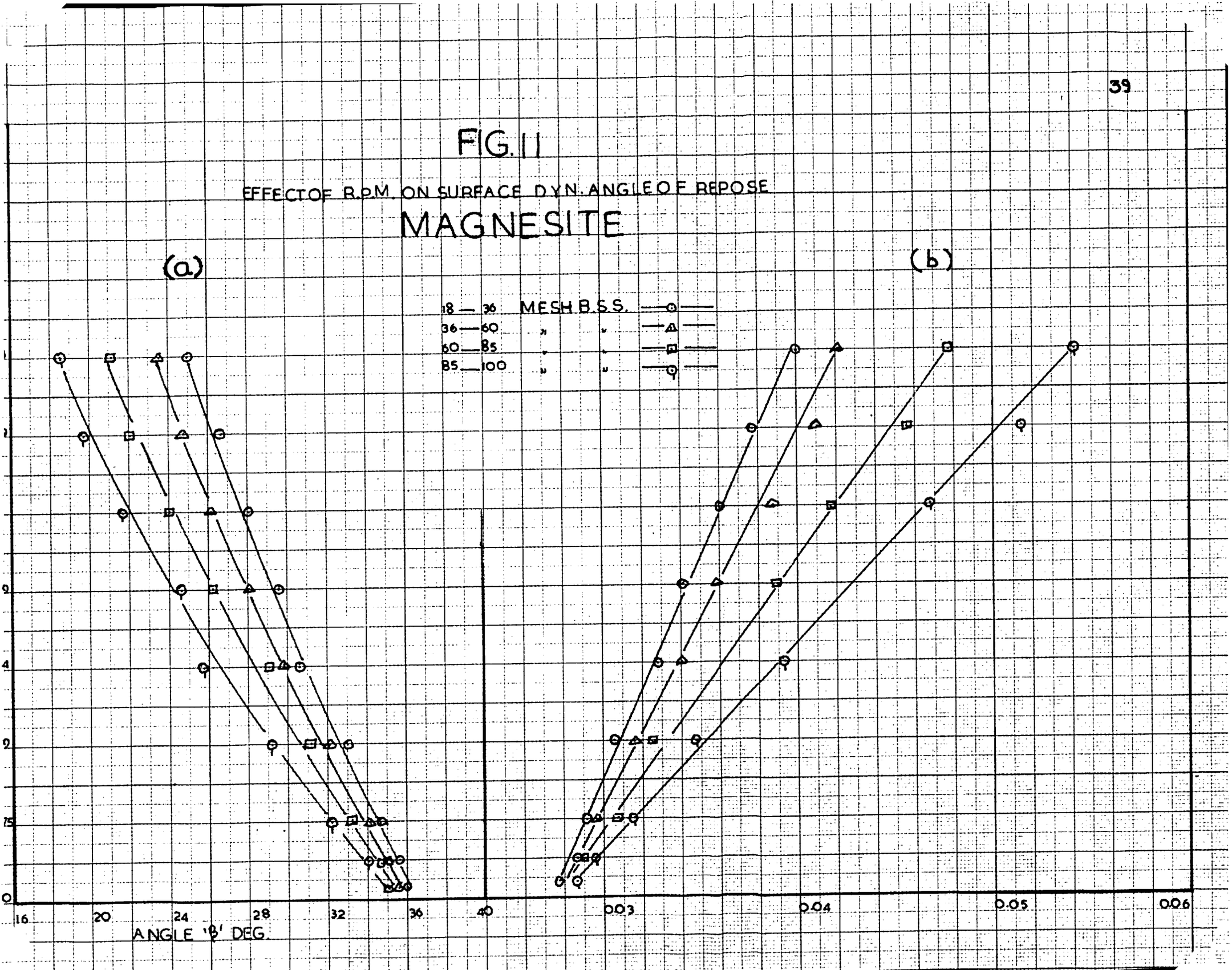
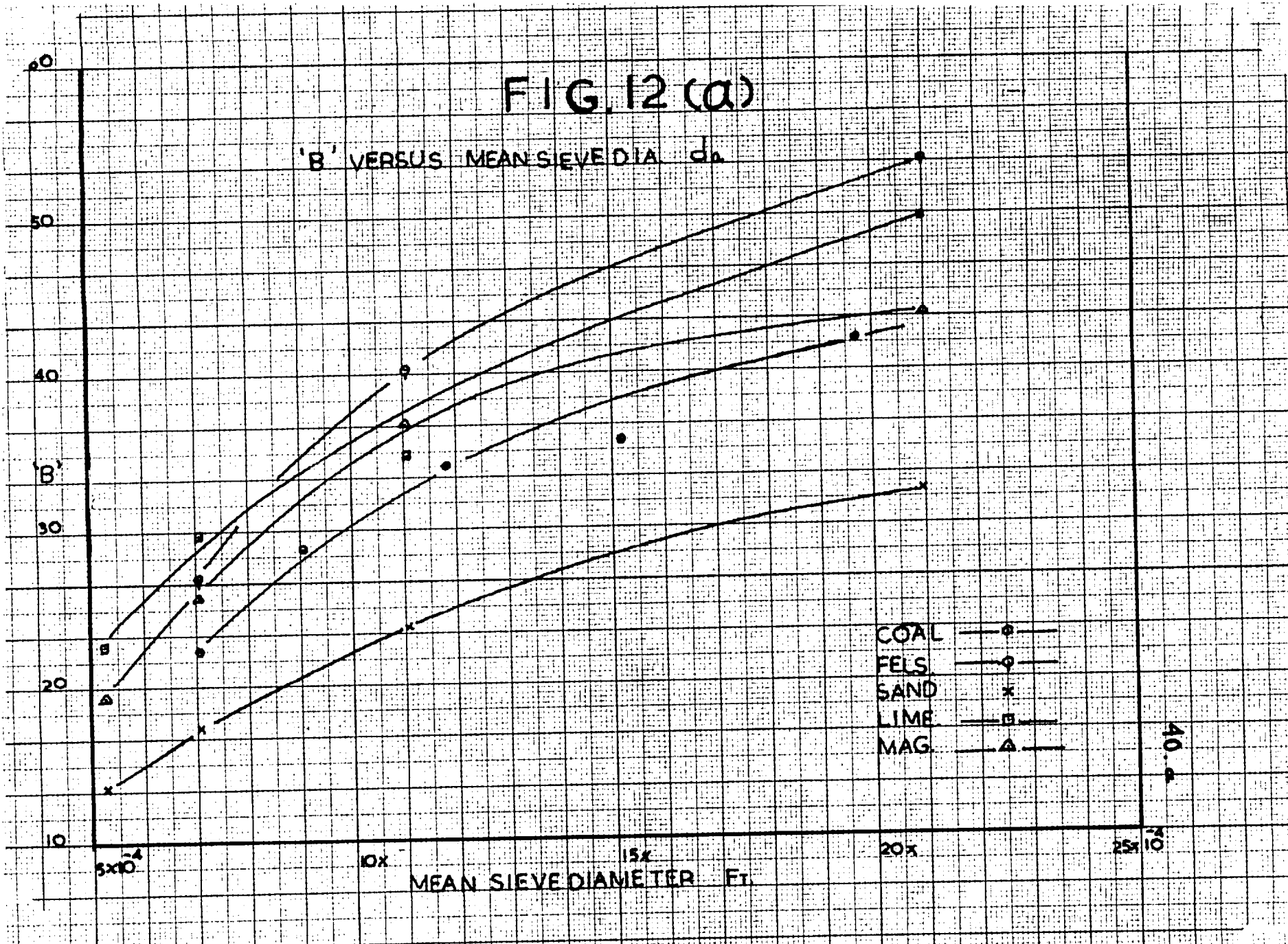


FIG. 12 (a)

'B' VERSUS MEAN SIEVE DIA d_m



40.P

FIG. 12 (b)

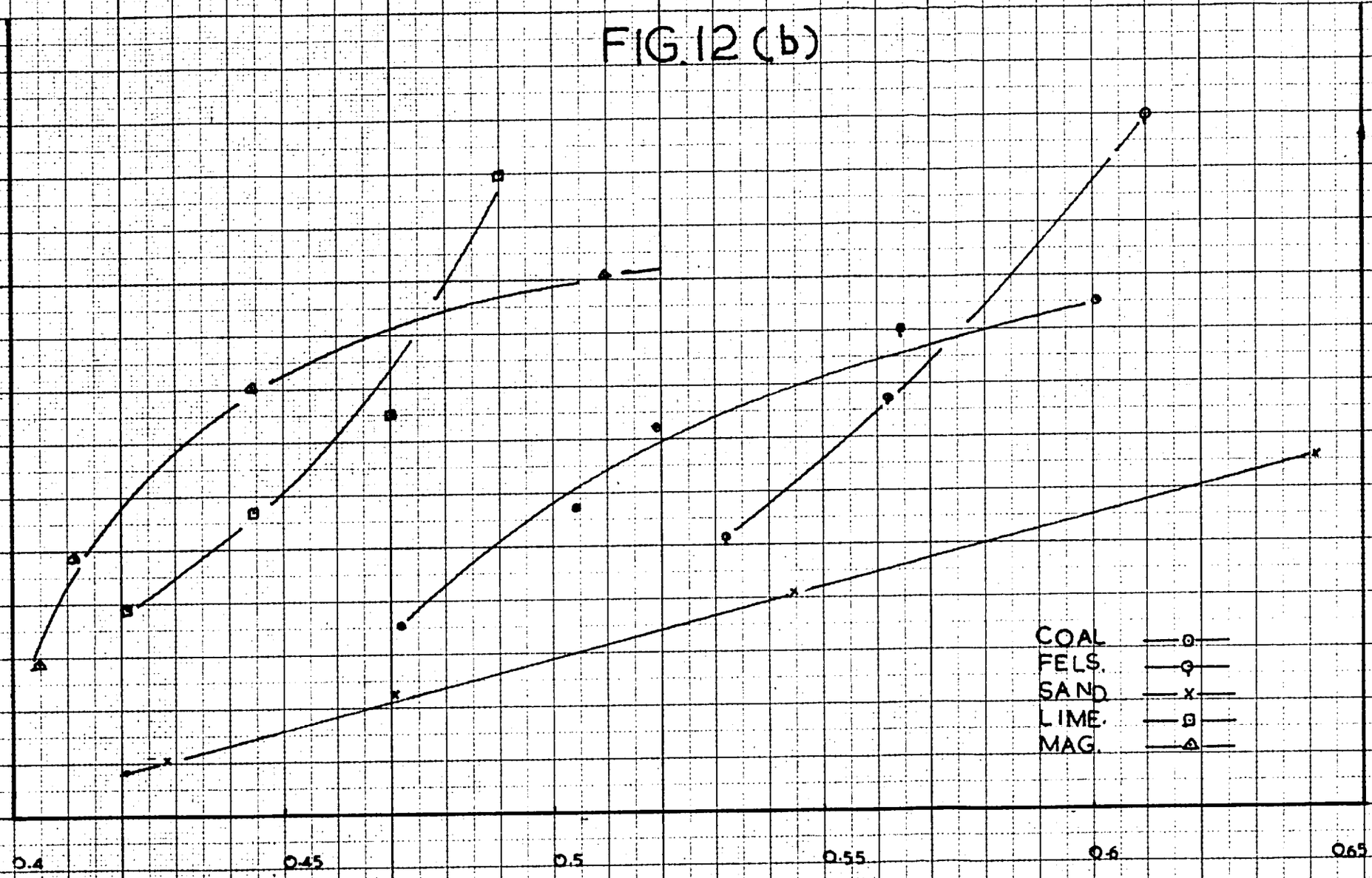


FIG 12 (b) 'B' VERSUS BULK DENSITY / TRUE DENSITY

TABLE (5)

VALUES OF EMPIRICAL CONSTANTS 'A' AND 'B'

NO.	MATERIAL	TRUE DENSITY lbs/C.FT.	(18-36) MESH			(36-60) MESH			(60-85) MESH			(85-100) MESH						
			A	B	B/A	A	B	B/A	A	B	B/A	A	B	B/A	A	B	B/A	
						(18-30)*			(30-36)*			(36-52)*			(52-60)*			(60-85)*	
1.	COAL	88.51	1.1962	42.055	35.155	1.0164	35.942	35.360	0.9873	34.259	35.371	0.8231	29.073	35.199	0.6355	21.805	34.344	
2.	FELSPAR	129.2	1.4738	53.4	36.294	1.143	40.05	35.039	0.785	27.185	34.630	—						
3.	SAND	165.6	0.919	32.224	35.096	0.6796	23.787	35.001	0.5004	17.430	34.829	0.3798	13.364	35.186				
4.	LIMESTONE	166.0	1.333	49.840	37.389	0.9158	34.772	37.968	0.8074	29.904	37.037	0.6209	22.885	37.432				
5.	MAGNESITE	208.3	1.196	43.610	36.630	1.0286	36.712	35.611	0.7177	26.166	36.405	0.543	19.673	36.230				

OVERALL AVERAGE VALUE OF $(B/A) = 35.796$

(*) SIZE DISTRIBUTION OF COAL

CHAPTER 3.

1. Free Curved Surface.

It has already been shown (see Plate 1) that the plane inclined surface of a granular bed, in a slowly rotating cylinder, is made up of two distinct parts, namely AB and BC (Figure 6). As the speed increases, the lower part BC remains plane while the upper part changes its profile as may be seen in Plates 1 and 2 for coal and magnesite. A set of these curves for coal (-18+22 mesh B.S.S.) are shown in Figure 13(a) and with curves superposed in Figure 13(b). Figure 13(a) also shows that the increase of speed results in the position of the point P, point of departure of the granules from the cylinder wall, shifting to higher levels.

The theory underlying the trajectories of the particles is complicated and must take into account their free-flight, mutual interactions and changes in apparent weight due to their peripheral speeds.

2. Free Flight.

Let us assume that the particle after leaving the cylinder wall at P (Figure 14a) follows a curved path, without coming into contact with other particles and

FIG. 13

EFFECT OF R.P.M. ON FREE SURFACE (UPPER PART)

COAL 18 - 36 MESH B.S.S.

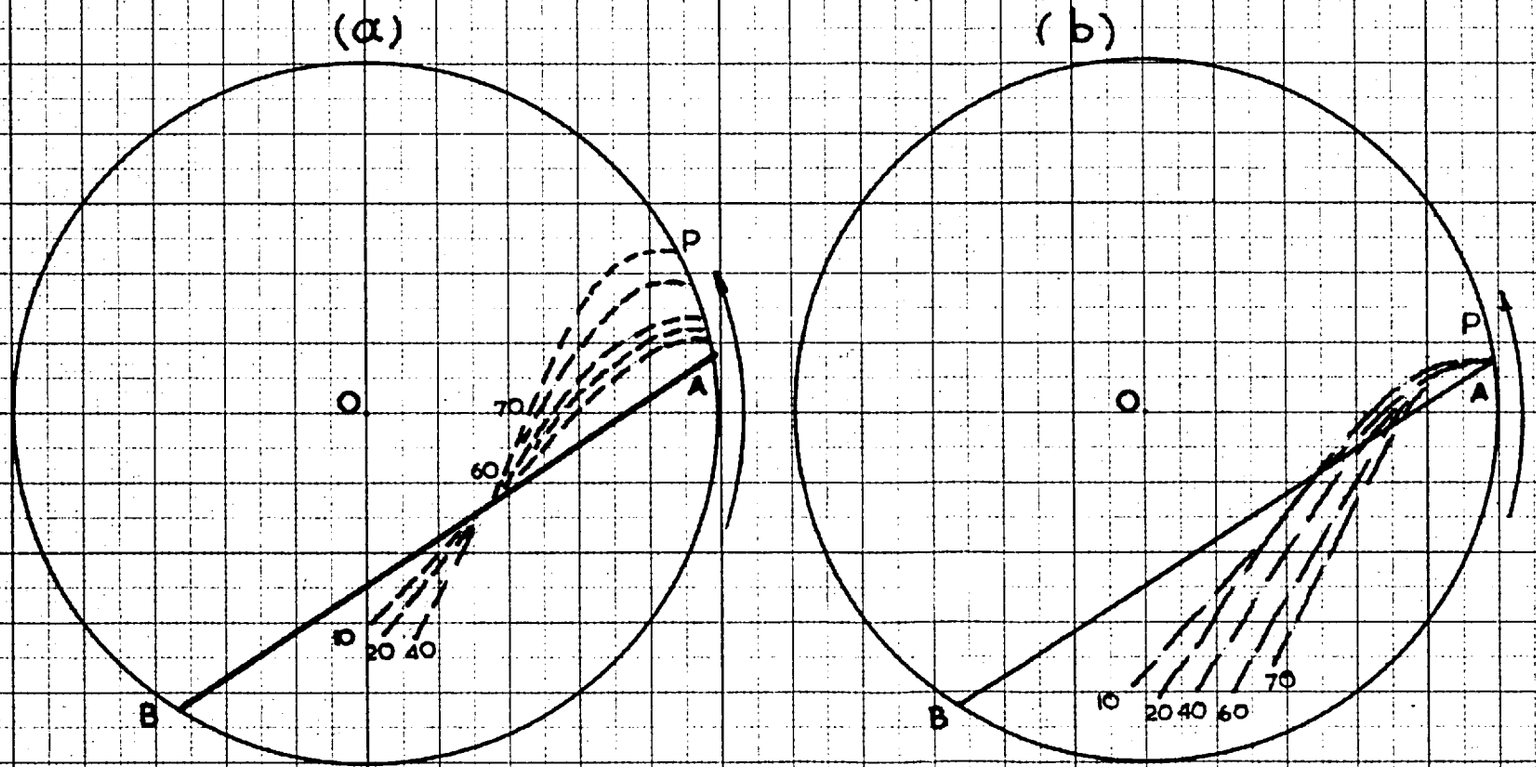
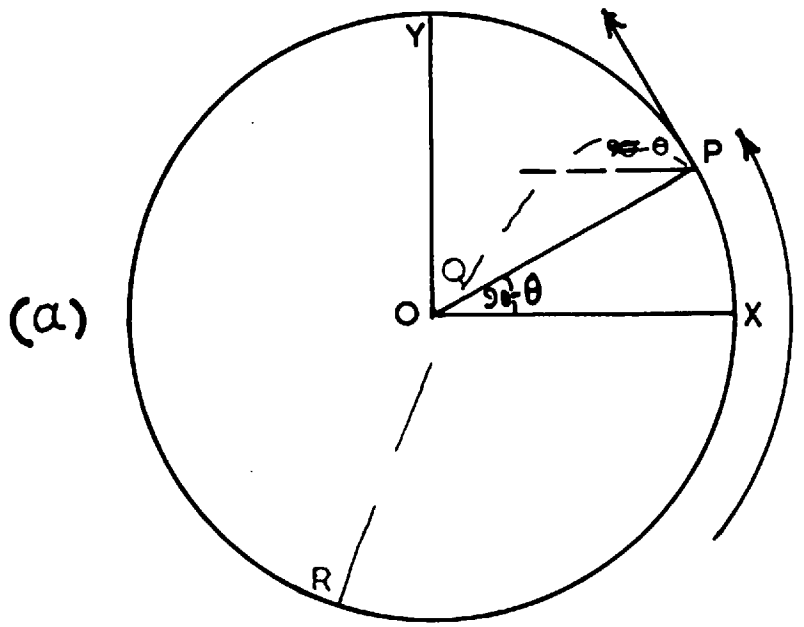
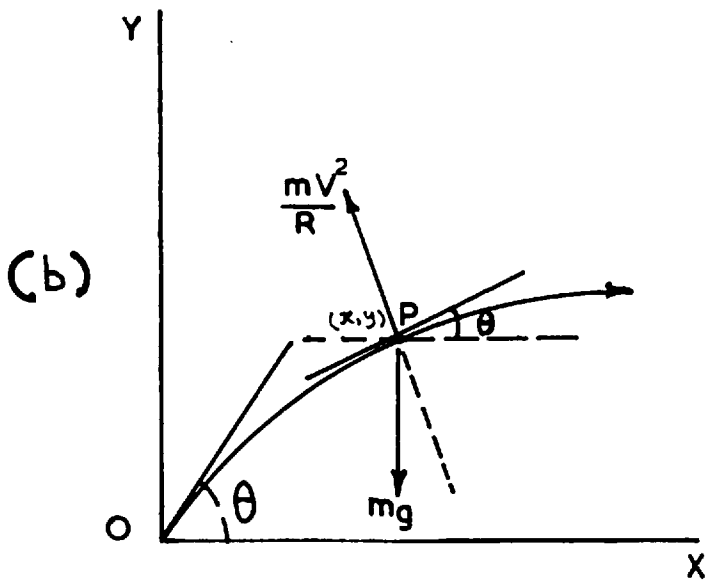


FIG.14





finally drops back to the main bed of particles, under the action of gravity. Let θ, be the angle of departure [5] of the particle and V ft./sec. its velocity. Resolving the velocity V, into its respective components along the x-axis and y-axis, we get:

Velocity component in the direction of x-axis

$$= x' = V \cos \theta \qquad (24)$$

Velocity component in the direction of y-axis

$$= y' = V \sin \theta - gt \qquad (25)$$

Integrating equations (24) and (25) with respect to time t, we get:

$$\int x' = \int V \cos \theta \text{ or } x = Vt \cos \theta \qquad (26)$$

$$\text{and } \int y' = \int V \sin \theta - g \int t \text{ or } y = Vt \sin \theta - \tfrac{1}{2} g t^2 \qquad (27)$$

Eliminating t between equations (26) and (27) and solving for y :

$$y = x \tan \theta - \frac{g x^2}{2 V^2 \cos \theta} \qquad (28)$$

The above expression is that of a parabola and when solved for x and y, at speeds 20, 30, 40, 50, 60 and 70 r.p.m., the results tabulated in Tables 8 (a), (b), (c), (d), (e) and (f) (see Appendix), are obtained. The corresponding curves are shown in Figure 15 (a), (b), (c), (d), (e), (f),

together with those obtained by actual experiment and a third set calculated by a method due to Gow which is referred to later.

It will be seen that approximate agreement between the calculated and the empirical curves is obtained only at higher speed, viz. 70 r.p.m. It would appear, therefore, that mutual interaction of the particles is playing an important part in determining the form of their trajectories.

3. Gow's Equation and Pushing Effect.

Gow, Campbell and Coghill [3] have criticised the concept of free flight and stressed that the granules while describing curved paths remain in contact with each other, in such a way that each exerts a pushing-effect on the one immediately in front of it. This results in a "greater throw" when compared with that due to free-flight only. The final relationship given by these workers is based on the assumption that the velocity of a granule remains essentially constant over the ascending part of the curve and is virtually the same as that of the rotating cylinder.

In Figure 14(b), where the granule is at a given

position, on the ascending part of the curved path, the forces acting on it are the centrifugal force $\frac{mV^2}{R}$ acting in a radial direction and the weight of the granule mg, acting vertically downwards. When the granule is in flight, the two forces are in equilibrium, i.e.

$$\frac{m\,V^2}{R} = -mg\cos\theta \qquad (29)$$

R is the radius of curvature of the curved path and may be expressed by :

$$R = \frac{[1 + (dy/dx)^2\ ]^{3/2}}{d^2y\ /dx^2} \qquad (30)$$

Also $$\cos\theta = \frac{dx}{dS} = \frac{1}{[1 + (dy/dx)^2\ ]^{1/2}} \qquad (31)$$

where dS is a small distance over the curved path. Both the values of the radius of curvature R and cos θ, when substituted in equation (29), yield the following results:

$$-g/V^2/g = \left\{\frac{[1 + (dy/dx)^2]^{3/2}}{d^2y\ /dx^2}\right\} \left\{\frac{1}{1 + (dy/dx)^2}\right\}^{1/2}$$

$$= \frac{1 + (dy/dx)^2}{d^2y\ /dx^2}$$

or $$\frac{d^2y/dx^2}{1 + (dy/dx)^2} = -\,g/V^2 \qquad (32)$$

Integrating Equation (32), we get :

$$\tan^{-1} dy/dx = - g/V^2 . x + C$$

In this equation $g/V^2 . x$ may be expressed in degrees, so multiplying by 57.29, we get :

$$\tan^{-1} dy/dx = -57.29\ g/V^2 . x + C$$

or $$dy/dx = \tan [-57.29\ g/V^2 . x + C] \qquad (33)$$

When x = 0, y = o, equation (33) reduces to

$$dy/dx = \text{Tan } (C)$$

and hence $C = \theta$ $[\because dy/dx = \tan \theta]$

Thus when the value of C is substituted in equation (33) we get: $dy/dx = \tan (\theta - 57.29\ g/V^2 . x)$

Integrating the above expression, we get:

$$y = \frac{V^2}{g}\left[\ln \cos (\theta - 57.29\ g/V^2 . x)\right] + C' \qquad (34)$$

At origin O, where x = 0 and y = 0, the above equation reduces to give,

$$C' = - \frac{V^2}{g}\left[\ln \cos \theta\right] \qquad (35)$$

Thus equation (34) may be rewritten as :

$$y = \frac{V^2}{g}\left[\ln \cos (\theta - 57.29\ \frac{g}{V^2} . x)\right] - \frac{V^2}{g}[\ln \cos (\theta)]$$

$$= \frac{V^2}{g}\left[\frac{\ln \cos (\theta - 57.29\ g/V^2 . x}{\cos \theta}\right]$$

$$\text{or } y = 2.3025 \frac{V^2}{g} \left[\log_{10} \frac{\cos(\theta - 57.29\ g/V^2 .\ x)}{\cos \theta} \right] \quad (36)$$

The above expression represents the ascending part of the curve traced by the granules after leaving the shell. The curved paths have been worked out for 30, 40, 50, 60 and 70 r.p.m. and are tabled in Tables 9(a), (b), (c), (d) & (e). (see Appendix). See also Figure 15 (b-f).

It will be seen that the curves give a fair representation of the trajectories for speeds up to 40 r.p.m. and thereafter diverge to an increasing extent.

4. Modified Gow's Equation.

An attempt has been made to modify Gow's equation so as to take into account friction effects between the particles.

Referring to Figure 16(a), let a spherical granule of radius r roll down an inclined plane at angle θ. OX represents the X-axis and OY the y-axis, both being in the same vertical plane. We have then the following three equations of motion [30]

$$m \ddot{x}_c = W \sin \theta - F \quad (37)$$

$$m \ddot{y}_c = W \cos \theta - R \quad (38)$$

and $$I_c \ddot{\theta} = F \times \text{[illegible]} \quad (39)$$

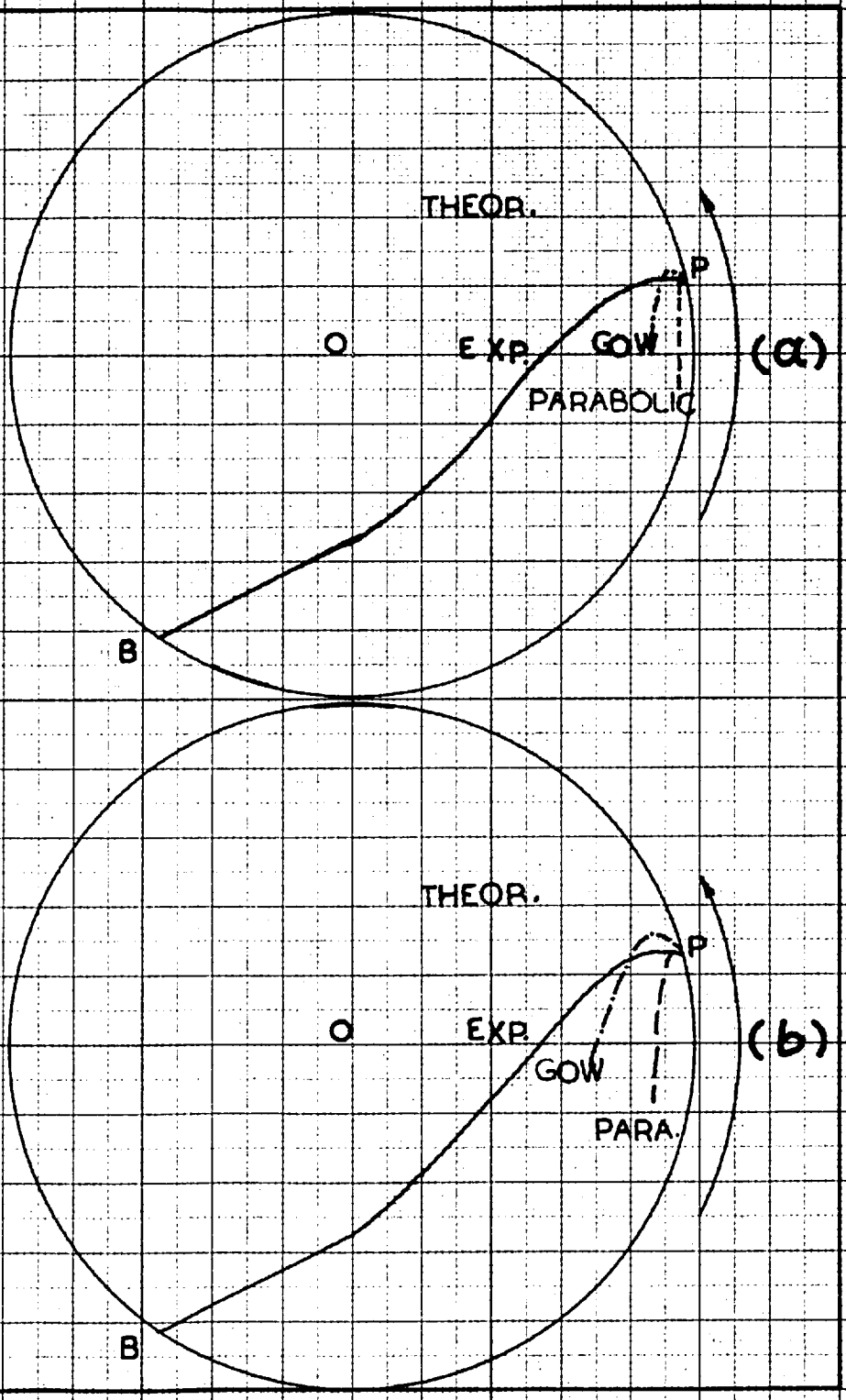

R.P.M.
20
THEOR.
P
O
EXP.
GOW
PARABOLIC
(a)
B
R.P.M.
30
THEOR.
P
O
EXP.
GOW
PARA.
(b)
B

FIG. 15

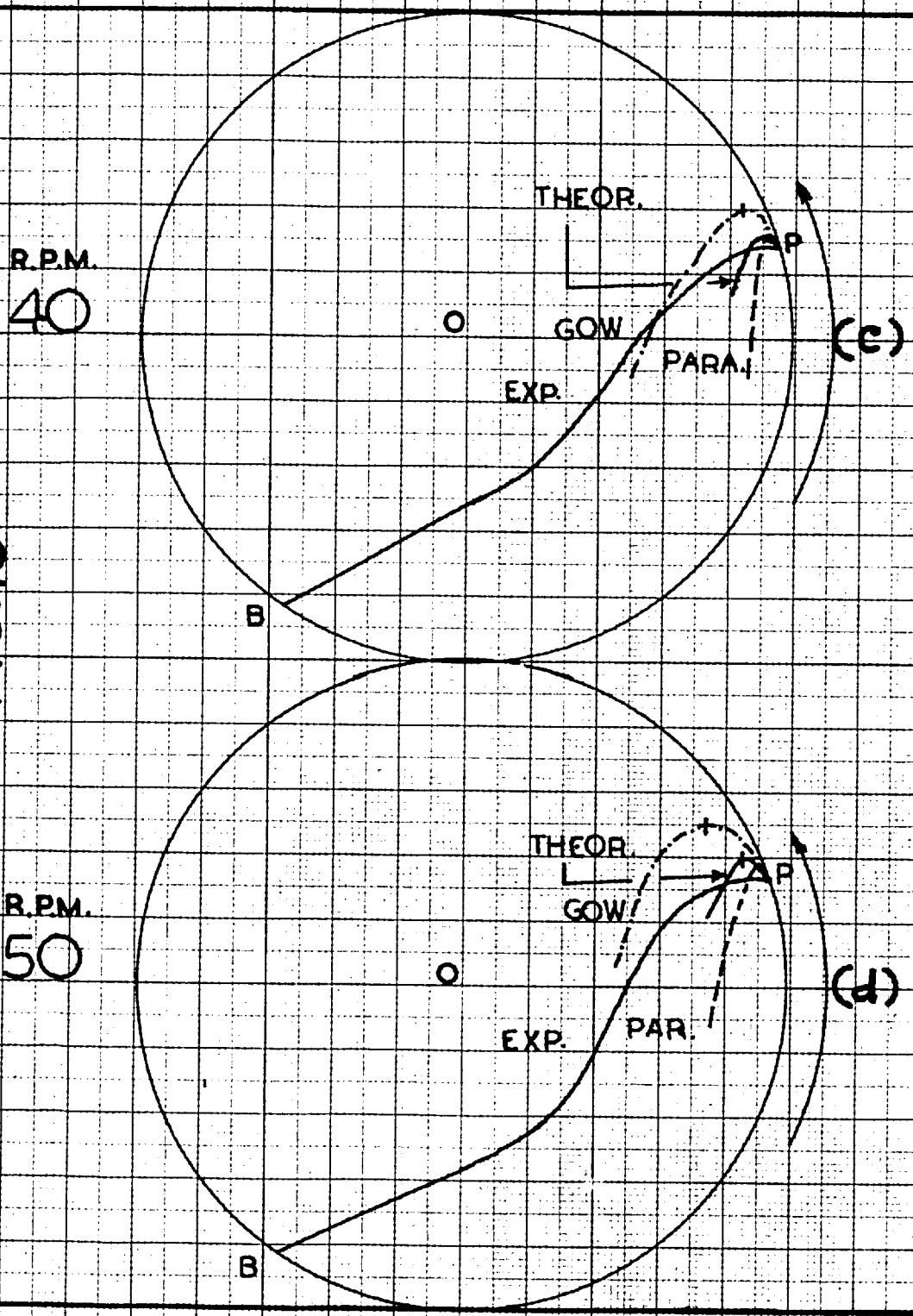


FIG.15

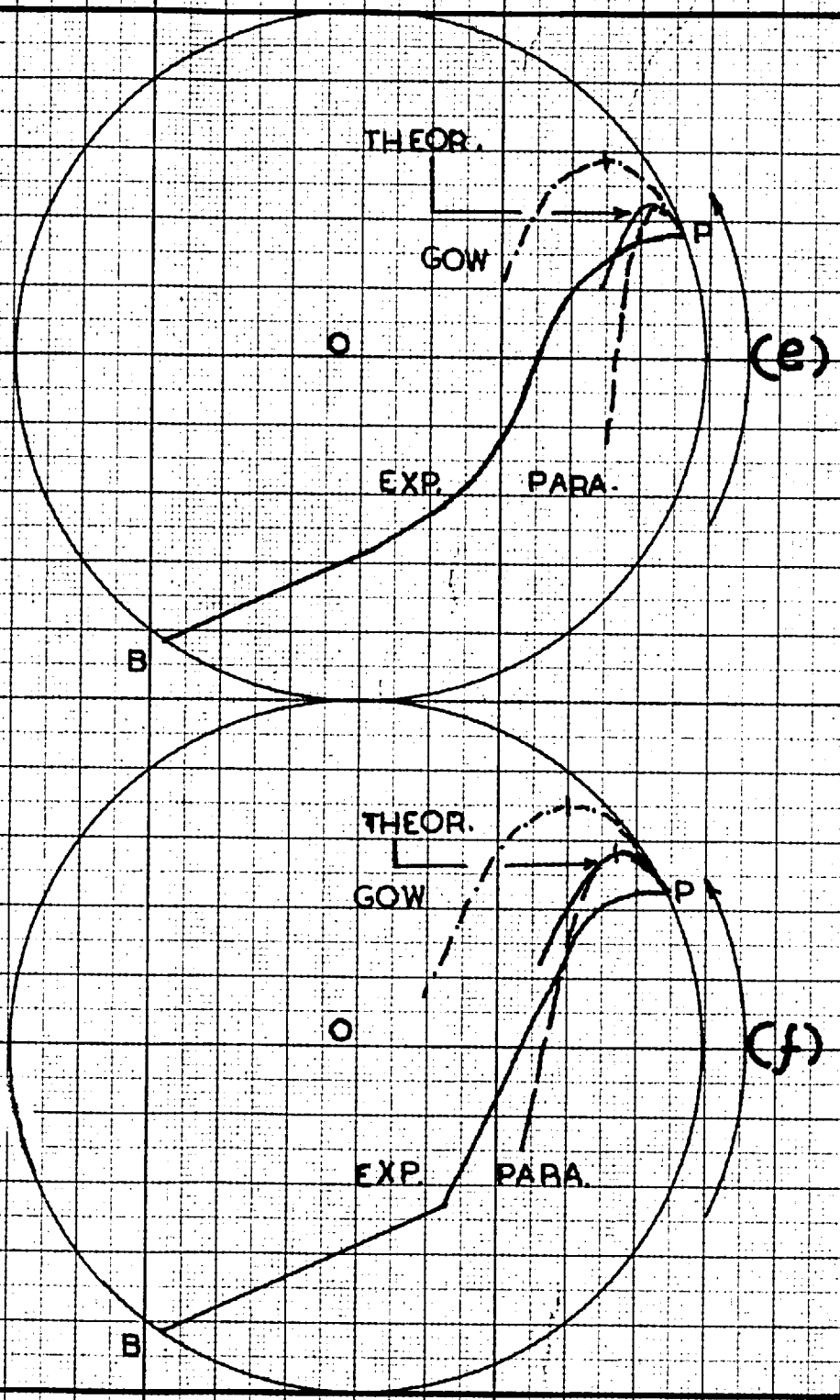
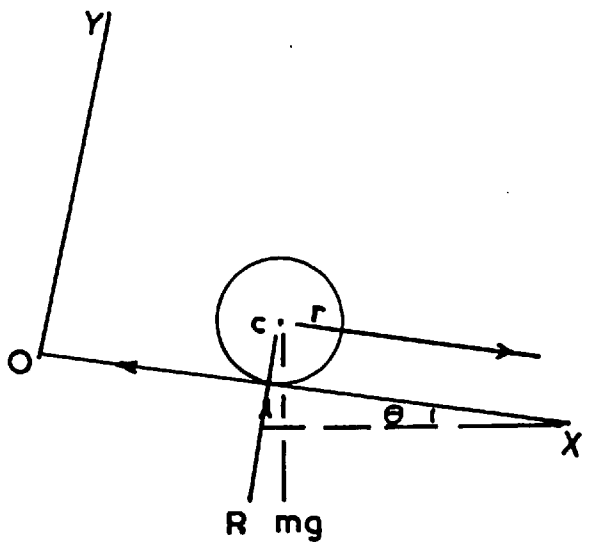


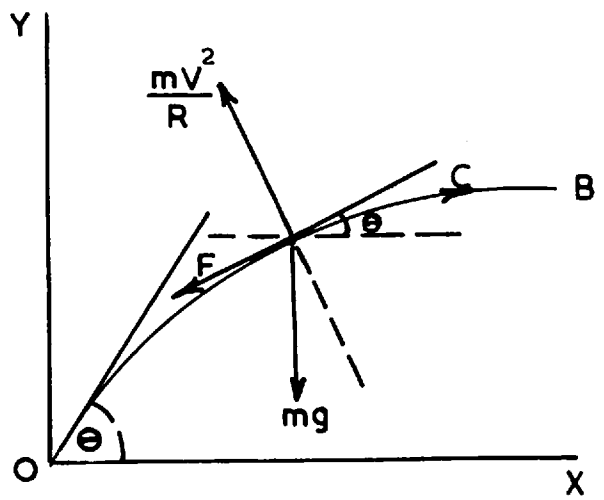
FIG.15

FIG. 16

(a)



(b)



where mg = weight of the body, (W)
$\ddot{x}_c$ = Acc. along x-axis.
$\ddot{y}_c$ = Acc. along y-axis.
$\ddot{\theta}$ = Angular acc. of the spherical granule.
I_c = Moment of inertia of the body,
F = Frictional forces,
R = Reaction to the normal forces.

Since there is no sliding, the velocity at the point of contact 'A' at any time is zero, i.e. the point A is the instantaneous centre of rotation. Thus the angular velocity $\dot{\theta}$ of the rolling body can be expressed as $\dot{x}_c/r$, which on differentiation yields $\ddot{\theta} = \ddot{x}_c/r$. Substituting this value in equation (39) we get :

$$I_c \times \ddot{x}_c/r = F \times r \qquad (40)$$

Eliminating F between equations (37) and (40),

$$(m + I_c/r^2)\ (\ddot{x}_c) = mg \sin \theta \qquad (41)$$

whence

$$\ddot{x}_c = \frac{g \sin \theta}{1 + i_c^2/r^2} \qquad (42)$$

where i_c is the radius of gyration of the body with respect to its geometric axis. The ratio $1/1 + i_c^2/r^2$, in the case of spherical bodies is equal to 5/7.

Substituting the value of the said ratio in equation (42), we get :

$$\ddot{x}_c = 5/7 \times g \sin \theta \qquad (43)$$

Again, when the value of $\ddot{x}_c$ is substituted in equation (37), we get,

$$m \times 5/7\ g \sin \theta = mg \sin \theta - F$$

$$\text{or} \quad F = 2/7\ mg \sin \theta \qquad (44)$$

Referring back to Figure 16 (b), where a particular granule leaves the surface of the rotating cylinder at O and describes the curve OCB. Assuming that there is no slip between the granular mass and the cylinder wall, then the granule P will be moving with the same velocity as that of the shell, remaining in contact with the granular mass.

The forces acting on the granule, the centrifugal force $\frac{mV^2}{R}$, the weight of the granule mg, and the frictional forces, can be expressed by the following relationship:

$$\frac{\text{Frictional Forces}}{\text{Normal Forces}} = \text{Coefficient of Friction}$$

$$\text{i.e.} \quad F/N = \mu \quad \text{or} \quad F = \mu \times N \qquad (45)$$

Substituting the values of the respective forces, we get

$$F = \mu \left(\frac{mV^2}{R} + mg \cos \theta \right) \qquad (46)$$

But $F = -2/7\ mg \sin \theta$ (see equation 44), then we have:

$$-2/7\ mg \sin \theta = \mu \left(\frac{mV^2}{R} + mg \cos \theta \right)$$

$$\text{or} \quad 1/\cos \theta \times R = -(2/7\ \mu \tan \theta + 1)\ g/V^2 \qquad (47)$$

since $\cos\theta = \dfrac{1}{\sqrt{1 + (dy/dx)^2}}$

and $R = \dfrac{[1 + (dy/dx)^2]^{3/2}}{d^2y/dx^2}$

equation (47) becomes,

$$\frac{d^2y/dx^2}{1 + (dy/dx)^2} = -g/V^2 \left[\frac{2 \tan\theta + 7\mu}{7\mu} \right] \qquad (48)$$

This is precisely the same form as obtained by Gow in equation (32) and when developed on similar lines, the final relationship obtained may be expressed as follows:

$$y = 2.3025 \frac{V^2}{gK} \left[\log_{10} \frac{\cos(\theta - 57.29 \times g/V^2 . K.x)}{\cos} \right]$$

$$\text{where } K = \frac{2 \tan\theta + 7\mu}{7\mu} \qquad (49)$$

Equation (49) represents the ascending part of the path traced out by the outermost layer of the granules, taking into account the frictional characteristics of the material under examination.

Employing equation (49), the co-ordinates x and y, as they appear in Tables 10 (a), (b), (c) and (d) for 40, 50, 60 and 70 r.p.m. (see Appendix), have been graphically presented in Figure 15 (c), (d), (e) and (f). These graphs indicate that unlike Gow's equation the modified form gives rather better agreement with the experimental curves.

5. Effect of Apparent Change in Weight of Particles on their Trajectories.

The apparent weight of a body in a rotating cylinder is a function of both the centrifugal force and its position on the periphery.

Consider a granule lying on the inner surface of the cylinder. When the cylinder rotates, the granule begins to move along the shell, in the direction of rotation and reaches a height determined by its weight, the friction between the particle and walls of the cylinder and the speed of rotation. Since the sliding friction is smaller than the static friction, this position will be unstable and the particle will tend to return to its original position. When the particle is in some position P (Figure 18), its apparent weight is given by :

$$\text{Apparent weight} = Wa = mg\left(1 + \frac{V^2}{rg}\cos\theta\right) \qquad (50)$$

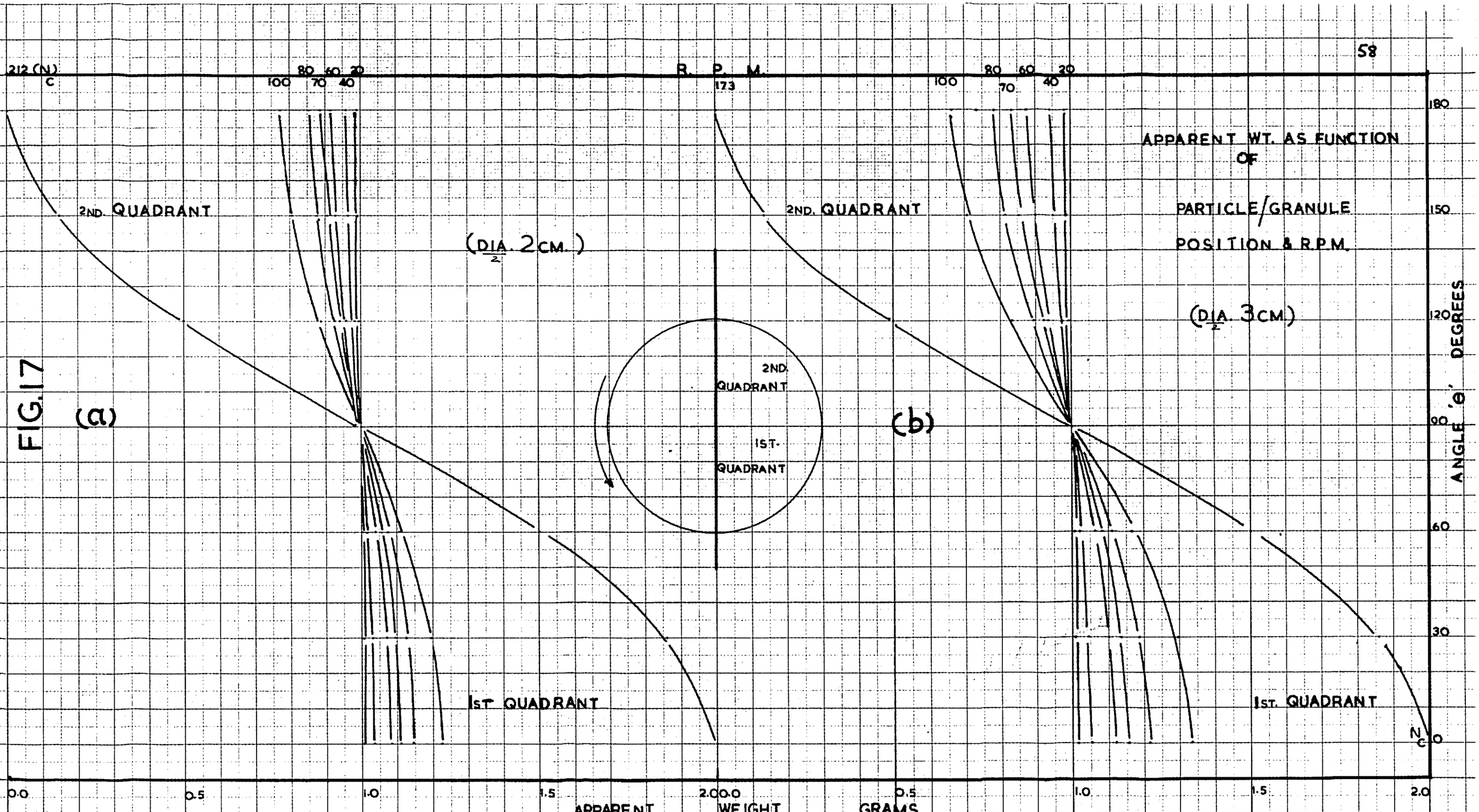
where Wa = apparent weight in grams,
V = peripheral speed in cm/sec.,
θ = the angle subtended by the granul e P at the centre O,
g = gravitational constant.

The above relationship may be expressed in a more convenient form :

$$Wa = mg\left(1 + 0.561 \times 10^{-5}\, D\, N^2 \cos\theta\right) \qquad (51)$$

where Wa = apparent weight in grams, D = diameter of cylinder in cm., N = r.p.m., and θ = the angle as defined above.

FIG. 17


212 (N)/C
R. P. M.
173
100 80 70 60 40 30
2ND. QUADRANT
(DIA. 2 CM.)
(a)
2ND. QUADRANT
1ST. QUADRANT
1ST. QUADRANT
(b)
APPARENT WT. AS FUNCTION OF PARTICLE/GRANULE POSITION & R.P.M.
(DIA. 3 CM.)
180
150
120
90
60
30
0
ANGLE 'θ' DEGREES
0.0
0.5
1.0
1.5
2.0
APPARENT WEIGHT GRAMS

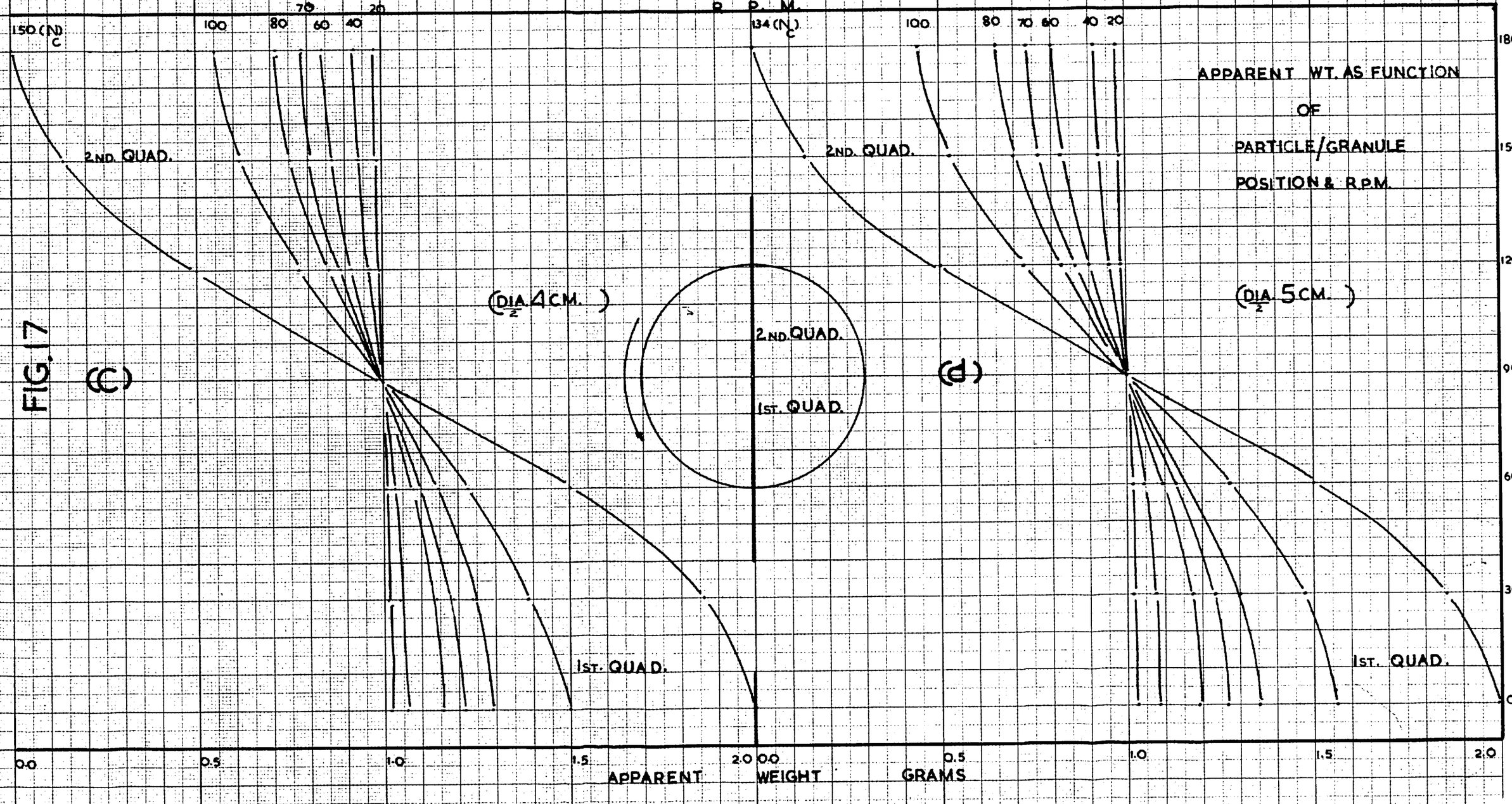

R. P. M.
150 (N_c)
100
80
70
60
40
20
2ND. QUAD.
(DIA. 4 CM.)
1ST. QUAD.
(c)
134 (N_c)
100
80
70
60
40
20
2ND. QUAD.
(DIA. 5 CM.)
1ST. QUAD.
(d)
2ND. QUAD.
1ST. QUAD.
APPARENT WT. AS FUNCTION OF PARTICLE/GRANULE POSITION & R.P.M.
ANGLE 'θ' DEGREES
180
150
120
90
60
30
0
0.0
0.5
1.0
1.5
2.0
APPARENT WEIGHT GRAMS

FIG. 17

APPARENT WT. AS FUNCTION OF R.P.M.

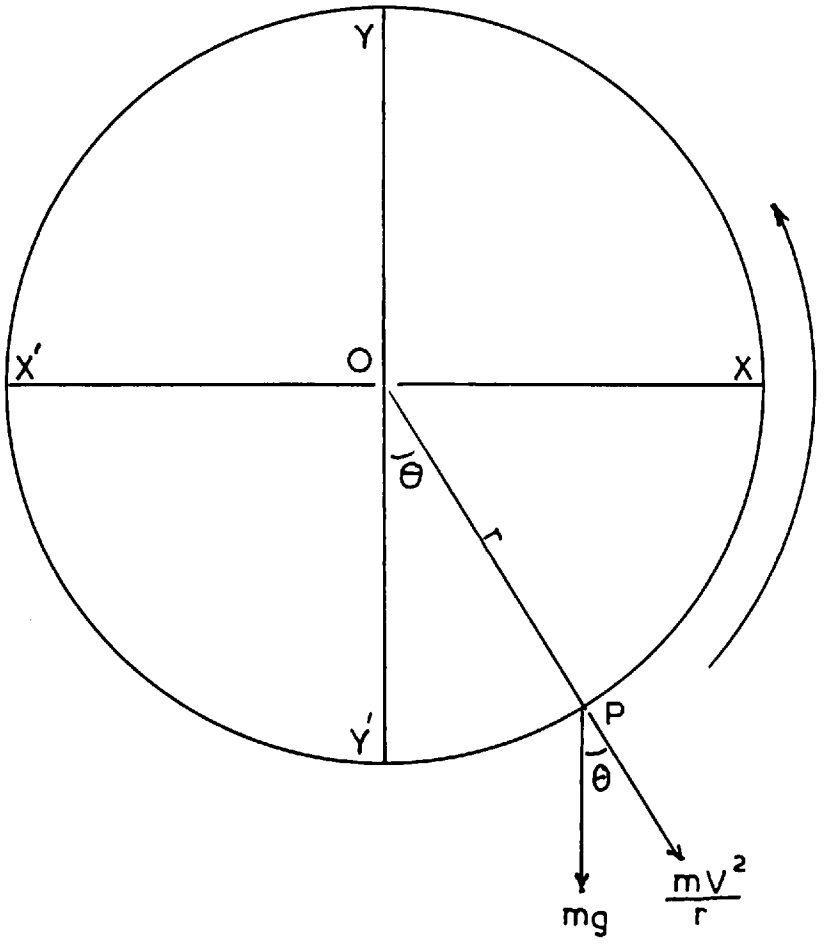


FIG. 18

With the help of the above equation, the apparent weights of one gram of granular mass were calculated for speeds ranging from 20 r.p.m. to the critical speed when the value of angle θ and the distance of the particle from the centre of the circle are given. These values have been graphically presented in Figure 17 (a), (b), (c) and (d).

It will be seen from the curves that in a cylinder of radius 5 cm., rotating at 70 r.p.m., the apparent weight of the granule when the angle θ is 116 degrees, comes to about 0.87 grams.

6. The Proposed Construction.

Knowing the static angle of repose of the material and the maximum value of θ' for any given speed, it is possible to construct the profile of the moving bed in the following manner:

Let AB represent (see Figures 19 and 20) the surface of the material at its static angle of repose and let HOP represent the maximum value of the angle θ'. P will be the point of departure of a particle originating at the periphery.

1. Referring to Figure 19, with O as centre, describe 5 semi-circles of radii 1,2,3,4 and 5 cm., concentric to the circle of reference.

2. Join P with O, to cut the semi-circles in P', P", P‴ and P⁗.

3. From P, P', P", P‴ and P⁗ drop perpendiculars to meet the horizontal line OH at L, L', L", L‴ and L⁗.

4. With A,C, D, ..., the points generated by the intersection of semi-circles and the static surface AB, as centres and radii equal to PL, P'L', P" L", ... describe arcs to cut the semi-circles in U, R, S, ...

5. Join P, U, R and S to give the curve PURS - the curved surface.

The above construction is graphically presented for coal and magnesite (-18+36) mesh B.S.S., at 10, 20, 40 and 70 r.p.m. in Figures 19 and 20. It will be seen that the constructed curves are in fair agreement with the experimental ones. It may also be seen that the construction is not possible at 5 r.p.m. where the point P lies too close to B, i.e. the dynamic surface is situated very near to the static surface AB.

It will further be noticed that the constructed curves are somewhat higher in position than the experimental ones which means that the change in apparent weight along the constructed curves is smaller than the experimental ones.

The values of apparent weights along both types of curves, i.e. the constructed and the experimental ones, can readily be compared by making use of Figure 17 (a), (b), (c) and (d).

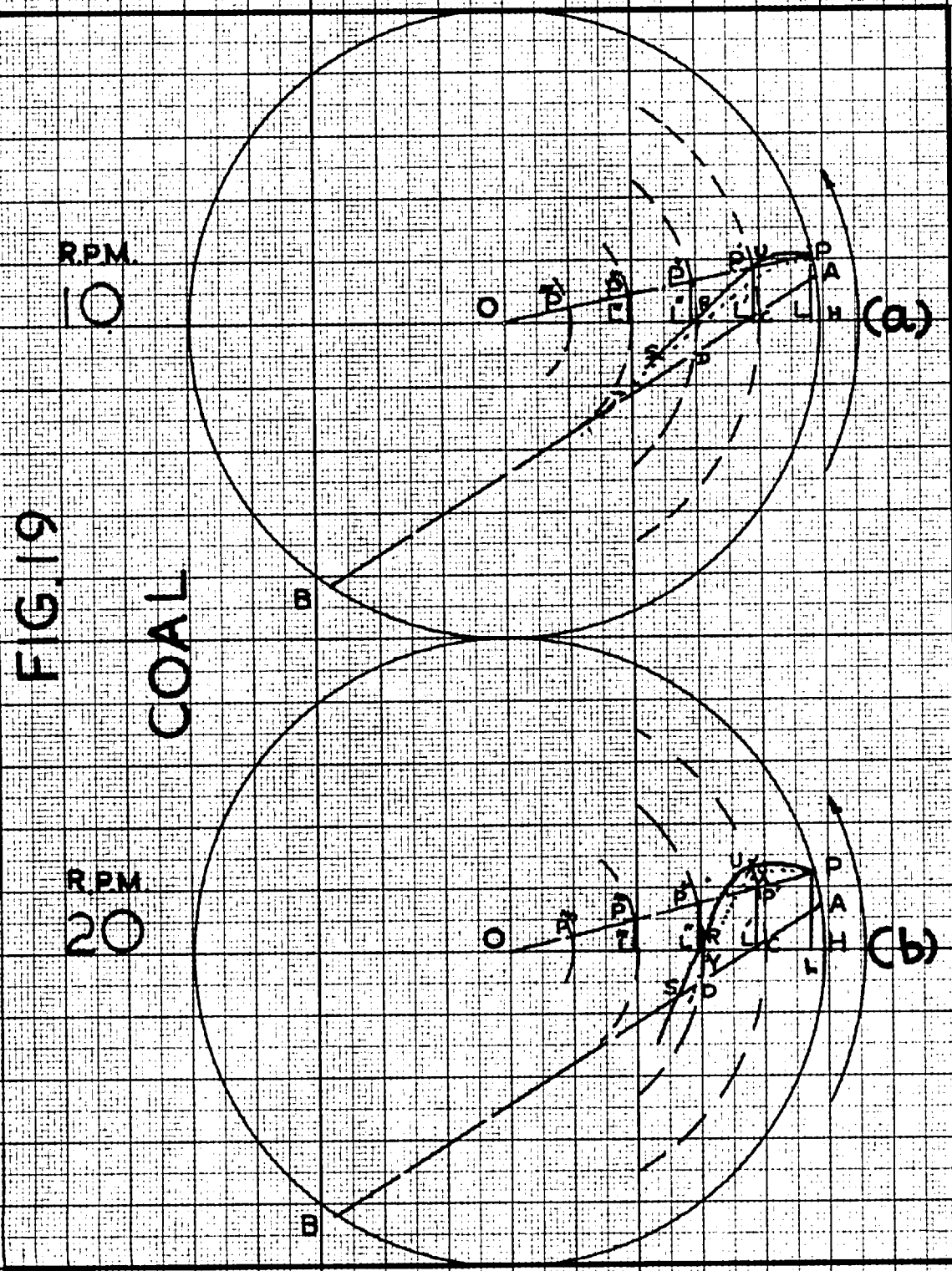
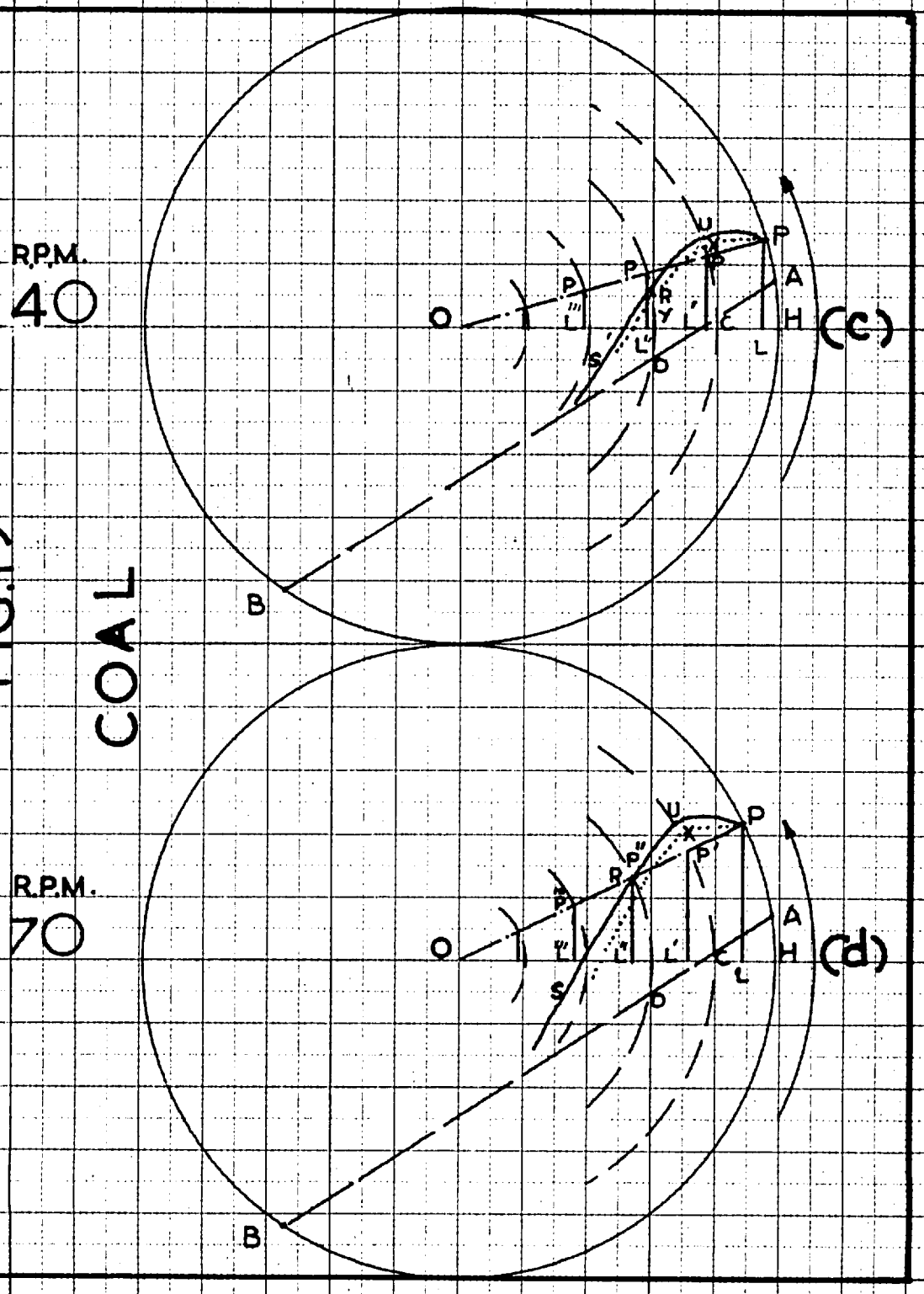


FIG. 19

FIG.19

COAL



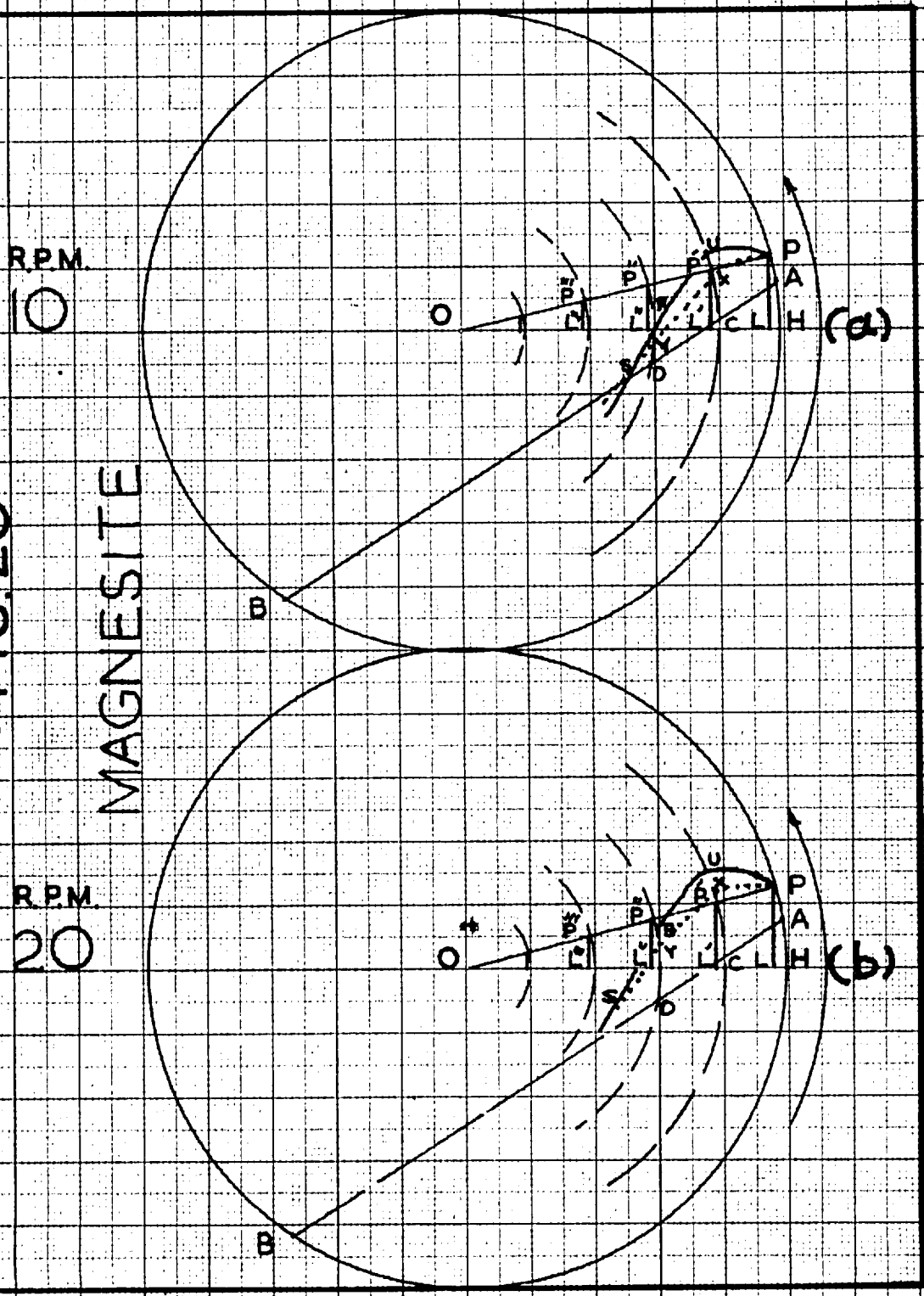
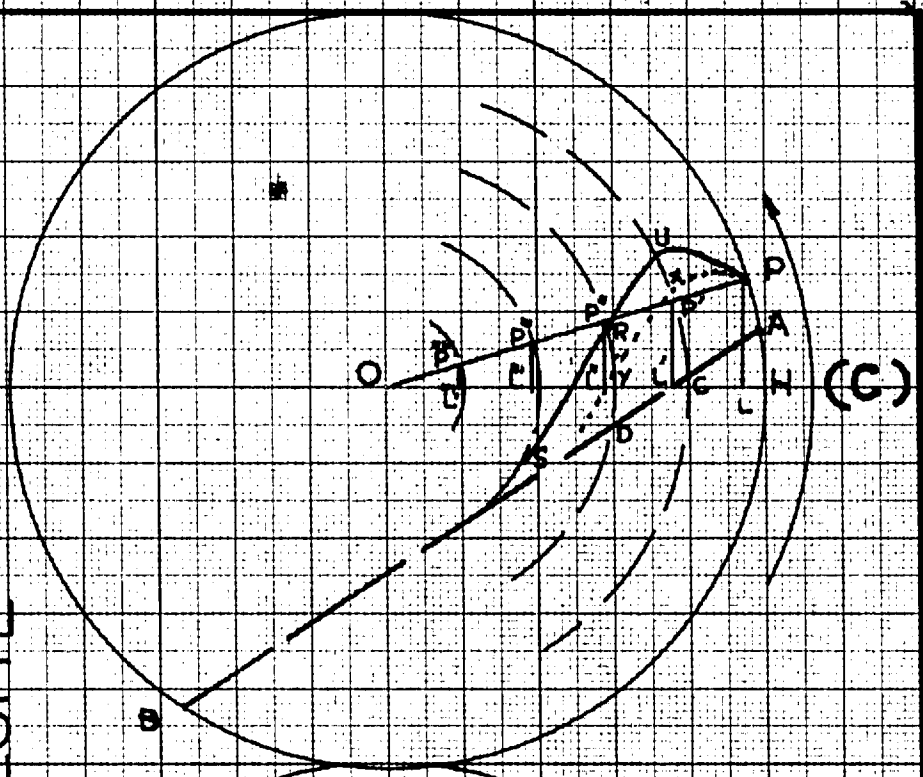


FIG. 20 MAGNESITE

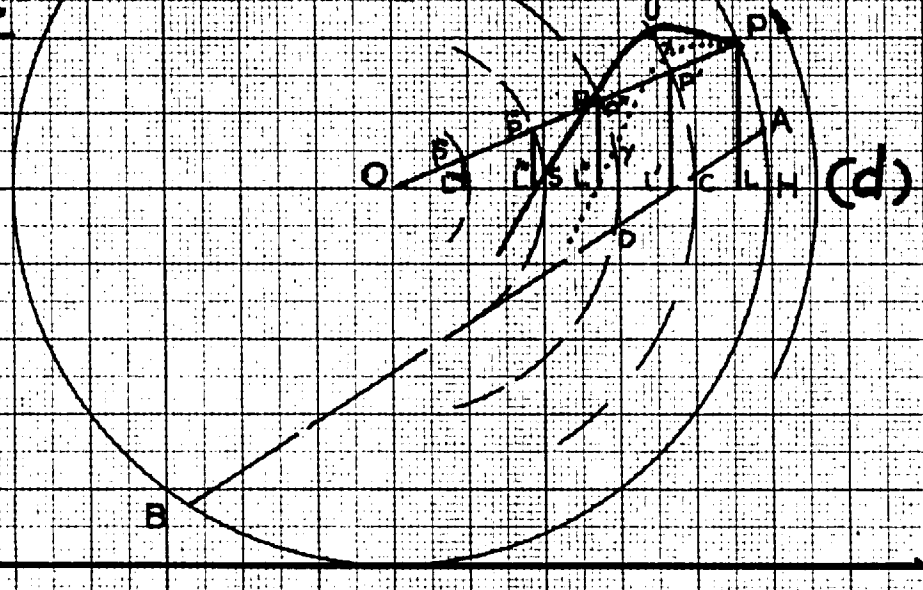
FIG.20

MAGNESITE

R.P.M.
40



R.P.M.
70



SECTION 2.

CHAPTER 4.

1. Introduction.

In setting up apparatus for studying the passage of granular material through an inclined rotary cylinder, it is necessary to arrange for supplying the material at various uniform feed-rates. The simplest method is to allow it to flow from a hopper through an orifice of known size, taking advantage of the fact that the rate of flow is known to be independent of the head of material above the orifice. As it was proposed to use a wide range of material in the experiments, it was necessary, however, to determine the effect of such factors as the density, the orifice diameter and particle size, on the rate of flow or discharge.

A survey of the literature indicated that although a considerable amount of work had been published on the flow of solids through orifices and numerous empirical equations suggested, there was no well established theory which would enable a feed hopper to be designed from the first principles.

2. Literature Survey.

The earliest work on solid flow through orifices appears to be that of Ketchum [31] in 1911, who used a glass lined container, fitted with a circular orifice and showed that the discharge rate Q, was proportional to the cube of the orifice diameter and was independent of the head H.

Later in 1929, Deming and Mehring [14] while studying granular flow through apertures, proposed the following equation:

$$Q = \frac{1.66\, D^{2.5} \cdot \rho_a}{\mu[34.6 + (67.4 + 444 \sin \tfrac{1}{2}\phi\,]\,[d_a/D + 0.130 - 0.161\mu]} \qquad (52)$$

where Q = discharge rate in grams/sec.
D = orifice diameter in mm.
d_a = particle diameter in mm.
ρ_a = bulk density, grams/cc.
μ = coefficient of friction
α = angle of repose - degrees
and ϕ = (180-2α), cone angles.

The above authors used conical bottomed cylindrical vessels, with the angles equal to (180-2α), where α is the angle of repose. Thus it would appear that for every material under test, the cone would have to be altered according to the angle of repose. Their work was limited to one

material, namely potassium nitrate over a wide range of particle size, i.e. 8 to 100 mesh, the potassium nitrate particles being spherical. Thus the proposed relationship includes only a bulk-density term, the true density remaining constant, a circumstance which limits its application.

Takahashi [32] in 1933, carried out a series of experiments on a wide range of materials such as sand, leadshots, vegetable seeds and different mixtures of sulphur and sand and showed that the velocity of flow V of the granules through an orifice depends on the orifice diameter, the particle size and the coefficient of friction:

$$V = \frac{k\sqrt{g \times D}}{f(\mu) + a(d_a/D)} \qquad (53)$$

where V = velocity of the emerging granules in ft/sec.
k and a= constants depending on the materials used
D, d_a and μ have the same significance as described earlier.

Takahashi has not defined the function $f(\mu)$ and it will be noted that his equation contains no terms involving the true or bulk-density.

Newton, Dunham and Simpson [33] in 1945, showed that for catalyst particles of 0.1 to 0.2 inches in diameter the discharge rate Q, through a flat bottomed cylinder

containing an orifice, may be expressed in terms of the orifice diameter and the material head :

$$Q = 0.141\ D^{2.96} \times H^{0.04} \qquad (54)$$

$$f = 1.80\ D^{0.96} \times H^{0.04} \qquad (55)$$

where Q = discharge rate in lbs./sec.

f = discharge rate per unit area of the cross section (lbs/(sec)(sq.in.)

H = material head. H is in feet and D is in inches.

Both the above mentioned equations show that contrary to the findings of many other workers, the flow rates have a dependence on the head H. The authors have moreover pointed out that both the equations are only applicable when the ratio D/d_a exceeds 6; lower values of ratio either tended to block the orifice or make the flow irregular.

The most comprehensive work on gravity flow of spherical solids is that of Rausch [34] in 1948, who arrived at the following correlation:

$$Q = 0.294.C.\rho_a . A_o\sqrt{\frac{g \times D}{2 \tan\beta}} \times (D/d_a)^{0.3} \qquad (56)$$

where C depends on the ratio D/d_a. For $D/d_a = 12.3$, the value of C = 0.91.

He used tubes of 3 to 8 inches in diameter and the orifices 1/16 to 2 inches diameter and obtained data for particles

of bulk density ranging from 45.5 lbs/c.ft. (radish seed) to 420.5 lbs/c.ft. (lead shot) and particle diameter from 0.005 inches (iron powder) to 0.6 inches (steel ball bearings).

Shirai [35] in 1952 showed that for sand, quartz and earth powder (30 to 150 mesh) flowing from vertical glass pipes 0.5 to 1 inch diameter, through orifices ranging in size from 2.3 mm. to 9.0 mm. in diameter:

$$Q = 0.472 \times \rho_a \sqrt{\frac{g\, D^5}{2\mu}} \qquad (57)$$

where Q, ρ_a, D and μ have the same significance and are expressed in F.P.S. units.

Brown and Hawkesley [36] in 1953 studied qualitatively the mechanism of flow from a hopper through an orifice and showed that there exists at least five distinct regions of movement in the hopper.

Franklin and Johanson [21] in 1955 studied the effects of the variables density, orifice and particle diameter, the material head and the angle of repose. The materials employed covered a wide range of specific gravity (i.e. from 7.34 lbs/c.ft. for puffed rice to 676 lbs/c.ft. for lead shot), which were shown to give flow rates expressed by the following equation:

$$Q = 1.66 \times 10^{-2} \frac{\rho_t \times D^{2.93}}{(6.288\mu_i + 23.16)(d_a + 1.889)} \qquad (58)$$

where μ_i = coefficient of friction based on the internal dynamic angle of repose.
Q, ρ_t, D and d_a are as already defined
D and d_a are both in inches.

The authors used the conventional drum-method for determining the internal dynamic angle of repose and showed that this angle is smaller than the surface dynamic angle of repose.

Fowler and Glastonbury [37] in 1959 studied the effects of the variables density, orifice and particle diameter on the discharge rate, using different shapes of orifices, namely circular, ellipsoidal, rectangular, square, pentagonal, hexagonal and triangular. By use of dimensional analysis they arrived at the equation:

$$Q = 0.236 \rho_a A_o \sqrt{2gD_h} (D_h/d_s)^{0.185} \qquad (59)$$

where A_o = area of the orifice (sq.ft.)
D_h = hydraulic diameter (ft)
$= \frac{4 \times \text{cross-section}}{\text{perimeter}}$
d_s = spherical diameter of the particle.

It may be noted that the proposed relationship does not take into account either the true density or the frictional characteristics of the material.

Brown and Richards [38] in 1959 measured the flow of spherical glass beads (0.03 to 0.1 cm. in diameter),

rounded yellow sand (-12+36 mesh) and sharp grey sand (-18+120 mesh range), for a number of flat-bottomed cylindrical vessels ranging from 1.45 to 14.6 cm. diameter, through circular orifices from 0.112 to 5.03 cm. diameter, located at the centre of the base.

Based on their experimental results, they have shown that the discharge rate Q could be expressed as follows:

$$Q = 2.24\ D^{2.5} \times \frac{V}{\sqrt{g\ D_h}} \qquad (60)$$

where Q = discharge rate in tons/hour

V = mean linear velocity = $Q/\rho_t x A_o$ (cm/sec)

D and D_h have the same significance as before but are expressed in cms.

The proposed correlations have been summarised in Table 6 which shows that the equation proposed in the present work is in good agreement with the observed values.

Table (6).

SAND (-18 + 22) Mesh B.S.S.

Orifice Diameter D Ft. = 0·03125; Cross Section A_o.S.Ft. $=0.715 \times 10^{-3}$; Particle size da Ft. = 2.541×10^{-3}; True Density lbs/C.Ft. = 165·127; Bulk Density lbs/C. Ft. = 104·5; Cone Angle = 120.

No.	Authors	Equations Proposed.	Coeff. of Friction	Q obs. lbs/sec.	Q cal. lbs/sec.
1.	Deming & Mehring.	$Q = \dfrac{1.66\, D^{2.5}\, \rho_a}{\mu\left[34.6+(67.4+444\sin\frac{\phi}{2})\right]\left[\frac{d_a}{D}+0.130-0.161\mu\right]}$ g/sec.	0.6745	0.615 $\times 10^{-2}$	0.514 $\times 10^{-2}$
2.	Newton, Dunham & Simpson.	$Q = 0.141\, D^{2.96} \times H^{0.04}$ lbs/sec.	-	"	0.775
3.	Rausch.	$Q = 0.294\, C p_a A_o \sqrt{\frac{gD}{2\tan\beta}} \left(\frac{D}{d_a}\right)^{0.3}$	-	"	3.65 $\times 10^{-2}$
4.	Shirai.	$Q = 0.472.p_a.\sqrt{\frac{g\, D^5}{2\,\mu}}$	0.6745	"	0.416 $\times 10^{-2}$
5.	Franklin and Johanson [8]	$Q = \dfrac{1.66 \times 10^{-2}\, p_t\, D^{2.93}}{(6.288\,\mu_i+23.16)(d_a+1.889)}$ lbs/sec.	0·65	"	0.293 $\times 10^{-2}$
6.	Fowler and Glaston-Bury.	$Q = 2.36 p_{at} A_o \sqrt{2gD_h}\ (D_h/d_s)^{0.185}$	-	"	3.98 $\times 10^{-2}$
7.	Present Worker.	$Q = 9.302\times10^{-3} p_t D^{2.5} g^{0.5} (D/\mu\, d_a)$	0.6745	~~0.615~~ 2.75 $\times 10^{-2}$	~~0.642~~ 2.76 $\times 10^{-2}$

3. Description of the Proposed Feed Hopper.

The feed hopper consists of a vertical glass cylinder A, one foot high and 0.51 ft. in internal diameter, as shown in Figure 21. The lower end of the cylinder is connected to an inverted brass cone (B) by a flanged joint, the cone-angle being 60 degrees.

The brass cone is fitted with a one inch diameter outlet pipe, accommodating a butterfly valve (D), which controls the feed rate to the rotary cylinder.

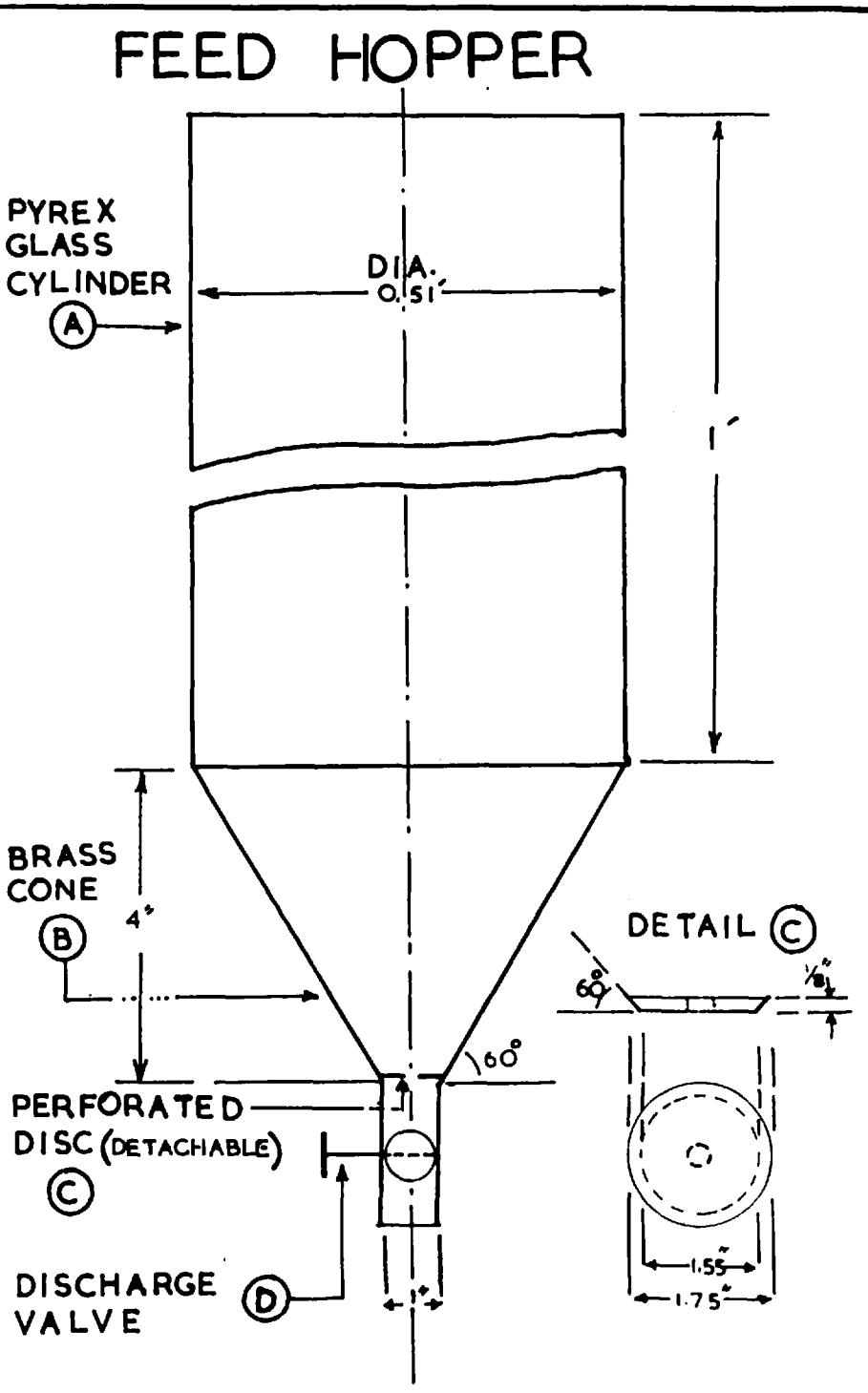
In order to study the flow through apertures, circular brass discs with different sized perforations, namely 0.25, 0.375 and 0.5 inches, were inserted in the apex of the cone, as shown in the diagram.

Testing the Output of the Feed Hopper.

The output of the feed hopper can be tested either by installing the perforated discs of the known aperture size or simply using the butterfly valve (V). The first approach is preferable since the aperture is well defined and of symmetrical form.

The output for a given aperture may be measured quite simply. The perforated disc is plugged (plug not shown in the diagram). The feed hopper is then filled

FIG.21


FEED HOPPER
PYREX GLASS CYLINDER
A
DIA. 0.51"
1'
BRASS CONE
B
4"
60°
PERFORATED DISC (DETACHABLE)
C
DISCHARGE VALVE
D
1"
DETAIL C
60°
1/8"
1.55"
1.75"

Testing the Output of the Feed Hopper.

The output of the feed hopper can be tested either by installing the perforated discs of known aperture size or simply using the butterfly valve V. The first approach is preferable since the aperture is well-defined and of symmetrical form.

The output for a given aperture may be measured quite simply. The perforated disc is plugged (plug not shown in the diagram). The feed hopper is then filled with the material under test and its surface levelled. The plug is removed and the time of discharge of 500 cc. of the material together with the change in the material head are noted. This step is repeated about ten times, till the level of the material in the hopper falls to the base of the cone.

4. Experimental Results.

(1) Effect of the Head of Feed-Material.

In order to study the effect of the head on the discharge rate, four materials, namely, rape seed, coal, sand and haematite, the properties of which are given in Table 11, of particle size distribution (-18+22) mesh B.S.S., were used. The results for 0.25, 0.375 and 0.5 inches

FIG. 22 (a)

DISCHARGE RATE VS. HEAD

ORIFICE DIA. 0.25 IN.

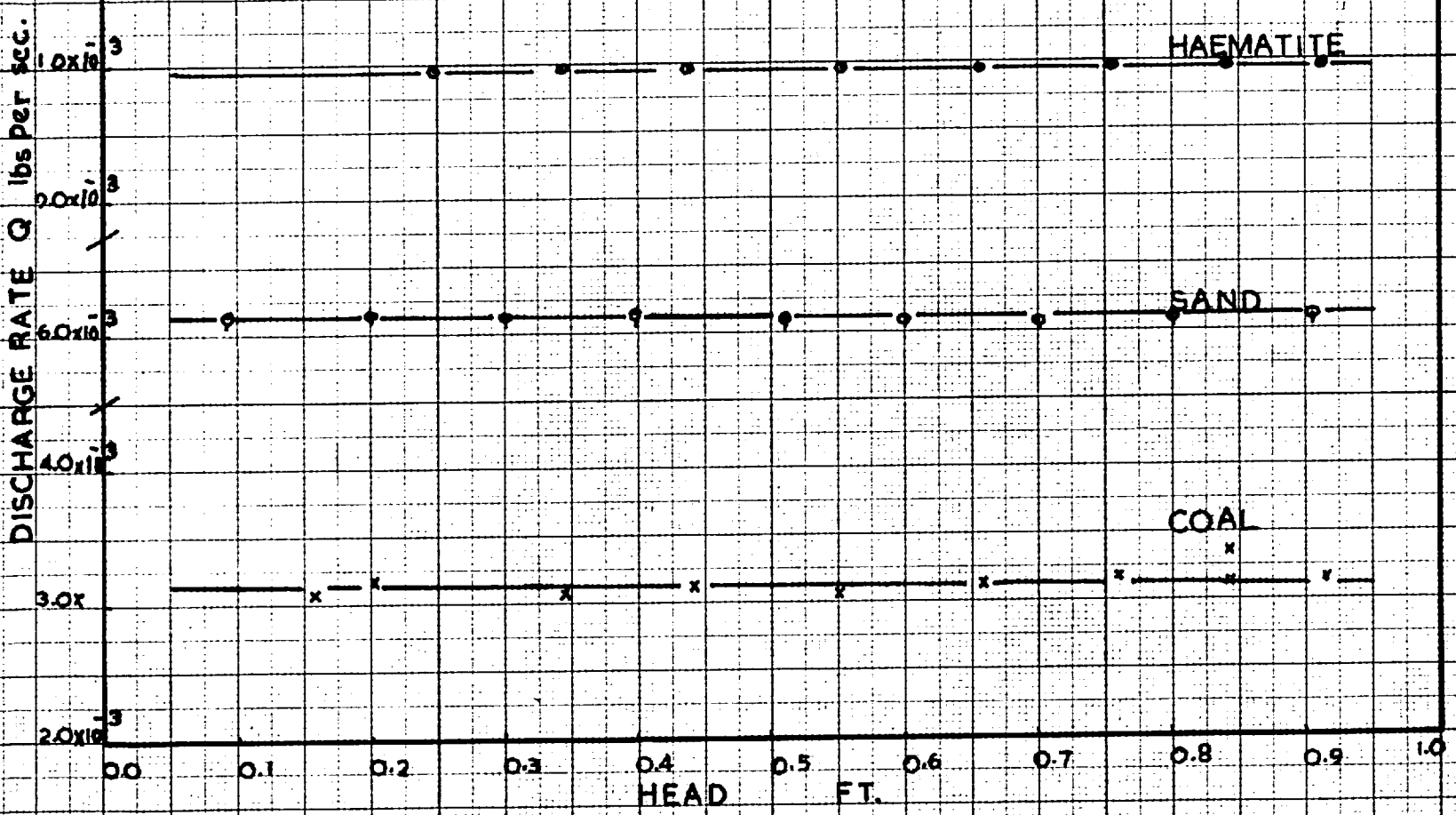


FIG. 22 (b)

DISCHARGE RATE VS. HEAD

ORIFICE DIA. 0.375 IN.

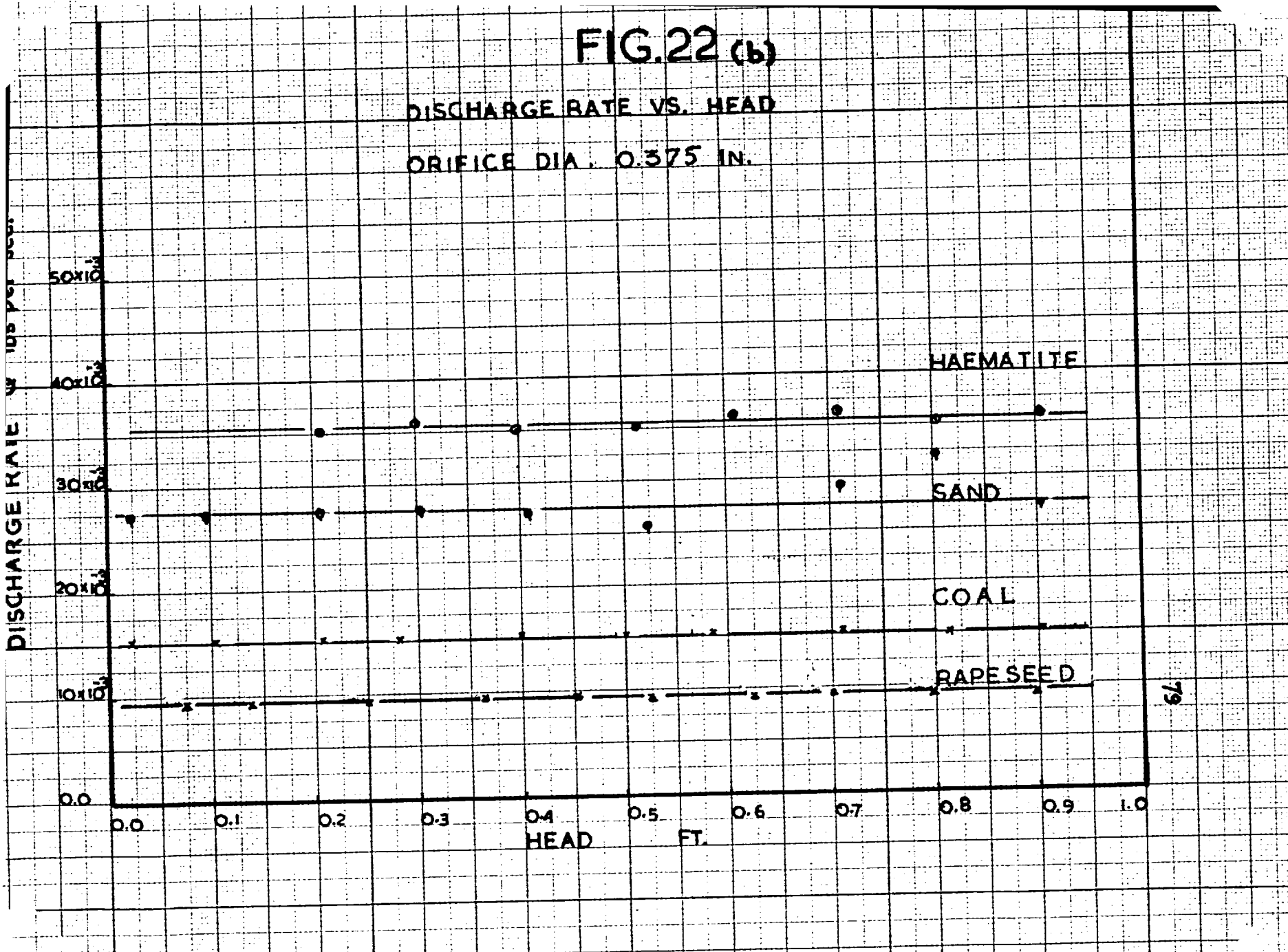
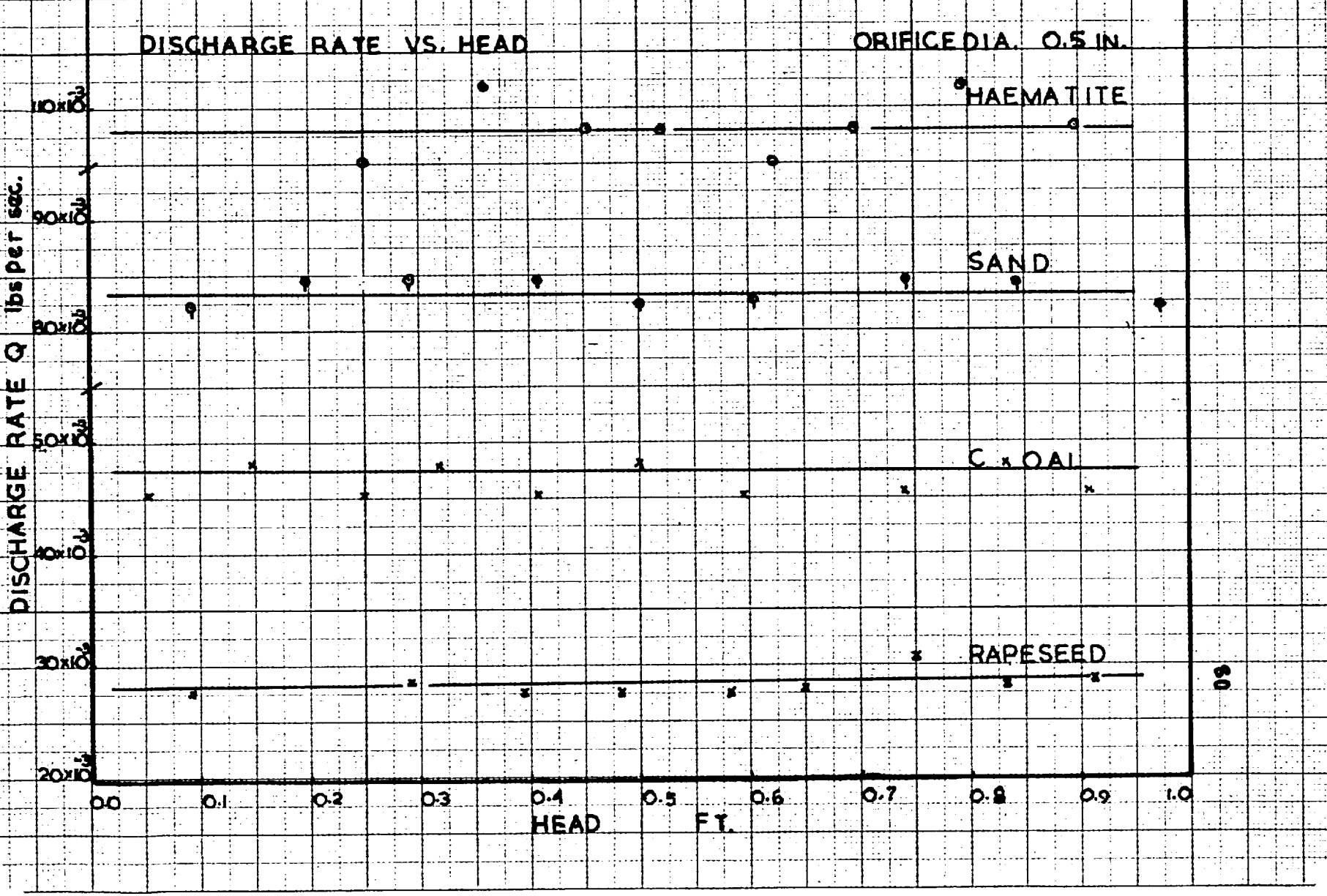


FIG. 22 (C)


DISCHARGE RATE VS. HEAD
ORIFICE DIA. 0.5 IN.
HAEMATITE
SAND
C x OAL
RAPESEED
DISCHARGE RATE Q lbs per sec.
10x10⁻³
90x10⁻⁴
80x10⁻⁴
50x10⁻⁴
40x10⁻⁴
30x10⁻⁴
20x10⁻⁴
0.0
0.1
0.2
0.3
0.4
0.5
0.6
0.7
0.8
0.9
1.0
HEAD FT.

diameter orifices are summarised in Tables 11, 12 and 13 (see Appendix) and are shown graphically in Figure 22 (a), (b) and (c). The data shows that the discharge rate Q is, in all cases, independent of the head H but very nearly directly proportional to the density.

2. Effect of Particle Size.

The discharge rates of sand having a size range (-18+22), (-18+44) and (-100+120) mesh B.S.S., were measured for three orifices and the results are tabulated below:

Table 7.

Effect of Particle Size on Discharge Rate.

No.	Particle Size. d_a ft.	$1/d_a$	Discharge Rate Q lb./sec. for Orifice Diameters 0.25 in.	0.375 in.	0.5 in.
1	2.541×10^{-3}	0.394×10^{3}	0.615×10^{-2}	2.75×10^{-2}	8.35×10^{-2}
2	1.981×10^{-3}	0.505×10^{3}	1.75×10^{-2}	4.0×10^{-2}	11.5×10^{-2}
3	0.454×10^{-3}	2.2×10^{3}	1.93×10^{-2}	5.73×10^{-2}	12.4×10^{-2}

On the basis of the above table, when the discharge rate, Q, is plotted against the reciprocal of the particle size, $1/d_a$, a set of converging straight lines, over a particle size range -18 to +44 mesh is obtained (see Figure 23). Beyond +44 mesh, the linear relationship between the discharge rate and $1/d_a$ ceases to hold and

at the same time it will be noted that the rise in the discharge rate when the particle size diminishes from -44 to +120 mesh, is insignificant. This might be due to an early stage of bridging or arch-formation, which results in an 'hindered-flow' of the material. The effect, namely the bridging or arch-formation over the discharge orifice, becomes more pronounced when the particle size is reduced further. Thus, when the sand of +200 mesh was used, no flow could be obtained, which apparently is due to complete bridging or arching over the discharge end.

In the present work, which is limited to a particle size distribution of (-18+22) mesh B.S.S., no great error will be introduced by assuming the discharge rate to be inversely proportional to the particle size d_a:

$$Q \propto 1/d_a \qquad (61)$$

3. Effect of Orifice Diameter.

In Figure 24, the discharge rate is plotted against the orifice diameter for different materials, based on Table 8. A log-log plot indicated that the discharge rate can be expressed, in terms of the orifice diameter, by the equation

$$Q = k\,(D)^{3.5} \qquad (62)$$

where k = a constant depending on the material under examination,

Q and D have the usual significance.

FIG. 23

EFFECT OF PARTICLE SIZE (d_a) ON DISCHARGE RATE (Q).

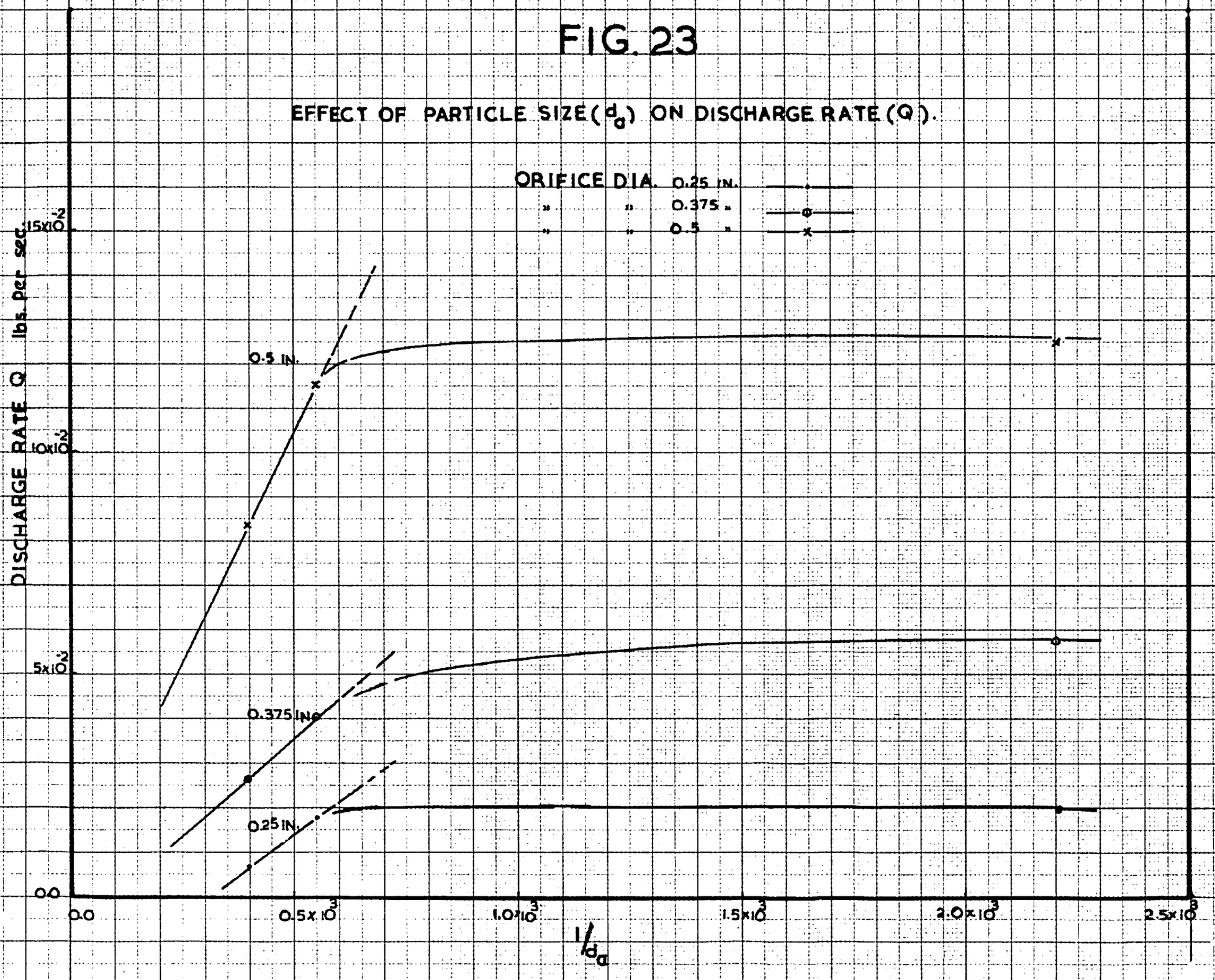


FIG 24

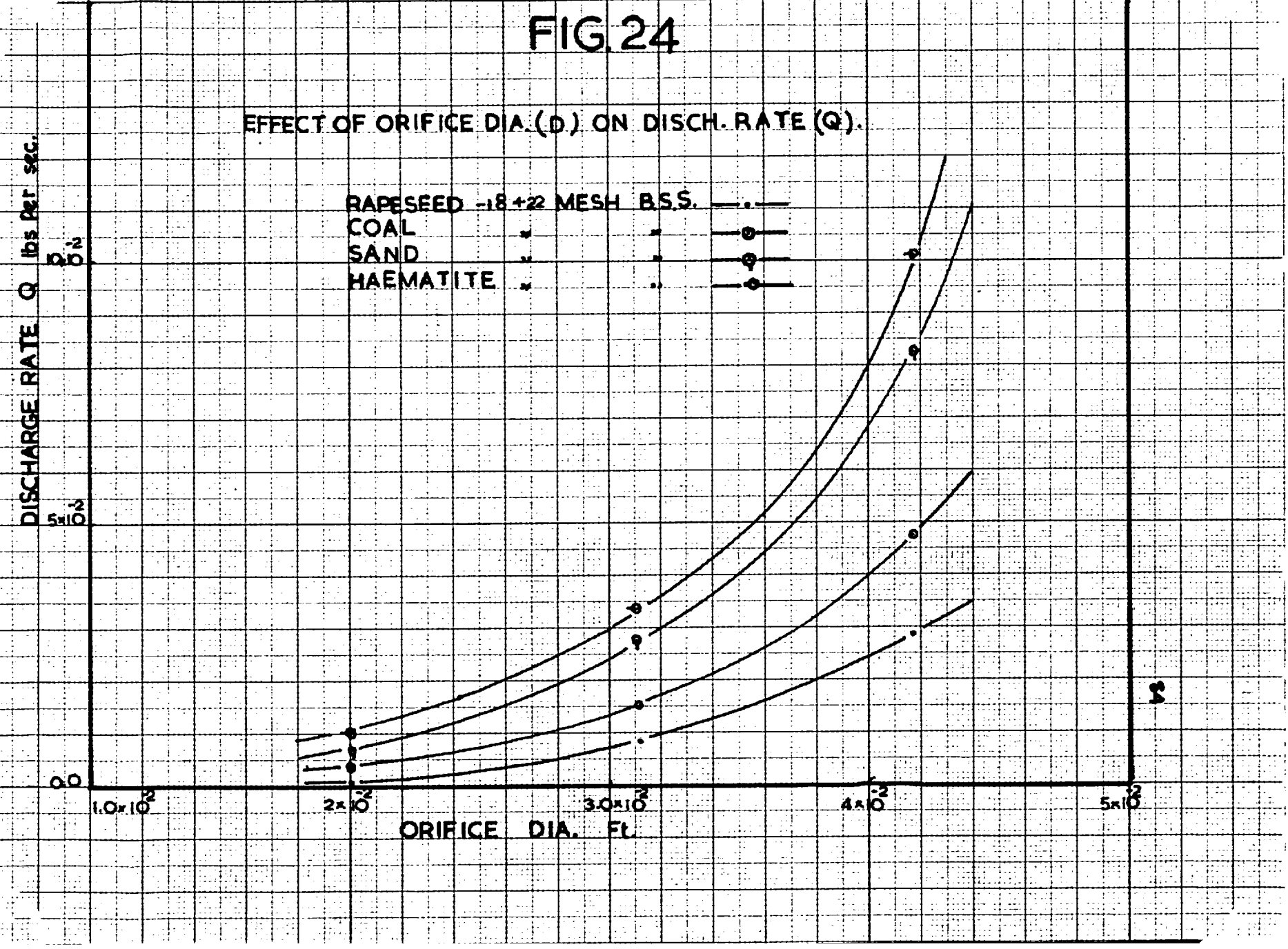

EFFECT OF ORIFICE DIA. (D) ON DISCH. RATE (Q).
RAPESEED -18+22 MESH B.S.S.
COAL
SAND
HAEMATITE
DISCHARGE RATE Q lbs per sec.
10.0
5x10⁻²
0.0
1.0x10⁻²
2x10⁻²
3.0x10⁻²
4x10⁻²
5x10⁻²
ORIFICE DIA. Ft.

Table 8.

Effect of Orifice Diameter on Discharge Rate.

No.	Material	Particle Size. d_a Ft.		Orifice Diameter D Ft.	Discharge Rate Q lb./sec.
			1.	0.02083	-
1	Rape seed	2.8×10^{-3}	2.	0.03125	0.885×10^{-2}
			3.	0.04166	2.85×10^{-2}
2	Coal	2.541×10^{-3}	1.		0.31×10^{-2}
			2.	-do.-	1.5×10^{-2}
			3.		4.75×10^{-2}
3.	Sand	2.541×10^{-3}	1.		0.615×10^{-2}
			2.	-do.-	2.75×10^{-2}
			3.		8.35×10^{-2}
4.	Haematite	2.541×10^{-3}	1.		0.997×10^{-2}
			2.	-do.-	3.59×10^{-2}
			3.		10.8×10^{-2}

4. Effect of Density.

The qualitative effects of density can be seen from an inspection of Figure 24, in which the curves for four materials are in order of their densities. Taking the density of rapeseed as datum and assuming the discharge rate to be proportional to the density, the set of curves shown in Figure 25 is obtained. Though the elimination of density has brought the curves close together, it is clear

that some other factors probably the coefficient of friction and/or the particle shape is influencing the discharge rate. That a linear relationship exists between the discharge rate and the density is shown by the lines in Figure 26. Confirmation of this relationship may also be obtained indirectly from equation (62), where the value of k is found to vary with the density of the relevant material, in accordance with the equation:

$$k = K (\rho_t)^{1.09} \qquad (63)$$

Equation (62) may therefore be rewritten:

$$Q = K (\rho_t)^{1.09} (D)^{3.5} \qquad (64)$$

where K = a constant equal to 0.195×10^2

5. Friction Effects on the Discharge Rate.

It is obvious that the discharge rate will depend to some extent on the interparticulate friction of the material and some evidence of this relationship is given by this work. Thus, when the discharge rate Q is plotted against $1/\mu$, where μ is the coefficient of friction based on the surface dynamic angle of repose (see Table 9), a set of converging straight lines (Figure 27) is obtained.

FIG. 25

EFFECT OF ELIMINATION OF DENSITY FROM DISCH. RATE VS. ORIFICE DIA.

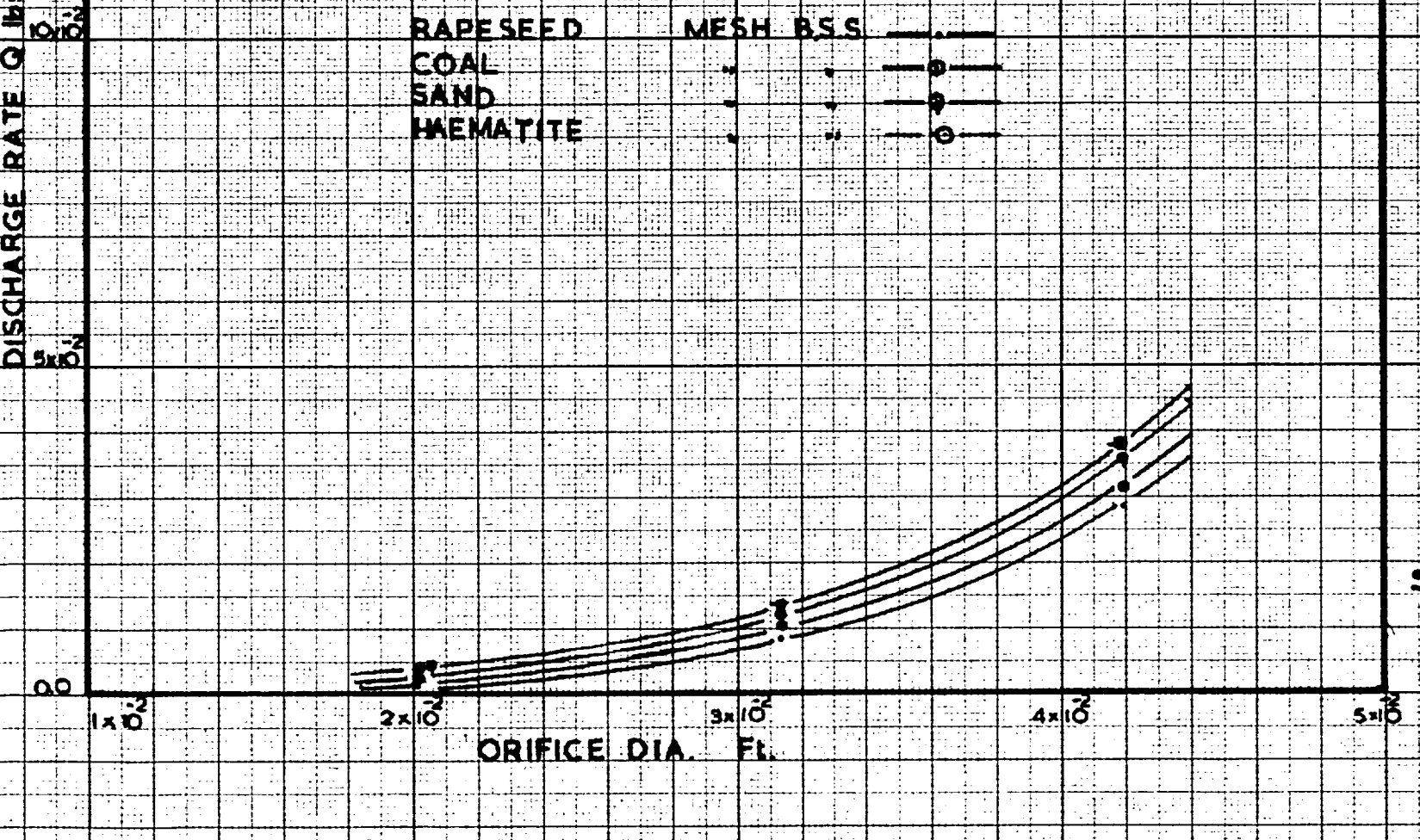


FIG. 26

EFFECT OF TRUE-DENSITY(ρ_t) ON DISCHARGE RATE(Q)

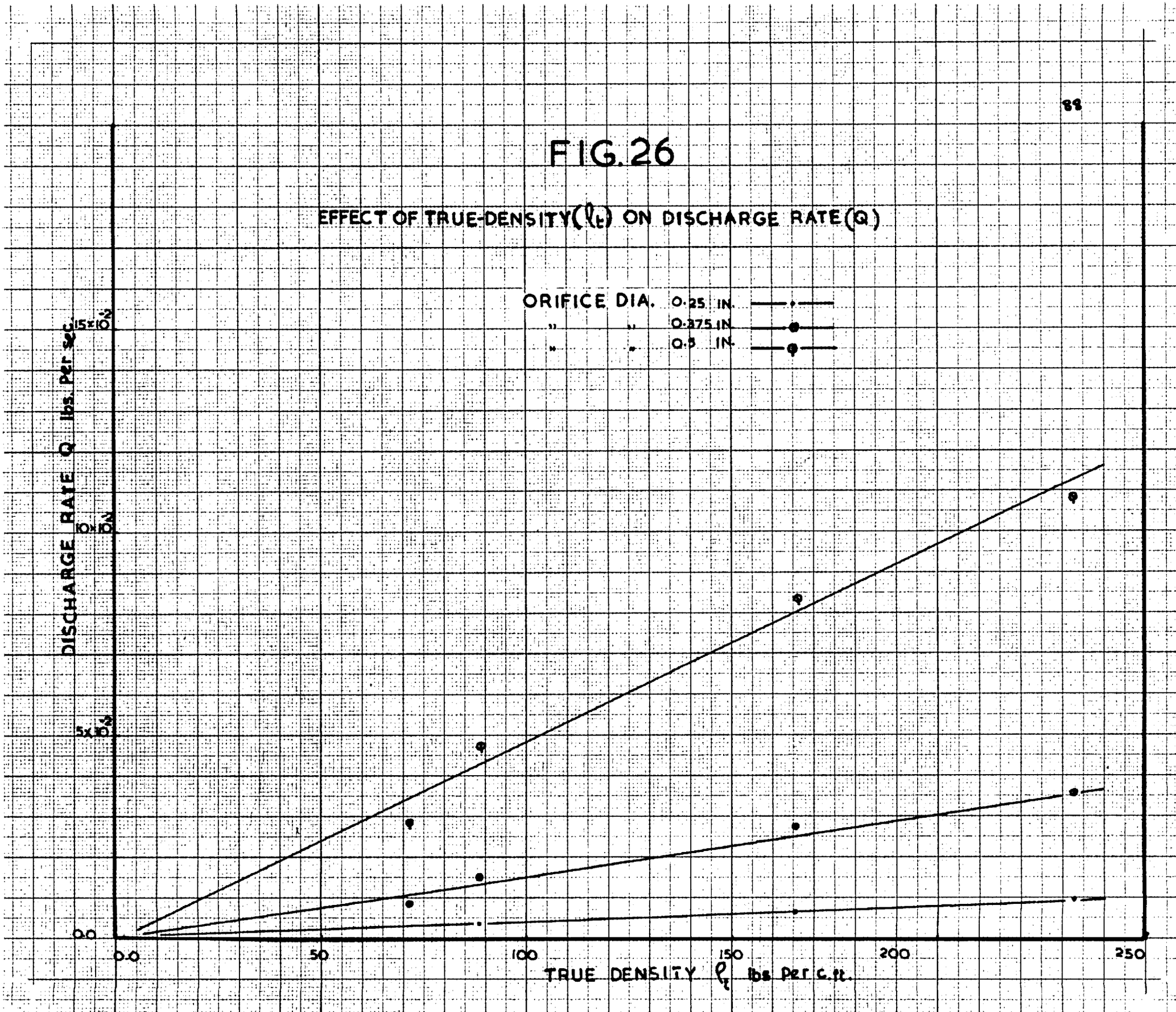


FIG. 27

EFFECT OF CO-EFFICIENT OF FRICTION ON DISCHARGE RATE

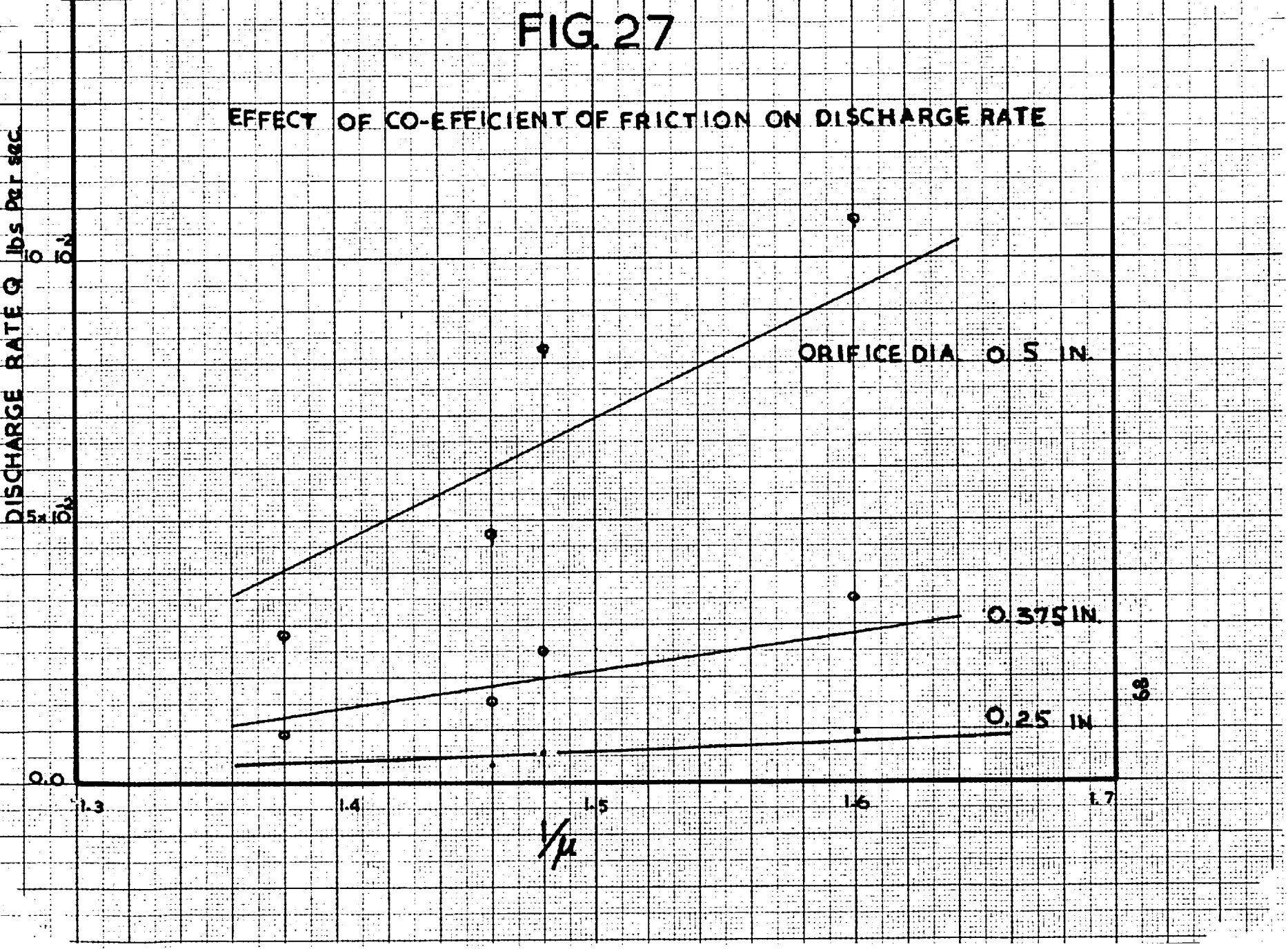


Table 9.

Variation of Discharge Rate Q with Coefficient of Friction, μ.

No.	Material		Discharge Rate Q lb/sec.	Coeff. of Friction μ (Dyn.)	$1/\mu$
		1.	-		
1	Rape seed	2.	0.885×10^{-2}	0.7265	1.38
		3.	2.85×10^{-2}		
2	Coal	1.	0.31×10^{-2}		
		2.	1.5×10^{-2}	0.6873	1.46
		3.	4.75×10^{-2}		
3	Sand	1.	0.615×10^{-2}		
		2.	2.75×10^{-2}	0.6745	1.48
		3.	8.35×10^{-2}		
4	Haematite	1.	0.997×10^{-2}		
		2.	3.59×10^{-2}	0.6248	1.6
		3.	10.8×10^{-2}		

5. Dimensional Analysis and Correlation.

It has been shown experimentally that the discharge rate Q depends on density, the orifice diameter, and the gravity g.[×] These quantities may be expressed in dimensional form as in the following table:

× the particle size and the coefficient of friction.

Table 10.

Dimensions of Different Variables involved.

No.	Name of quantity	Symbol	Dimensional Formula
1.	Discharge Rate	Q	MT^{-1}
2.	Density	ρ_t	ML^{-3}
3.	Orifice Diameter	D	L
4.	Particle Diameter	d_a	L
5.	Forces of Gravity	g	LT^{-2}

It will be seen that we have five variables and three fundamental kinds of units. There are, therefore, two dimensionless products, one of which is (D/d_a). Out of the remaining quantities we are particularly interested in Q, which can be combined with only three other quantities in order to get a dimensionless product. We will select ρ_t, D, g, to get :

$$Q = f\left[(\rho_t)^a \times (D)^b \times (g)^c \right]$$

i.e. $$M \times T^{-1} = f\left[M^a \times L^{b+c-3a} \times T^{-2c}\right]$$

Equating indices

$$a = 1$$
$$b + c - 3a = 0$$
$$2c = 1$$

whence $a = 1$, $b = 2.5$ and $c = 0.5$.

Hence thesecond dimensionless product will be $Q/\rho_t \times D^{2.5} \times g^{0.5}$, giving a final solution as

$$\frac{Q}{\rho_t \; D^{2.5} \; g^{0.5}} = k \; (D/d_a) \qquad (65)$$

It has been shown as well that the discharge rate Q is inversely proportional to the coefficient of friction μ. It is possible at this stage to introduce μ in the above equation (65), to give an expression of the type :

$$\frac{Q}{\rho_t \; D^{2.5} \; g^{0.5}} = K \; \frac{D}{\mu \; d_a} \qquad (66)$$

The value of K can be determined by plotting $\frac{Q}{\rho_t \; D^{2.5} \; g^{0.5}}$ against $(D/\mu d_a)$ as shown in Figure 28. Its value when substituted in equation (66) gives a final relationship as given below:

$$Q = 9.302 \times 10^{-3} \; \rho_t \; D^{2.5} \; g^{0.5} \; (D/\mu \; d_a) \qquad (67)$$

where Q, ρ_t, g, D, μ and d_a have the same significance as described earlier.

The overall deviation of the above equation 67 is $\pm$ 2.5% as shown in Table 11.

TABLE (11)

No.	Material	Particle Size da Ft.	Density lbs/C.Ft ρ_t.	Coeff. of friction (Dyn) μ	Orifice Diameter D, Ft.	Orifice Cross-Section Ao Sq.Ft	Discharge Rate Q lbs/sec.	$\frac{Q}{\rho_t\sqrt{D^5 g}}$	$D^{2.5}$	(D/da)	$(\frac{D}{da\,\mu})$	$Q_{Cal.}$ lbs/sec.
					0.02083	0.341×10^{-3}	-	-	0.688×10^{-4}	7.44	10.34	-
1.	Rapeseed	2.8×10^{-3}	71.170	0.7265	0.03125	0.715×10^{-3}	0.885×10^{-2}	0.127	1.736×10^{-4}	11.15	15.35	0.995×10^{-2}
					0.04166	1.36×10^{-3}	2.85×10^{-2}	0.199	3.542×10^{-4}	14.90	20.6	2.75×10^{-2}
					0.02083		0.31×10^{-2}	0.0984		7.88	11.5	0.337×10^{-2}
2.	Coal	2.54×10^{-3}	88.651	0.6873	0.03125	— do —	1.50×10^{-2}	0.173	— do —	12.32	17.9	1.45×10^{-2}
					0.04166		4.75×10^{-2}	0.266		16.40	23.9	4.48×10^{-2}
					0.02083		0.615×10^{-2}	0.105		7.88	11.7	0.642×10^{-2}
3.	Sand	2541×10^{-3}	165.127	0.6745	0.03125	— do —	2.75×10^{-2}	0.170	— do —	12.32	18.3	2.76×10^{-2}
					0.04166		8.35×10^{-2}	0.251		16.40	24.4	7.55×10^{-2}
					0.02083		0.997×10^{-2}	0.115		7.88	12.6	1.01×10^{-2}
4.	Haematite	2.54×10^{-3}	242.528	0.6248	0.03125	—do —	3.59×10^{-2}	0.151	— do —	12.32	19.8	4.38×10^{-2}
					0.04166		10.8×10^{-2}	0.221		16.40	26.3	11.95×10^{-2}

% Overall Deviation $\pm$ 2.5%

FIG. 28

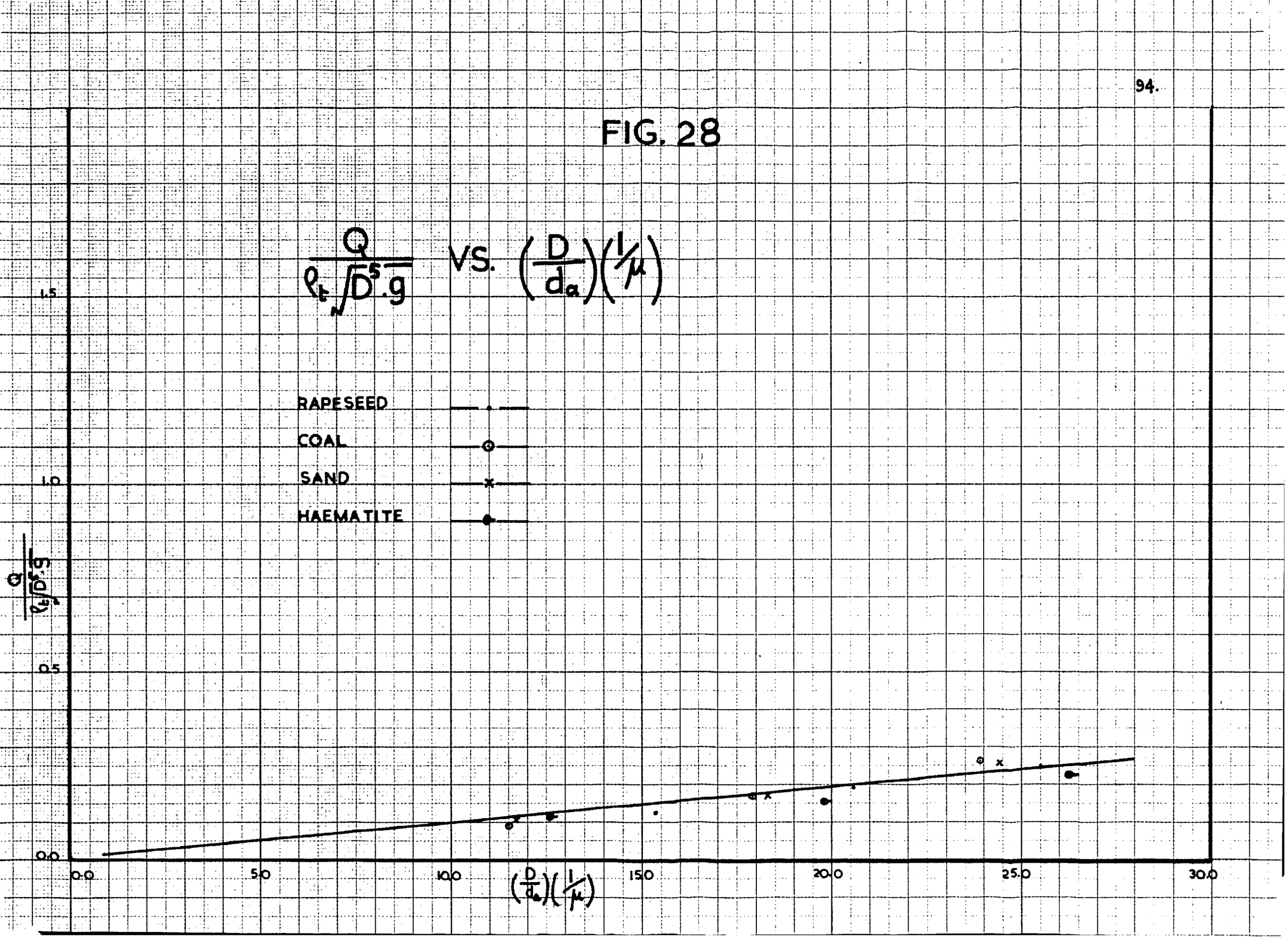
$$\frac{Q}{\rho_t \sqrt{D^5 . g}} \text{ vs. } \left(\frac{D}{d_a}\right)\left(\frac{1}{\mu}\right)$$

RAPESEED —·—

COAL —⊙—

SAND —×—

HAEMATITE —●—



SECTION 3.

CHAPTER 5.

1. Introduction.

The motion of granules in a cylinder rotating on a horizontal axis, has been described in the first part of the thesis. When the cylinder is inclined, the situation is altered; in the normal case the granules after rising in circular paths concentric with the cylinder, slide down the free inclined surface of the charge at an angle approximately equal to the angle of the inclination of the cylinder. The cylinder is in fact acting as a conveyor, the rate of conveying being related to its speed of rotation and its angle of inclination.

The time of passage of a granular material or its residence time in the cylinder depends on a number of variables, the more important of which are the cylinder length and diameter, the number of revolution per minute, the slope of the cylinder and finally the dyn. angle of repose of the material. The effect of these variables on the average time of passage has been studied by a number of workers and several correlations have been proposed. But as will appear from the

literature survey, there is still a serious lack of data relating to the behaviour of different materials.

In this work, the effect of the more important variable on the time of residence, has been studied for a number of materials including granular - starch, coal, felspar, sand and haematite of specific gravity ranging from 1·14 to 3·888 g/cc and for a particle size range (- 18 + 22) mesh B.S.S. (The physical properties are given in Table (14) in Appendix).

An attempt has been made to analyse the problem and derive a relationship between the time of passage, the dimensions of the cylinder and the properties of the feed-material.

2. Literature Survey.

One of the earliest studies of the operation of a rotary-kiln is that of Sullivan, Maier and Ralston (20) in 1927. They employed kilns 7 feet long and of four different diameters namely 3, 6, 11½ and 19¾ inches. The interior of the shell was made rough by coating it with material under examination. Though their measurements of the angle of repose covered about eleven materials with a value of the angle varying from 24·4 degrees for lead-shots to 55·6 degrees for saw-dust,

the kiln performance data given by these authors appears to be limited to two materials namely sand and quartz. The empirical equation proposed by these authors is:

$$t = \frac{1.77\ L\sqrt{\beta}}{D\ N\ S} \qquad (68)$$

where t = Time of passage minutes.

L = Length of cylinder ft.

D = Diameter " " ft.

S = Slope of " " Degrees.

β = Dyn. angle of repose.

N = Revolutions per minute.

The use of angular measure rather than a trignometric function in the above equation is said to give "more exact figures".

Ginstling, Zilberman and Gvazdev (39) in 1939, while studying the movement of reactants employed in the manufacture of Sod. sulphate ($2\ NaCl + H_2SO_4 \longrightarrow Na_2SO_4 + 2HCl$), in a 26 feet long by 2 feet diameter rotary kiln, inclined at an angle of 4.7 degrees, showed that the time of passage could be expressed by:

$$t = k \frac{L}{377{\cdot}5\ DN \tan S} \quad \text{Hrs.} \qquad (69)$$

where k = A constant depending on the physical properties of the material and the volume of the hold-up. For Nacl, it was found to be 2·95.

D, N and S, have the same significance as already defined.

Smith (40) in 1942 proposed an equation for co-current and counter-current dryers fitted with 18 flights:

$$t = \frac{6\ k\ L}{D\ N\ S} \qquad (70)$$

where k = A constant which changes from 0·2 to 0·5 for counter flow and 0·2 to 0.7 for parallel flow, according to the combination of the material characteristics and air velocity in the dryers,

and D, N, S are as already defined.

According to the author, the value of k originated as a factor of ignorance and remained a factor of experience. The values of k for both the co-current and counter - current air-flow, when the number of flights is 18,

vary as indicated above.

Prutton, Miller and Schuette (41) in 1942, employed a number of materials including saw-dust, sand and Fuller's earth, in a stainless steel cylinder 4 feet long and 8 inches in diameter, fitted with flights and a driving mechanism to give a speed variation of 2·1 to 6·32 R.P.M; they showed that:

$$t = \frac{k \times L}{D\ N\ S} \pm m\ V \qquad (71)$$

where k = A constant depending on the number of flights and their design. For 6 flights k = 3·3 and for 12 flights k = 4·5.

m = A constant which depends on two factors namely the material characteristics and the method of operation i.e. for co-current flow m varies from 0·015 to 0·045 and for counter-current flow, its value changes from 0·02 to 0·08.

The other symbols have the same significance as given before.

Bayard (42) in 1945 pointed out that the time of passage through a rotary-cylinder, could be

calculated from the cyclic-motion of the granules, if the number of such cycles over the cylinder length is known. His experimental observations were confined to a 4 feet diameter by 30 feet long kiln, inclined at a slope of ½ inch per foot length and rotating at 2 R.P.M. Based on these experiments, he showed that:

$$t = \frac{0.037\ (\beta + 24)\ L}{D\ N\ S_1} \qquad (72)$$

where S_1 = Slope of the cylinder in inches per foot of the cylinder length.

and t, β, L, D and N are as already defined.

For a better understanding of heat-transfer within a rotary-dryer, Friedmann and Marshall (43) in 1949 laid more emphasis on the study of the factors which directly influence the hold-up and dusting in a rotary-dryer. They used a 1 foot diameter by 6 feet long stainless steel cylinder, fitted with 8, one-inch by 5.5 feet evenly spaced flights.

When the feed-rate F was plotted against the rate of rotation N, for a given hold-up, they found that F varied with N, raised to a power varying from 0.78 to 0.98. The general form of their equation is:

$$x = \frac{0.294\ F}{D\ N^{0.9} S_1} \qquad (73)$$

where x = Hold-up as a percent of the dryer volume.

F = Feed-rate C.Ft./(hr)(sq.ft.) (Dryer's cross-section).

and S_1 = Slope of the cylinder expressed in feet per foot cylinder length.

Since $t = \frac{L\ x}{100\ F}$, the equation (73) may be rewritten:

$$t = \frac{0.176\ L}{D\ N^{0.9} S_1} \qquad (74)$$

Pickering, Feakes and Fitzgerald (44) in 1951 developed a theoretical equation based on the cyclic movement of the granules in a rotary cylinder and showed that:

$$t = \frac{\pi}{180} \times \frac{\theta/2}{\sin \theta} \left[\frac{L \sin \beta}{\pi D N \sin S} \right] \qquad (75)$$

where θ = The angle subtended by the bed at the centre of the circle of reference.

Other symbols are as defined before.

When θ approaches 90 degrees, as a close approximation,

the kiln formula may be reduced to:

$$t = \frac{L \text{ Sin } \beta}{\pi D N \text{ Sin } S} \qquad (76)$$

In order to determined experimentally the effect of R.P.M. (1 to 4) on the residence time, the authors employed a small rotary kiln 11 feet in effective length and 16¾ inches in diameter, the inside being lined with fire-bricks. Their results showed that the time of passage t, is inversely proportional to the rate of rotation N.

Saeman (45, 48) has given a theoretical equation for the time of passage of a material through a rotary cylinder. For non-uniform hold-ups i.e. when the slope of the bed is greater than the slope of the cylinder, he finds:

$$t = \frac{L \text{ Sin } \beta}{\pi D N (S_2 + \psi \text{Cos } \beta)} \qquad (77)$$

where ψ = The difference between the slope of the bed and the cylinder, i.e.

$$\phi - S_2 = \psi \text{ Radins.}$$

Other symbols are as defined before.

For uniform hold-up, where the slope of the bed virtually equals the slope of the cylinder, equation (77) has been

simplified to:

$$t = \frac{L \sin \beta}{\pi D N S_2} \qquad (78)$$

Table (12)

Comparison of Proposed Correlations

Sand (- 18 + 22) Mesh B.S.S.

L = 2·1 feet, D = 0·3386 ft., S = 4 deg.

R.P.M. = 10, $\beta = 34^{\circ}$.

	No.	Name of Authors.	Proposed Correlations.	Time of passage (Observed)	Time of passage (Calculated)
EMP.	1.	Sullivan, Maier & Ralston.	$t = \frac{1.77L\sqrt{\beta}}{D N S}$	1·45	1·65
	2.	Ginstling and Zilberman.	$t = \frac{0.525L}{DN \tan S}$	"	1·47
	3.	Bayard.	$t = \frac{0.037 (\beta + 24)L}{D N S_1}$	"	1·64
	4.	Friedman and Marshall.	$t = \frac{0.177 L}{D N^{0.9} S_1}$	"	2·03
	5.	Present Worker.	$t = \frac{1.181(\sin \beta - 0.434)L^{1.5}}{D N \sin (S + 2)}$	"	1·27

Table (12) - Contd.

THEO.	6. Pickering, Feakes and Fitz-gerald.	$t = \frac{L \sin \beta}{\pi D n \sin S}$	1·45	1·62
	7. Saeman.	$t = \frac{L \sin \beta}{\pi D N' S_2}$	"	1·58
	8. Present Worker.	$t = \frac{L \sin \beta}{\pi D N \sin (S + 2)} \times \frac{\sqrt{Dh_1 - h_1^2}}{\sqrt{Dh_1 - h_1^2} - \sqrt{Dh_2 - h_2^2}} \times (1 - r^{N'})$ $= \frac{0{\cdot}326\ L \sin \beta}{D N \sin (S + 2)}$ when $h_1 = 0{\cdot}144'$ $h_2 = 0{\cdot}04'$	"	1·21

3. Comparative Study of the Proposed and Existing Correlations.

In Table (12) the various empirical and theoretical equations referred to above as well as those resulting from the present work, are tabulated for comparison. The empirical equations given in the table may be expressed in the form:

$$t = k. \frac{L^x}{D\, N^y} . \frac{f(\beta)}{f(S)} \qquad (79)$$

where exponent 'x' varies from 1 to 1·5 and exponent 'y' varies from 0·9 to 1.

Similarly all the theoretical equations may be written in the form:

$$t = k. \frac{L}{D\, N} . \frac{f(\beta)}{f(S)} \qquad (80)$$

It will be seen that the time of passage in equation 1 to 4 is directly proportional to the length L of the cylinder, whereas in equation (5) (Table 12), the time varies with length, raised to power 1·5. Sullivan and Co-workers (20) do not appear to have made an experimental study of the effect of cylinder length and have argued that the effect of length of the kiln is self evident. "The rate of advance per foot is what

is being measured, so that the time of passage is directly proportional to the length". The authors have not mentioned whether $t \propto L$ under all conditions of movement of the granules? In Chapter (VI), it has been experimentally shown that $t \propto L$ only when the hold-up is moving under 'sliding-motion of granules' and if the hold-up is moving under cascading action, the relationship $t \propto L^{1.5}$ will hold. The reasons of this variation are discussed.

In equations 1, 2, 3 and 5 (Table 12) the time of passage is inversely proportional to both the diameter and the speed of rotation; In equation 4 the time is inversely proportional to the diameter and to the power of the speed varying from 0·78 to 0·98.

There is general agreement in all the correlations as to the effect of the cylinder slope.

Table (12) shows that in the empirical relationships, the dyn. angle of repose β, appears in different forms. Sullivan and co-workers (20) show that the time of passage t is proportional to the square root of the dyn. angle of repose β. Since Ginstling used only one material, his equation does not embody the dyn. angle of repose, which in fact is incorporated in the equations constant.

Bayard's equation shows that t is directly proportional to the angle β and he appears to have derived the expression $0 \cdot 037 \ (\beta + 24)$ by plotting the constant k for different materials against the respective angle of repose, which must have yielded a linear relationship.

The absence of a term interpreting the angle in equation 4 (Table 12), may be due to the presence of flights in the cylinder.

It is interesting to note that the ratio L/D, where L is the length and D is the diameter of the cylinder, varies from 4·2 to 28 as shown in the following table.

Table 13.

The ratio No.	Cylinder Length L/Cylinder Diameter D. Name of Worker.	L/D.
1.	Sullivan, etc. etc.	4·2 to 28.
2.	Guistling.	13
3.	Prutton, etc. etc.	6
4.	Bayard.	7·5
5.	Friedman and Marshall.	5·5
6.	Present Worker.	6·0

An examination of the theoretical equations 6,

7 and 8 (see Table 12), shows that the product $(\frac{\text{Sin } \beta}{D\ N})$ appears in all the correlations. In addition, Pickering's equation indicates that $t \propto \frac{1}{\text{Sin } S}$, Saeman's correlation suggests $t \propto \frac{1}{S_2}$ while the present correlation indicates that $t \propto \frac{1}{\text{Sin } \varphi}$, $\left[\propto \frac{1}{\text{Sin } (S + 2)} \right]$. Though the relationship $t \propto \frac{1}{\text{Sin } (S + 2)}$, has been verified experimentally in the present work for a number of materials (see Figs. 31, 32), Pickering and Saeman appear to have depended on the results of Sullivan and co-workers to test the proposed equations.

In equation (8), L' represents the length of the inclined bed, which may be expressed as L Sec ψ, where L is the cylinder length and the angle ψ is the difference between the slope of the bed ϕ and that of the cylinder S. The same equation also accounts for the variation of bed-depth down the cylinder and for the number of the cycles N', completed by a granule before reaching the end of the cylinder. For a constant hold-up (25% of the cylinder volume (approx.)), the proposed relationship may be reduced to:

$$t = \frac{0.326\ L'\ \text{Sin}\ \beta}{D\ N\ \text{Sin}\ (S + 2)} \qquad (81)$$

An overall examination of both the empirical and theoretical sets of equations will reveal that the number of variables which determine the time of passage, with the exception of the present theoretical correlation, is almost the same. In two of the empirical equations, namely those proposed by Ginstling and Friedman, the term β is missing, due to either the presence of flights in the cylinder or to the fact that only one material was used in correlating the variables.

CHAPTER 6.

1. Description of Apparatus.

The general set-up of the apparatus used in the present work to examine the effects of variables, on the average time of passage of granular material through a rotary-cylinder is shown in Plate 3 (a) and (b).

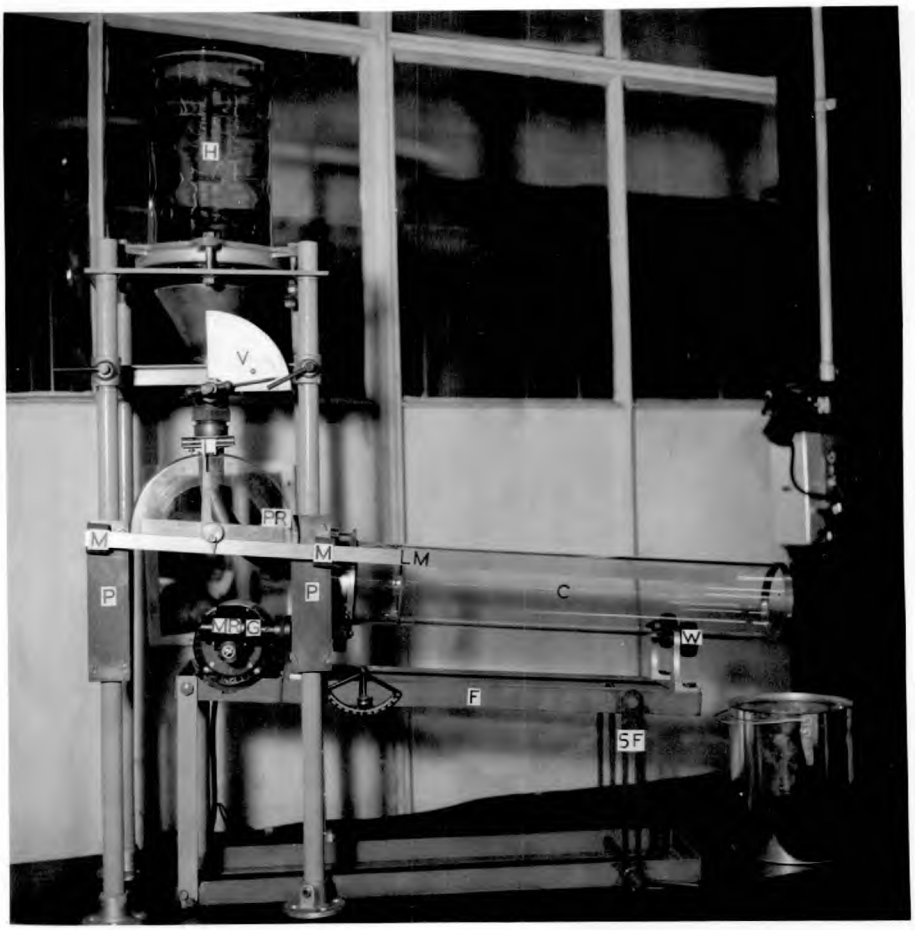
A glass cylinder C, 2.1 feet long and 0.339 feet in diameter, is supported by four 1.5 inches diameter rubber rollers W fitted onto the frame F. One of the rollers is driven by a motor Mr, through a gear-box G for obtaining variations of speed. Both the cylinder and motor are mounted on the same base, the slope of which can be altered by the help of a slotted guide-bar SF, fitted with lock nut.

The glass-hopper, H, is connected to a one-inch pipe through a butterfly valve V, to supply feed to the rotating cylinder at a desired rate.

A Clinometer LM (Plate 3 (b)), has been incorporated to measure both the inclination of the hold-up as well as that of the cylinder. The clinometer consists of a ¾-inches wide by 3 feet long aluminium angle bar, screwed to a pair of one-inch

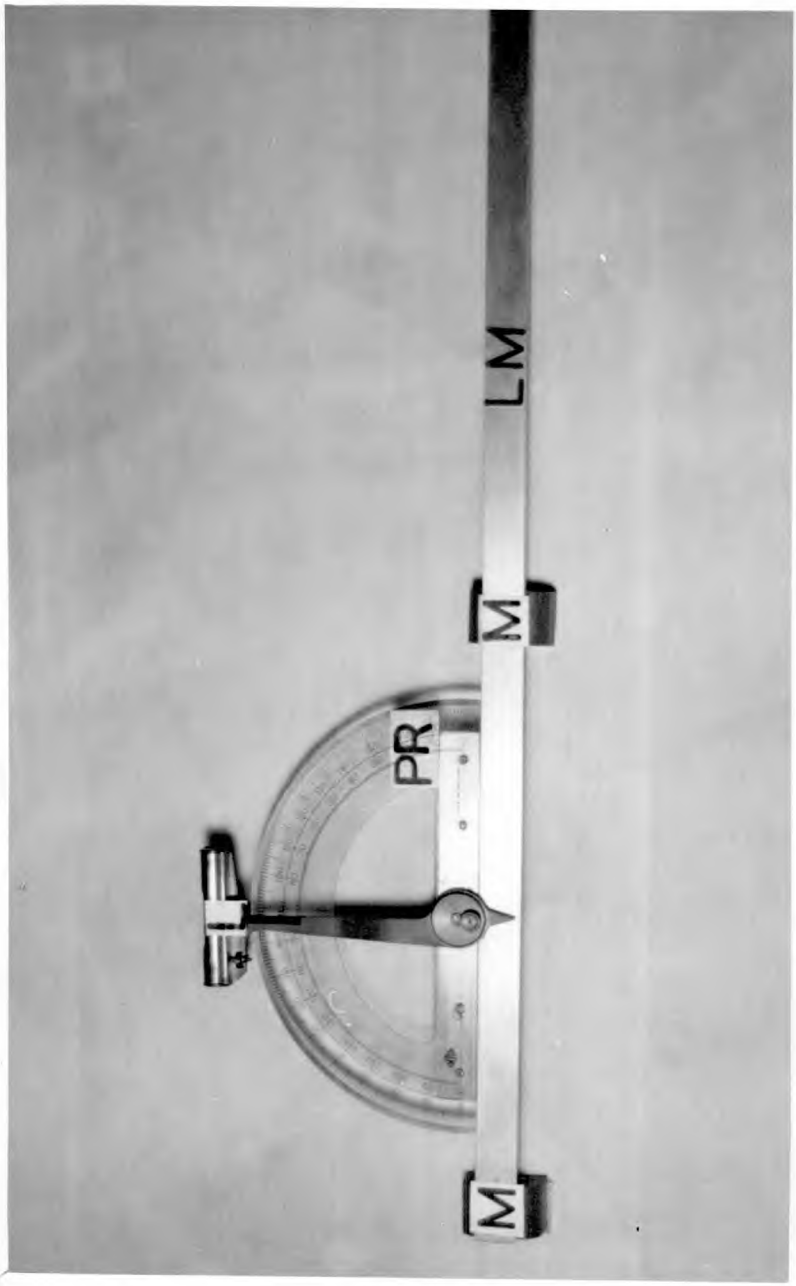
horse-shoe magnets MM. Between these two magnets, an 8-inches protractor PR and a sliding 2.5-inches spirit level, is fitted for level adjustments. Both these magnets slide freely in a vertical plane over two 6 x 1.5 inches steel platforms PP.

Plate 3 (a)



Apparatus for Studying the Average Time of Passage through Inclinfd Rotary-Cylinder.

Plate 3(b)



CLINOMETER

2. Experimental Procedure.

In order to find the time of passage of material through the cylinder, the cylinder is first set at the required inclination with the help of the clinometer. The motor is then switched on and the speed of the cylinder is adjusted to the desired R.P.M.

The hopper is then filled with the material under test and the necessary feed rate adjusted by means of the valve V. It will be noticed that after the material is spread along the cylinder length, it begins normally to cascade in the manner described in Chapter V. When the system has attained a state of equilibrium and the material is cascading, a known volume say 500 ccs of the discharged material is collected and weighed. If x lbs is the weight of the material discharged in y minutes, when the hold-up in the cylinder is z lbs, then the average time of passage is given by:

$$t = \frac{y \times z}{x} \text{ minutes.} \qquad (82)$$

3. Path of the Granules through the Inclined Cylinder.

During the passage of a granular material through the cylinder, the particles move under the

influence of centrifugal, gravitational and frictional forces. The relative magnitude of the forces may vary with the speed and the inclination of the cylinder, the nature of the surface of the granules and cylinder walls, and the shape and the density of the granules. The path traversed by the granules in any particular system will depend on the resultant of these forces.

Visual observation shows that one or other of the following systems may be established:

1. The whole bed may traverse the cylinder by cascading. In this case the thickness of the bed progressively diminishes towards the exit end of the cylinder and there is a pronounced end-effect at the exit-end. It is probable that during cascading there will be slip between the granules and the wall of the cylinder, the degree of slip depending on the coefficient of friction between the granules and the walls of the cylinder. A typical example of the cascading is shown in Plate (4).

2. The whole bed may slide down the cylinder with little or no relative movement of the granules. In these circumstances the bed is found to be of uniform thickness in the cylinder same for a short length

near the entry and the exit where the end-effects may be noted. Plate 7 (a), (b), (c) and (d) shows typical examples of sliding.

3. Cascading and Sliding.

In this case material near the feed-end is transported by cascade action but at some point cascading gives place to sliding. Typical examples are shown in Plate (5) and (6).

The time of passage of the material and the hold-up in the cylinder, will be governed by the mode of transport of the particles.

Plate 4.



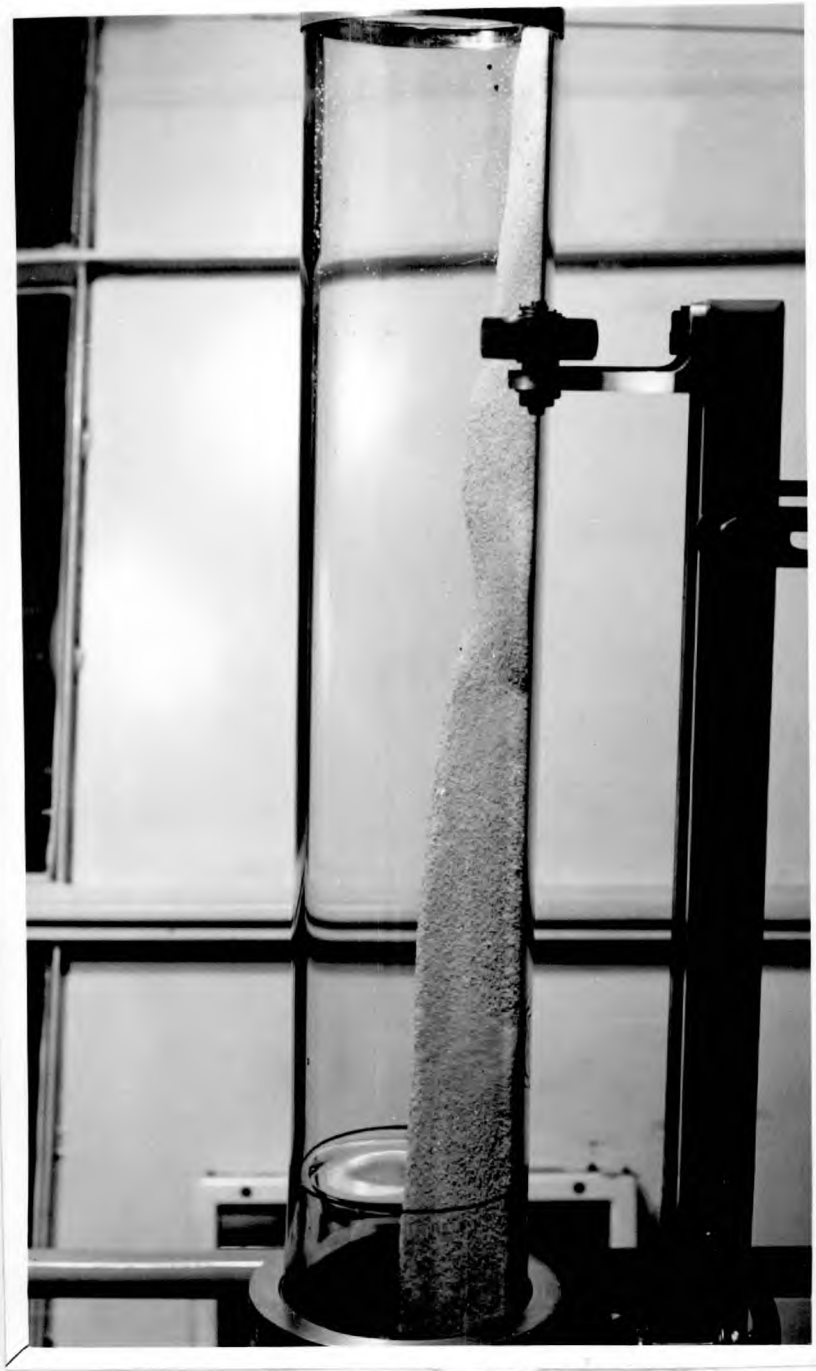
Cascading Motion of Granules
in an Inclined Rotary Cylinder.

Plate 5.



Cascading & Sliding Motion of Granules in Inclined Rotary-Cylinder.

Plate 6.



Cascading & Sliding Motion of Granules in Inclind Rotary-Cylinder.

Plate 7(a)



Sliding Motion of Granules
in an Inclined Rotary Cylinder.

Plate 7(b)



Sliding Motion of Granules
in an Inclined Rotary Cylinder.

Plate 7(c)



Sliding Motion of Granules
in an Inclind Rotary Cylinder.

Plate 7(d)



Sliding Motion of Granules
in an Inclind Rotary Cylinder.

4. Experimental.

As already described, the variables which were examined experimentally, are:

1. Inclination of the cylinder and the bed.
2. Length of the cylinder.
3. Diameter " "
4. Speed of rotation.
5. Dyn. angle of repose.

In addition to the above, certain other aspects of the granular-motion, in a rotary cylinder, which effect the time of passage, have been studied and are discussed later. They are:

1. Effect of Feed-Rate on Hold-up and the time of passage.
2. Bed slope vs kiln-slope.

The materials listed in Table (14) (see Appendix) were used. For each material two sets of experiments were usually carried out, one with 4 degrees slope and 2 R.P.M. (1 ft./min) and the second at the same slope but 10 R.P.M. (10 ft./min.). In determining the effect of cylinder inclination on the time of passage, various inclinations from 1 to 10 degrees were used. The choice of both the speed as

well as the cylinder-inclination is in accordance with usual kiln practices where the slope varies from 2 to 4 degrees (sometimes 2 to 4·7 degrees) and the speed limit covers a range of 18 to 36 ft./min. (46) for kilns and 30 to 150 feet for dryers (47).

Experimental Results.

1. Effect of Cylinder Inclination:

The effect of cylinder inclination S, on the average time of passage t, was studied for inclinations of 1 to 10° and for two different speeds i.e. 2 and 10 R.P.M. The results for different materials are presented in Tables 15 (a), (b), (c), (d) and (e) and 16 (a), (b), (c), (d) and (e) (see Appendix), and shown graphically in Fig. (29) and (30). Both these figures indicate that as the slope increases, the time of passage decreases and that the decrease in the time of passage is more pronounced from 1 to 5 than from 5 to 10 degrees.

It will also be seen that the relative position of the curves, with the exception of felspar, is in order of the surface dyn. angle of repose β of the materials, as indicated by the following table.

Table (14).

Time of passage vs Dyn. angle of Repose.

R.P.M. = 2, Cylinder Slope = 4 degrees.

No.	Material.	Size Distribution.	Dyn. angle of Repose (β, Deg.	Time of Passage. Minutes.
1.	Haematite.	(- 18 + 22)	37	8·32
2.	Felspar.	mesh B.S.S.	35·5	(4·92)
3.	Starch.		35	7·07
4.	Coal.	"	34·5	6·92
5.	Sand.		34	6·76
6.	Gravel(spherical)"		31	4·34

Since the value of the dyn. angle of repose of felspar, is close to that of starch and coal, it would be expected that the relevant curve would be somewhere close to those for coal and starch. Actually the curve for felspar occupies the lowest position in the series. The explanation of this abnormality appears to be associated with the effect of the combination of 'cascading and sliding' movement, which in case of felspar is much greater than with the other materials.

In accordance with the theoretical analysis, when 't' is plotted against $1/\sin\phi$, where t is the time of passage and ϕ is the slope of the bed, a set of

straight lines (see Figs. (31), (32)) is obtained.

It will be noted that instead of taking the slope of the cylinder, t has been plotted against the slope of the bed ϕ, which will be shown later, to equal $(S + 2)^{\circ}$ for a hold-up of approximately 25 percent. of the cylinder volume.

Effect of Cylinder-Inclination when the bed is Sliding.

The time of passage of the granular material has also been studied when the whole bed is sliding down the cylinder. The results for felspar and sand have been tabulated in Table 17 (a) and (b) (see Appendix) and graphically shown in Fig. (33).

These results indicate that save at one-degree cylinder slope, there exists a linear relationship between t and $^{1}/\text{Sin S}$, where t is the time of passage in minutes and S is the slope of the cylinder in degrees.

Thus it will be seen that the effect of slope is similar in both the cases namely under cascading-motion and sliding-motion of the bed. For the same cylinder inclination the time of passage with sliding system is shorter than in a cascading system.

FIG. (29)

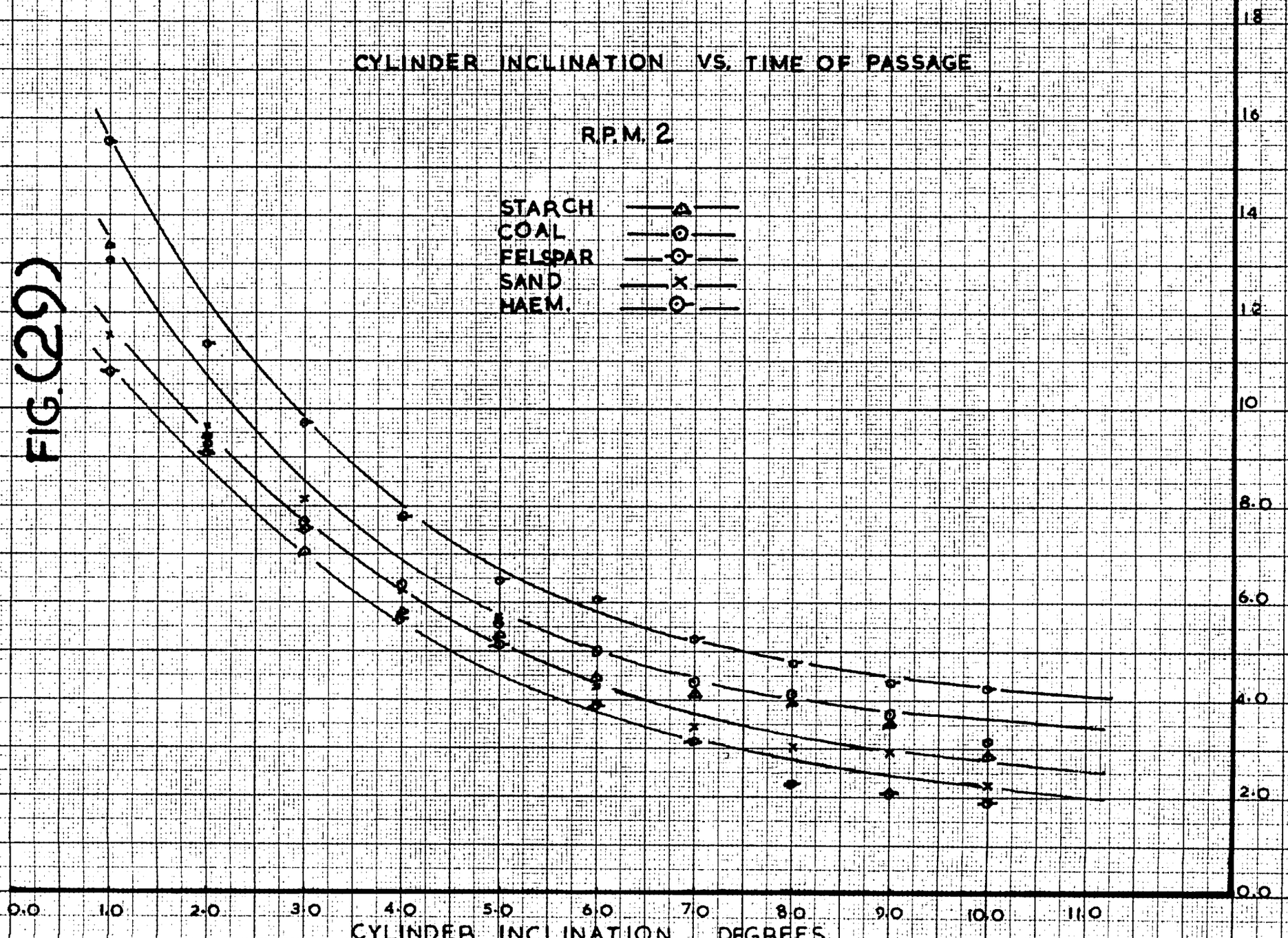
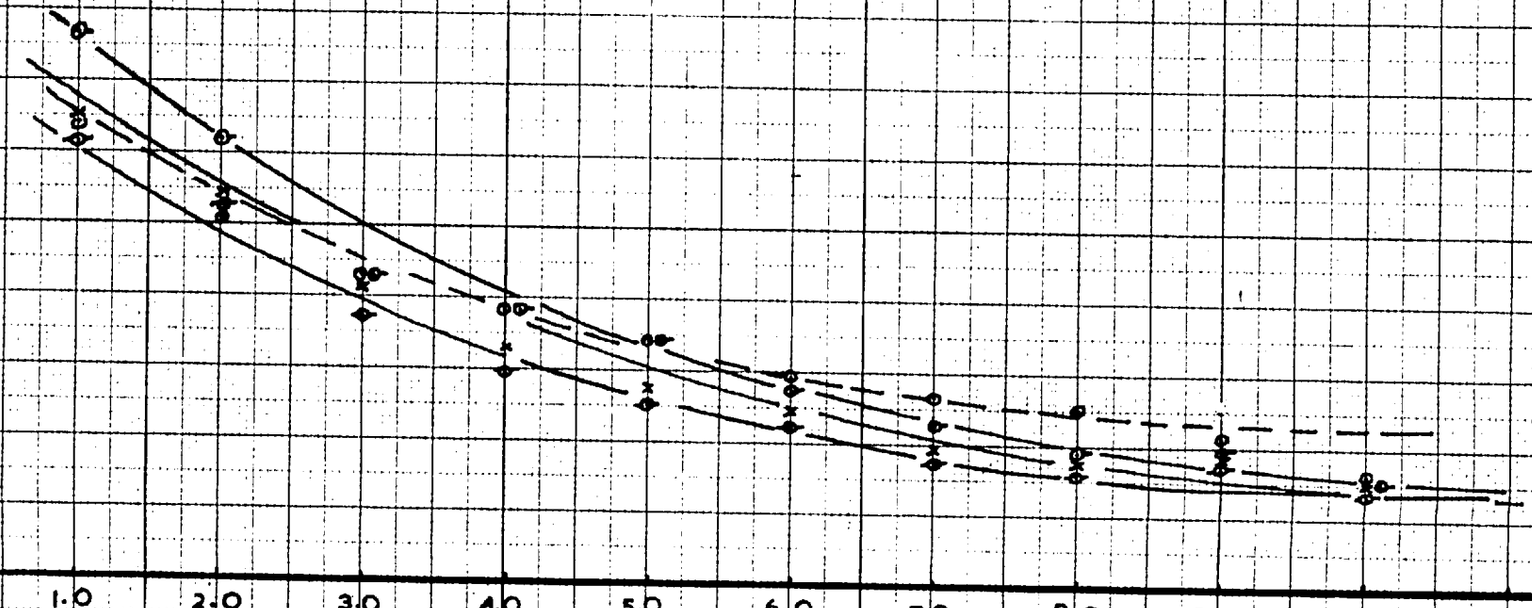

CYLINDER INCLINATION VS. TIME OF PASSAGE
R.P.M. 2
STARCH
COAL
FELSPAR
SAND
HAEM.
TIME OF PASSAGE MINUTES
0.0
2.0
4.0
6.0
8.0
10
12
14
16
18
0.0
1.0
2.0
3.0
4.0
5.0
6.0
7.0
8.0
9.0
10.0
11.0
CYLINDER INCLINATION DEGREES

FIG. (30)

CYLINDER INCLINATION VS. TIME OF PASSAGE

R.P.M. 10

STARCH
COAL
FELSPAR
SAND
HAEM.



TIME OF PASSAGE MINUTES

0.0 1.0 2.0 3.0 4.0 5.0 6.0 7.0 8.0 9.0 10 11

CYLINDER INCLINATION DEGREES

FIG. (31)

TIME OF PASSAGE VS. 1/SIN ϕ
R.P.M. 2

STARCH
COAL
FELSPAR
SAND
HAEM.

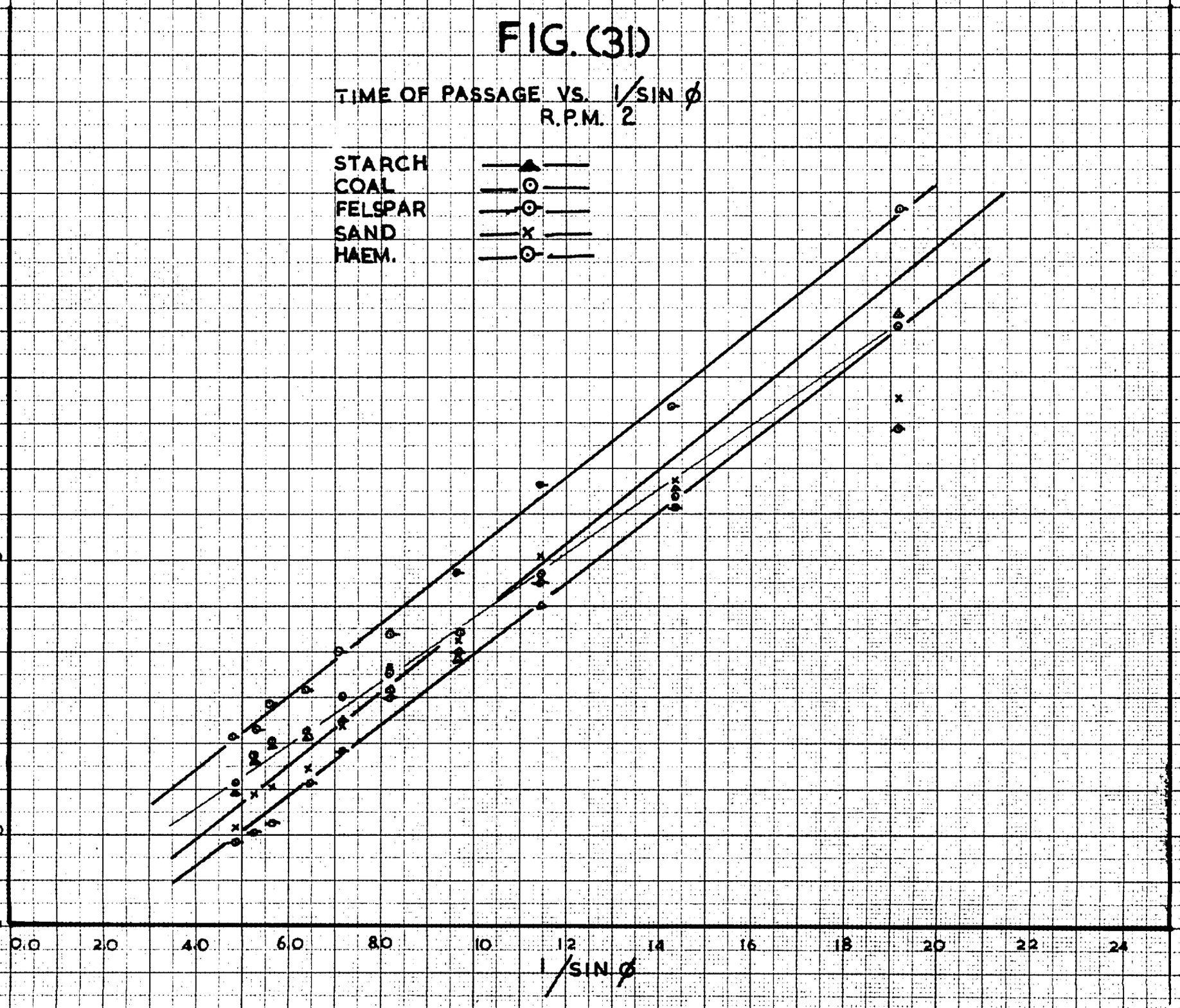
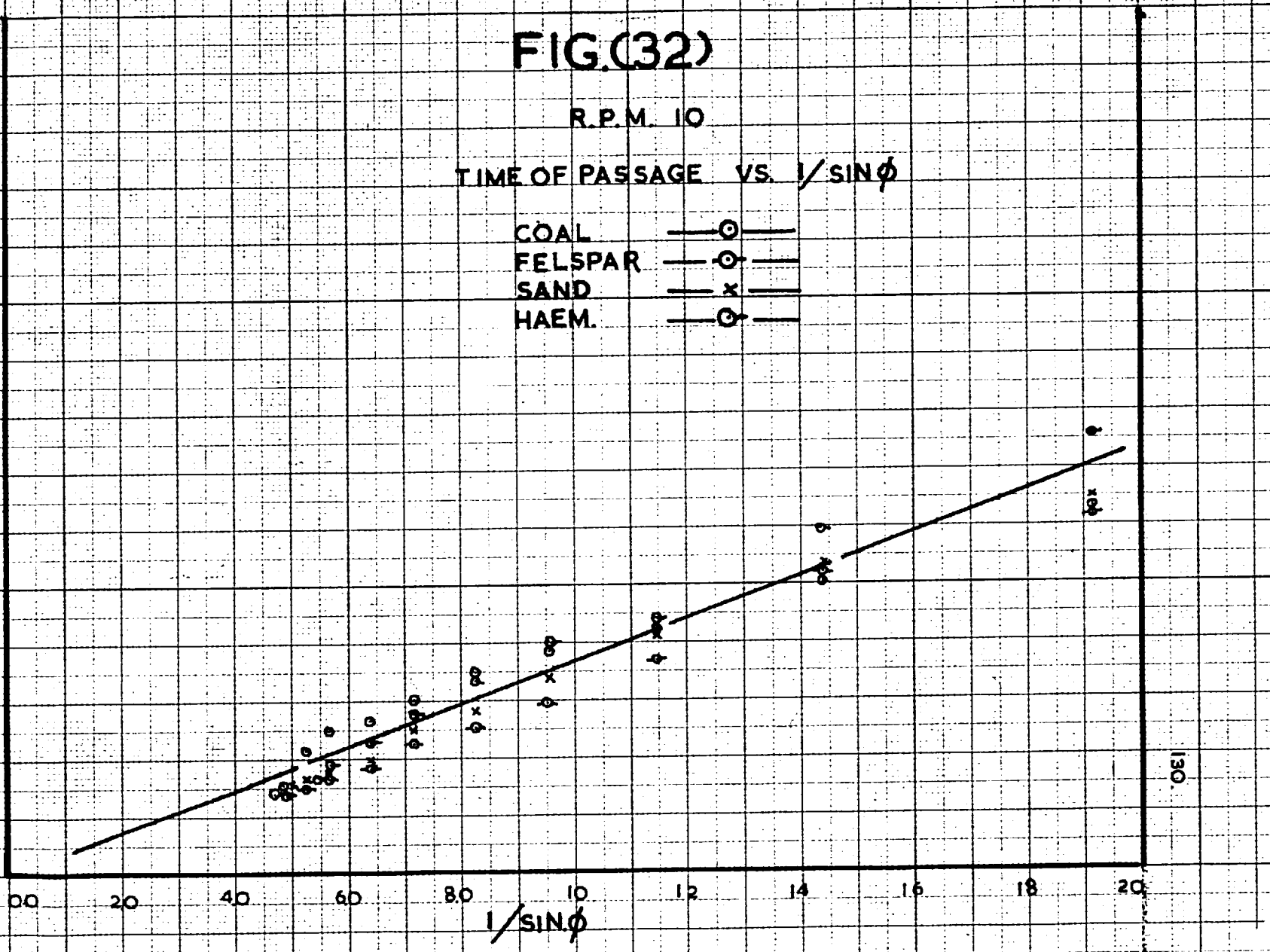


FIG.(32)

R.P.M. 10

TIME OF PASSAGE VS. $1/\sin\phi$

COAL —⊙—
FELSPAR —⊙—
SAND —×—
HAEM. —⊙—

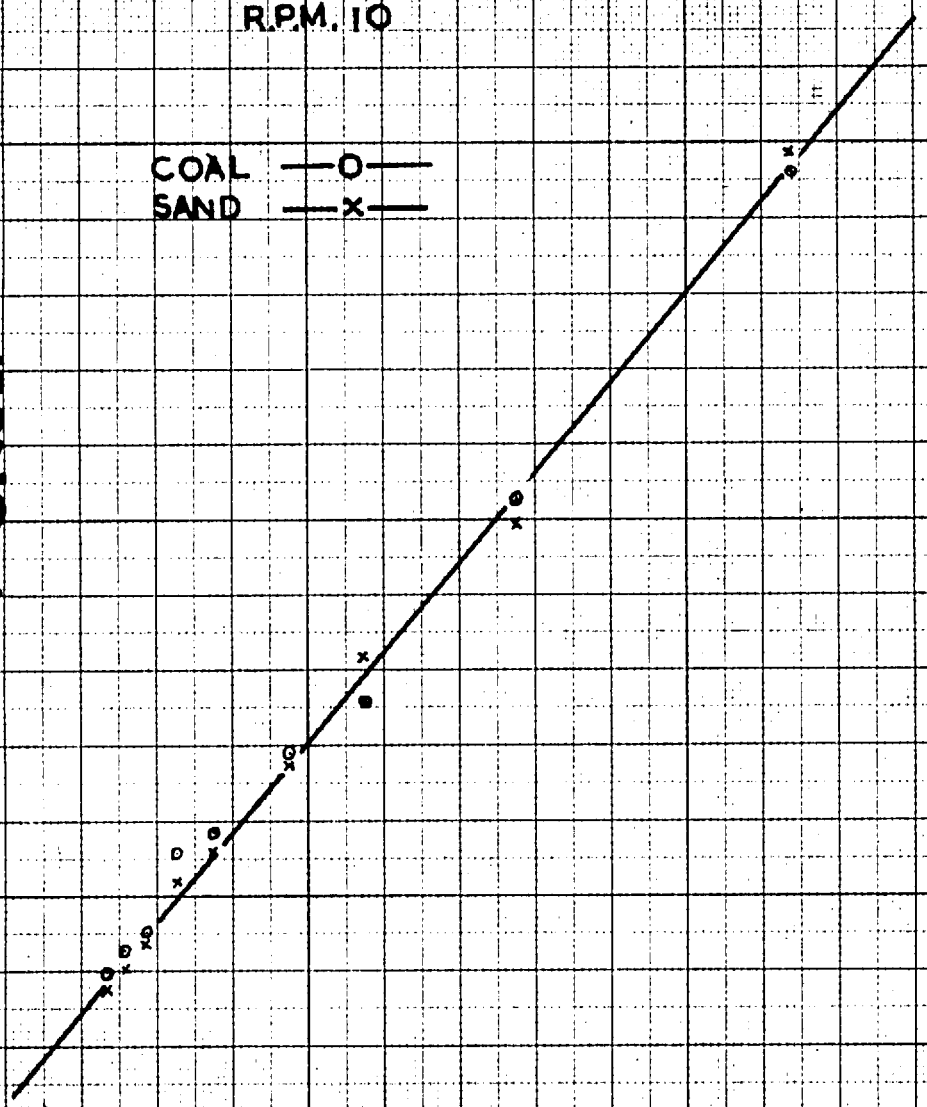


TIME OF PASSAGE VS. 1/SIN Ø

(SLIDING MOTION)

R.P.M. 10

COAL —O—
SAND —×—



2.0
1.5
1.0
0.5
0.0

TIME OF PASSAGE MIN.

00 10 20 30

1/SIN Ø

FIG. (33)

Effect of Cylinder Length.

It would at first sight seem probable that neglecting end-effects the time of passage of the material would vary directly with the length of the cylinder. In this work instead of using a number of cylinders of different lengths to determine the effect of length, only one cylinder was employed, the following procedure being adopted. The system was first brought into equilibrium with material flowing through it, at a constant rate. The motor and the feed - valve were then shut off simultaneously and a portion of the hold-up over a given cylinder length measured from the outlet-end, was drawn off, weighed and its time of passage calculated according to equation (82). This procedure was repeated each time changing the length over which the hold-up was withdrawn, until the entire cylinder length was covered.

Separate series of experiments were carried out for cascading and sliding beds.

1. Cascading Beds.

The results are summarised in Tables 18 (a),(b), (c), (d), and (e) and 19 (a), (b), (c), (d) and (e) (see

Appendix), which have been graphically presented in Figs. (34) and (35). Both these figures show that the placement of the curves is in order of the dyn. angle of repose, save in case of felspar. At low speeds the effect of the angle of repose is more pro - nounced than at higher speeds, where presumably the effect of 'slip' becomes significant.

A log-log plot shows that when the material is cascading, the relationship between the time of passage t and the cylinder length L, can be expressed by:

$$t = k\,(L)^{1.5} \qquad (83)$$

This result is contary to the experience of other workers who have shown or have assumed that $t \propto L$.

Since most of the experiments described in this thesis have been carried out with approximately 25% hold-up of the volume of cylinder, it was felt that the volume of the hold-up might have some effect on the relationship between t and L. Consequently, experiments with about 10 percent hold-up under cascading conditions were carried out with results tabulated in Table (15) and plotted in Fig. (36). A log-log plot indicated that even at low hold-up such as 10%, the relationship $t \propto L^{1.5}$ will hold, when the bed is

moving under cascading conditions.

Table (15)

Effect of Cylinder Length on the Time of Passage.

(Cascading Motion)

Coal.

Hold-up = 10% (approx.), R.P.M. = 10, Slope 4°

No.	Cylinder Length Ft.	Feed Rate lbs/min.	Hold-up lbs.	Time of Passage Min.
1.	0.5	0.797	0.187	0.238
2.	0.75	"	0.328	0.412
3.	1.0	"	0.485	0.610
4.	1.5	"	0.828	1.032
5.	1.75	"	1.031	1.30

2. Sliding Beds.

In order to determine the relationship between t and L, under sliding conditions, experiments were carried out on coal and sand (- 18 + 22) mesh B.S.S. The results are tabulated in Tables 16 (a) and (b) and graphically presented in Fig. (36).

Table (16).

Effect of Cylinder Length on the Time of Passage.

(under Sliding-Motion).

R.P.M. = 10, Slope = 4°

(a)

COAL.

No.	Cylinder Length Ft.	Feed Rate lbs/min.	Hold-up lbs.	Time of Passage.
1.	0·5	0·532	0·141	0·265
2.	0·75	"	0·219	0·412
3.	1·00	"	0·313	0·590
4.	1·5	"	0·50	0·940
5.	1·75	"	0·570	1·120

(b)

SAND.

1.	0·5	1·391	0·235	0·169
2.	0·75	"	0·391	0·281
3.	1·00	"	0·531	0·381
4.	1·5	"	0·814	0·585
5.	1·75	"	0·938	0·675

Fig. (36) indicates that t varies linearly with L i.e. $t \propto L$.

In continuation of the study of the sliding-motion of the bed, experiments were also carried out on

felspar and sand to show that the time of passage under 'sliding-motion' is shorter than the 'cascading-motion'. The results in Table (17) indicate that for felspar the time of passage under cascading-motion is 1·494 minutes and under sliding-motion 0·722 minutes and for sand they are 1·653 and 0·553 minutes respectively.

Table (17).

Sliding Motion vs Time of Passage.

R.P.M. = 10, Slope = 4^{o}

(a)

FELSPAR.

No.	Feed Rate lbs/min.	Hold-up lbs.	Time of Passage. (Sliding).	Time of Passage. (Cascading)
1.	1·215	0·876	0·721	
2.	1·528	1·096	0·715	
3.	1·930	1·426	0·739	
4.	2·530	1·797	0·712	
5.	3·865	2·813	0·727	
			Av: 0·722	1·494

(b)

SAND.

No.	Feed Rate lbs/min.	Hold-up lbs.	Time of Passage. (Sliding)	Time of Passage. (Cascading)
1.	2·360	1·281	0·544	
2.	3·240	1·968	0·557	
3.	4·860	2·609	0·537	
4.	5·558	3·016	0·543	
5.	6·479	3·813	0·587	
			Av: 0·553	1·653

These results also show that under sliding conditions the effect of increase in feed-rate (for felspar 1·215 to 3·865 lbs/min. and for sand 2·36 to 6·479 lbs/min.) on the hold-up is not very appreciable but its effects on the granular 'build-up' near the feed-end is quite distinct. Moreover, unlike the geometrical profile of the bed moving under cascading-motion, the hold-up in the cylinder is uneven and irregular in shape.

In the case of cascading, the granules move along circular arcs and in this way the distance travelled by a particular granule in contact with the glass-wall, over the whole cylinder length, would be

the sum of such arcs. Since the direct measurement of arc-length is not possible, we have summed up the corresponding chords, i.e. the lengths over which the granules slide on the inclined surface of the bed. Let these chords be denoted by C_1, C_2, C_3, ... C_{11}. Assuming that they have the same convergency ratio as shown by the convergent geometric series x_1, x_2, x_3, ... x_{11}, where x_1, x_2, x_3 ..... are the 'advancements' along the foot of charge as will be defined in Chapter VII, we may sum up the series C_1, C_2, C_3 ..... C_{11} with the help of the equation $\sum_{C_1}^{C_{11}} C = C_1/_{1 - r}(1 - r^{N'})$, where C_1 is the first term of the series, r the convergency ratio and N' the number of the chords. This equation when solved gives

$$\sum_{C_1}^{C_{11}} C = 11{\cdot}2 \text{ feet (approx.)}.$$

These chords have also been summed up by an alternate method i.e. by plotting the 'advancements' x_1, x_2, x_3 ..... x_{11} along the foot of the bed, as indicated in Fig. (37). The value of $\sum_{C_1}^{C_{11}} C$ by this method comes

out to be 10·5 feet. Thus it will be seen that if the material is truely cascading i.e. the cascading is not affected /to an appreciable extent by slip, the length covered will be approximately 10·5 to 11·2 feet, in a cylinder 2·1 feet long, whence it can be concluded that the time of passage will vary with some power of the cylinder length i.e. $t \propto L^n$, where n will always be greater than one. Experimentally, it has been shown that $n = 1·5$.

The study of the effect of the cylinder length on the time of passage has been supplemented using a 5·5 feet long by 1·08 feet diameter steel cylinder. The results both for cascading as well as sliding motion, have been tabulated in Table 20 (a) and (b) (see Appendix) and graphically presented in Fig. (38). These results confirm that for cascading the relation - ship $t \propto L^{1·5}$ and for sliding $t \propto L$ hold and are in agreement with the set of experiments carried out with the much shorter glass-cylinder.

FIG. (34)

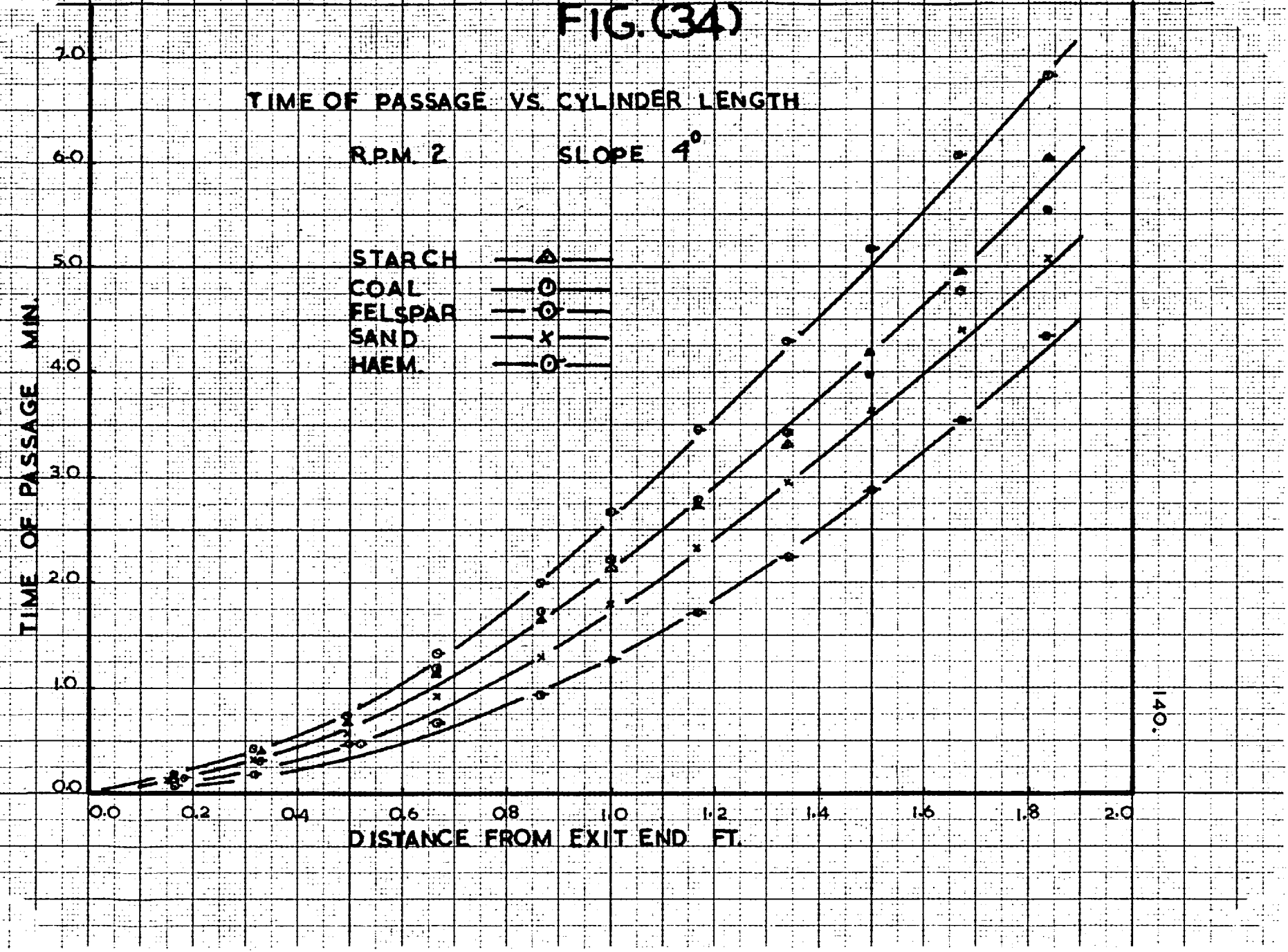

TIME OF PASSAGE VS. CYLINDER LENGTH
R.P.M. 2
SLOPE 4°
STARCH
COAL
FELSPAR
SAND
HAEM.
TIME OF PASSAGE MIN.
7.0
6.0
5.0
4.0
3.0
2.0
1.0
0.0
0.0
0.2
0.4
0.6
0.8
1.0
1.2
1.4
1.6
1.8
2.0
DISTANCE FROM EXIT END FT.

FIG.(35)

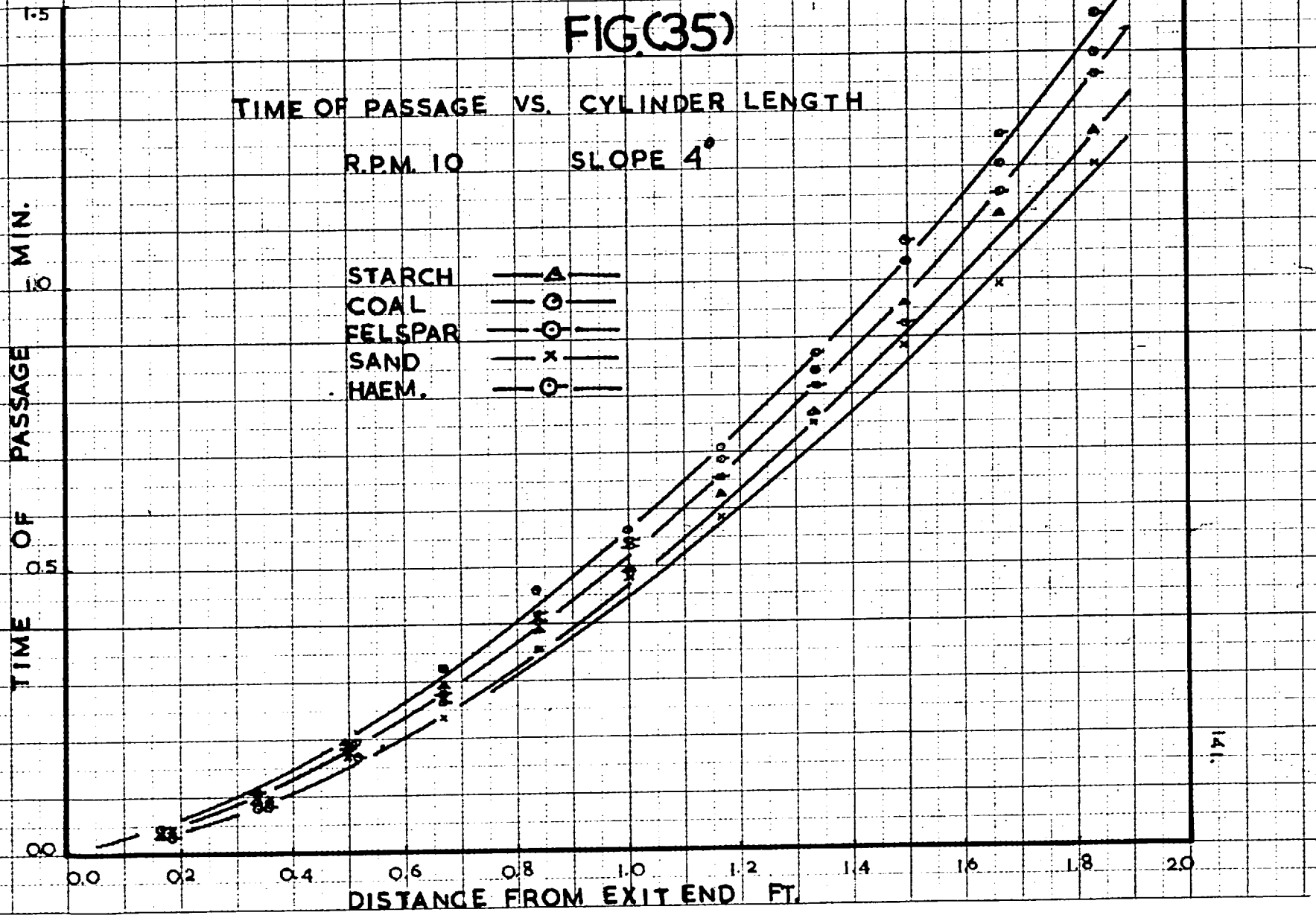

TIME OF PASSAGE VS. CYLINDER LENGTH
R.P.M. 10
SLOPE 4°
STARCH
COAL
FELSPAR
SAND
HAEM.
TIME OF PASSAGE MIN.
1.5
1.0
0.5
0.0
0.2
0.4
0.6
0.8
1.0
1.2
1.4
1.6
1.8
2.0
DISTANCE FROM EXIT END FT.

FIG.(36)

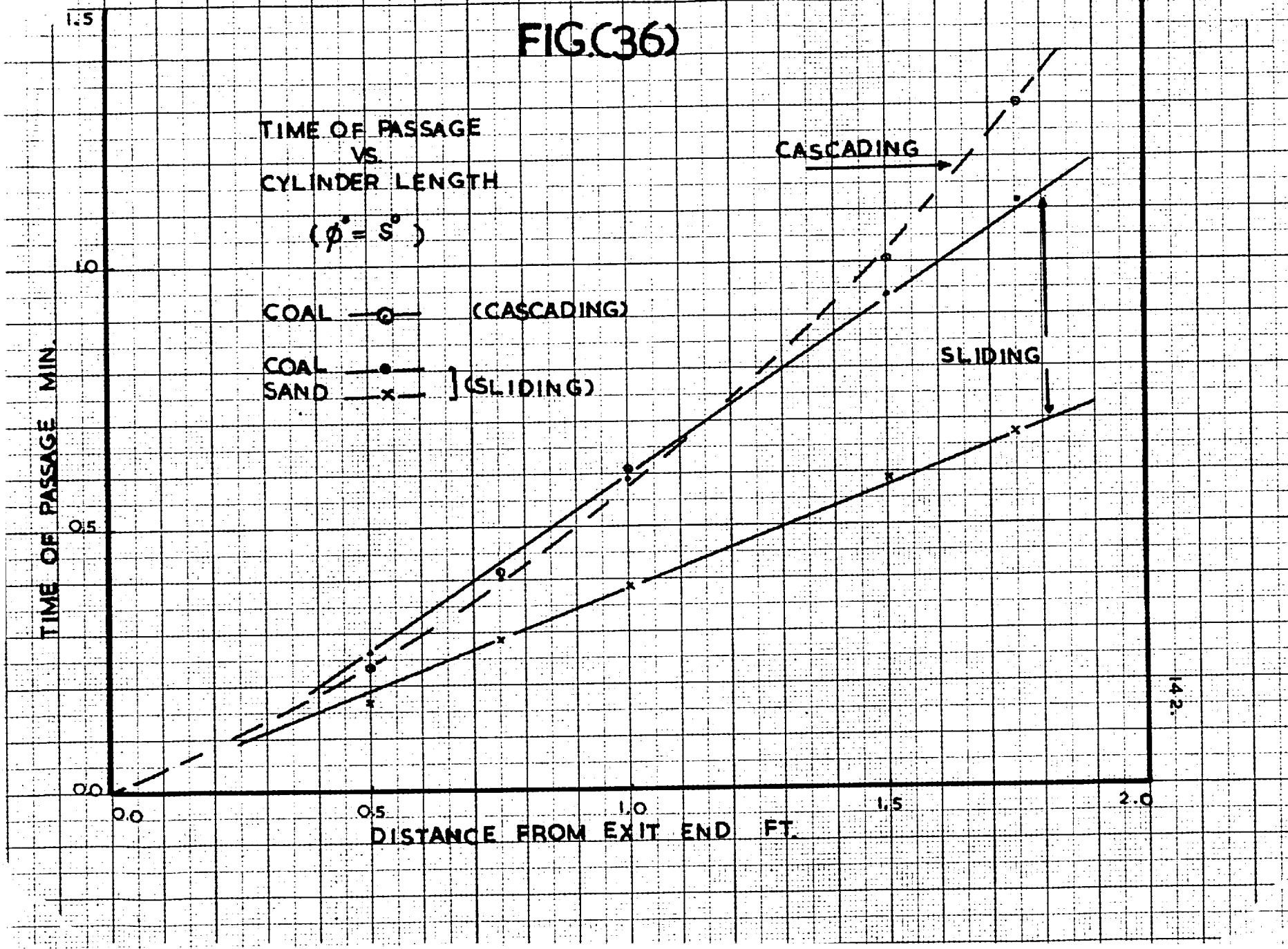
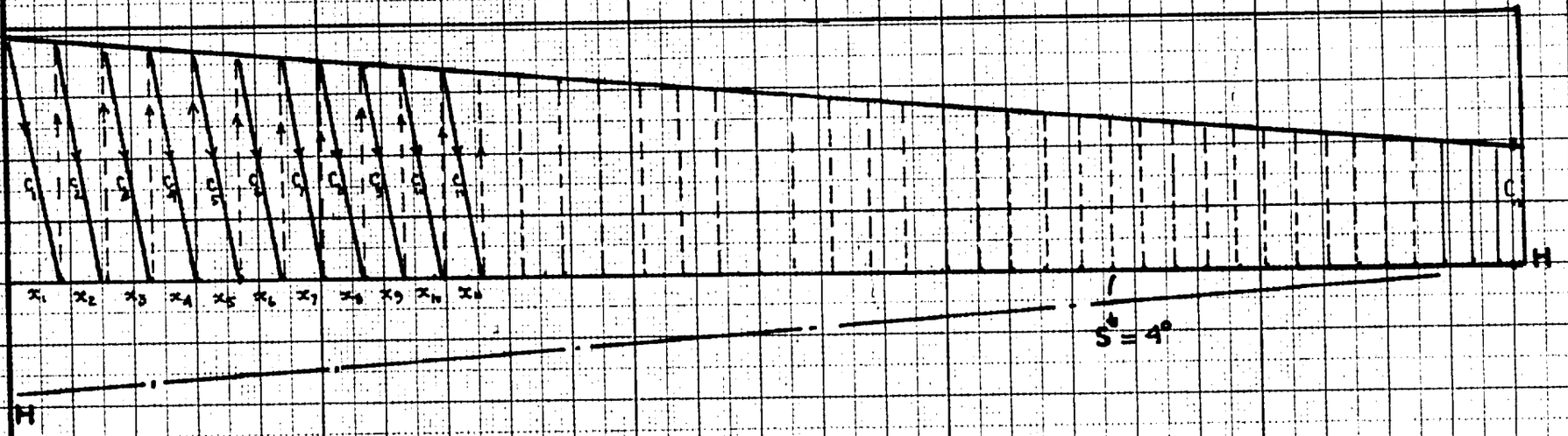

TIME OF PASSAGE
VS.
CYLINDER LENGTH
(ϕ° = S°)
CASCADING
COAL —o— (CASCADING)
COAL —•—
SAND —x—] (SLIDING)
SLIDING
TIME OF PASSAGE MIN.
1.5
1.0
0.5
0.0
0.0
0.5
1.0
1.5
2.0
DISTANCE FROM EXIT END FT.

FIG.(37)

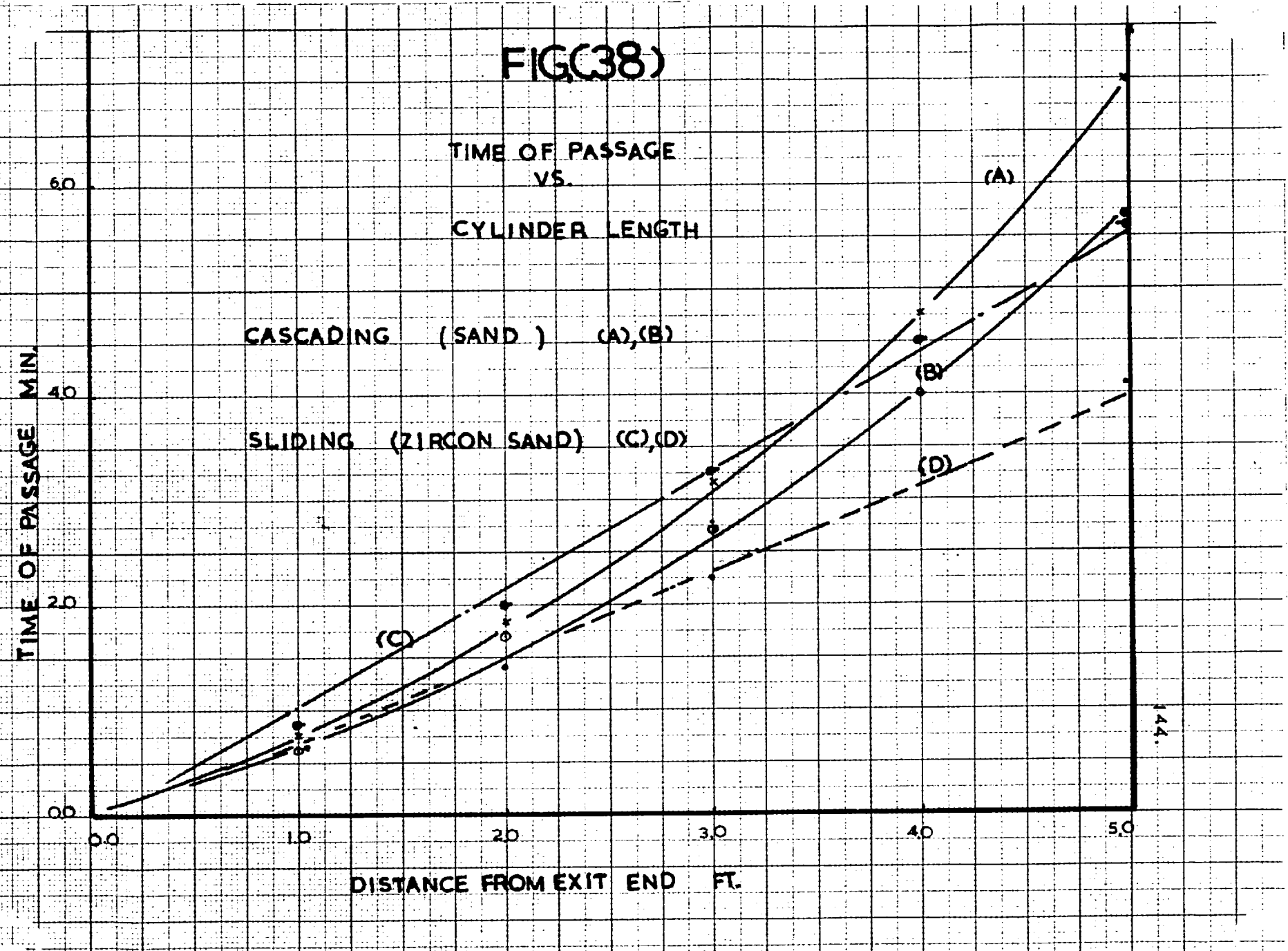
NUMBER OF CYCLES IN THE GRANULAR BED



SCALE 1 CM = 1 INCH

CYLINDER LENGTH FT.

FIG(38)

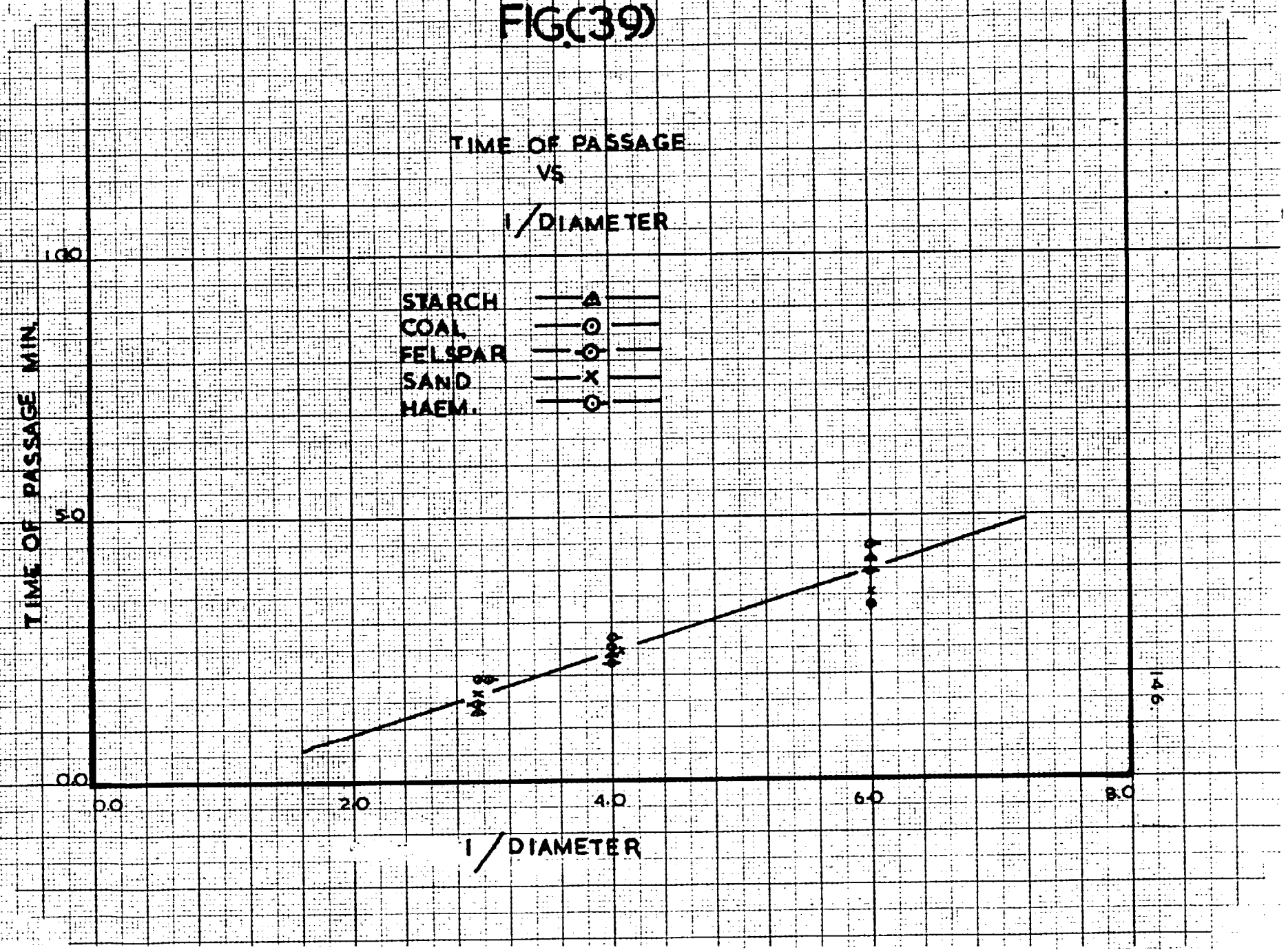

TIME OF PASSAGE
VS.
CYLINDER LENGTH
CASCADING (SAND) (A),(B)
SLIDING (ZIRCON SAND) (C),(D)
(A)
(B)
(C)
(D)
TIME OF PASSAGE MIN.
6.0
4.0
2.0
0.0
0.0
1.0
2.0
3.0
4.0
5.0
DISTANCE FROM EXIT END FT.

Effect of Cylinder Diameter.

Three cylinders having the same length but different diameters namely 0·166, 0·25 and 0·3386 feet, inclined at 4 degrees and rotating at 10 R.P.M., were used to examine the effect of diameter on the time of passage. The experimental results summarised in Tables 21 (a), (b), (c), (d) and (e) (see Appendix) and shown graphically in Fig. (39), indicate that as the diameter increases, the time of passage decreases. This is due to increase in the peripherical speed with diameter. Fig. (39) also shows that:

$$t \propto \frac{1}{D} \qquad (84)$$

FIG.(39)


TIME OF PASSAGE
VS
1/DIAMETER
STARCH
COAL.
FELSPAR
SAND
HAEM.
TIME OF PASSAGE MIN.
10.0
5.0
0.0
0.0
2.0
4.0
6.0
8.0
1/DIAMETER
146.

Effect of Cylinder Speed.

The results showing the effect of cylinder speed on the time of passage, over a range of 1 to 60 R.P.M., have been summarised in Table 22 (a), (b), (c), (d) and (e) (see Appendix) and plotted in Fig. 40 (a). A curve through the experimental points yield asymptotes both at the higher as well as the lower speeds.

Further when t is plotted against $^{1}/_{N}$, a set of converging straight lines (approaching the origin when N is infinitely large) as shown in Fig. 40 (b), is obtained.

When the speed of rotation is increased beyond say 60 or 70 R.P.M. and centrifugal forces become important, it is anticipated that the time of passage will gradually increase and will eventually become large at speeds above the critical speed of the cylinder, (135 R.P.M.). The dotted portion C.D.E. of the curve in Fig. 40 (a) illustrates this point. At high feed-rates and high speeds, it would be expected that there would be a concentric layer of granules rotating with the cylinder but not moving horizontally with a cascading core of granules travelling towards the exit end.

FIG.40(a)

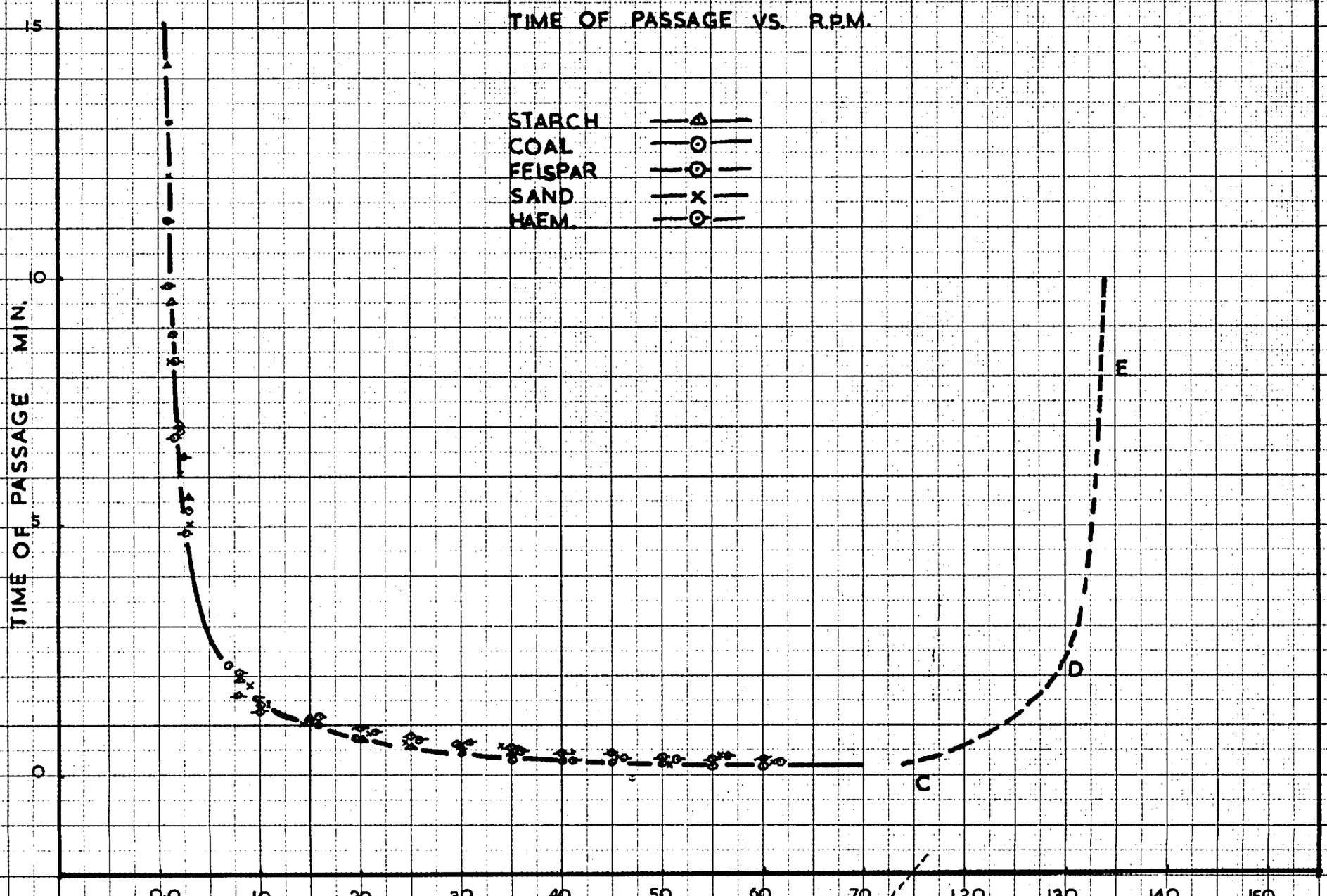
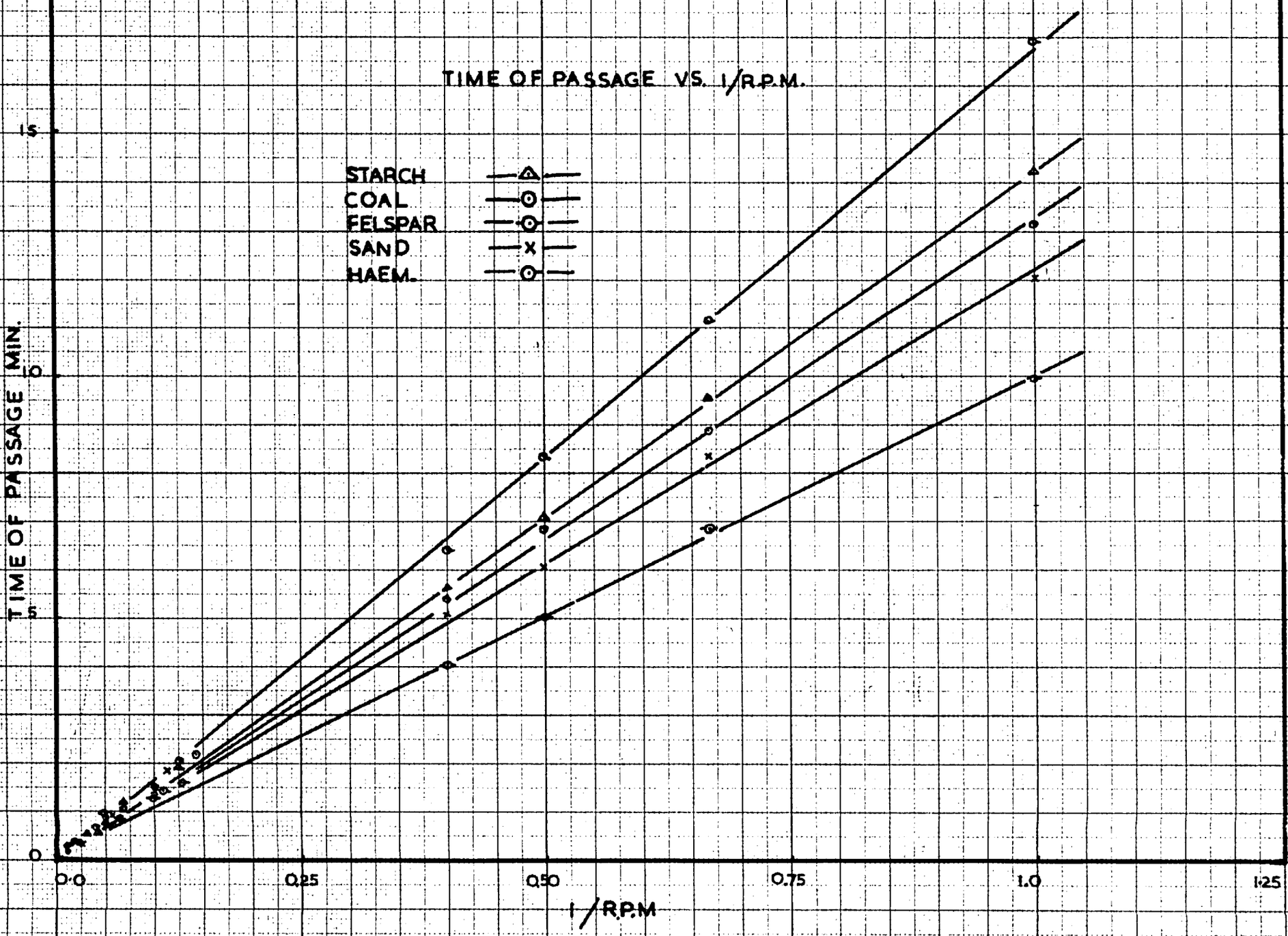

TIME OF PASSAGE VS. R.P.M.
STARCH
COAL
FELSPAR
SAND
HAEM.
15
10
0
TIME OF PASSAGE MIN.
E
D
C
0.0
10
20
30
40
50
60
70
120
130
140
150
REVOLUTIONS PER MINUTE

FIG.40(b)


TIME OF PASSAGE VS. 1/R.P.M.
STARCH
COAL
FELSPAR
SAND
HAEM.
15
10
5
0
TIME OF PASSAGE MIN.
0.0
0.25
0.50
0.75
1.0
1.25
1/R.P.M

Effect of the Dynamic Angle of Repose.

The dyn. angle of repose of the material gives a measure of the friction between the granules and the wall of the cylinder and hence the distance a granule will rise along the wall of a rotary cylinder.

Referring to Fig. (34) or (35), where the time of passage t of a number of materials, has been plotted against the length of the cylinder L, it will be noted that the relative position of the curves, with exception of that for felspar, is in the order of the dyn. angle of repose, as shown in Table (13). Felspar which has a dyn. angle of repose 35·5degrees, gives a low value for the time of passage - an anomaly which has already been noted and explained.

When the time of passage t is plotted against Sin β (Table 18). a straight line as shown in Fig. (41) is obtained indicating that:

$$t \propto \text{Sin } \beta \qquad (85)$$

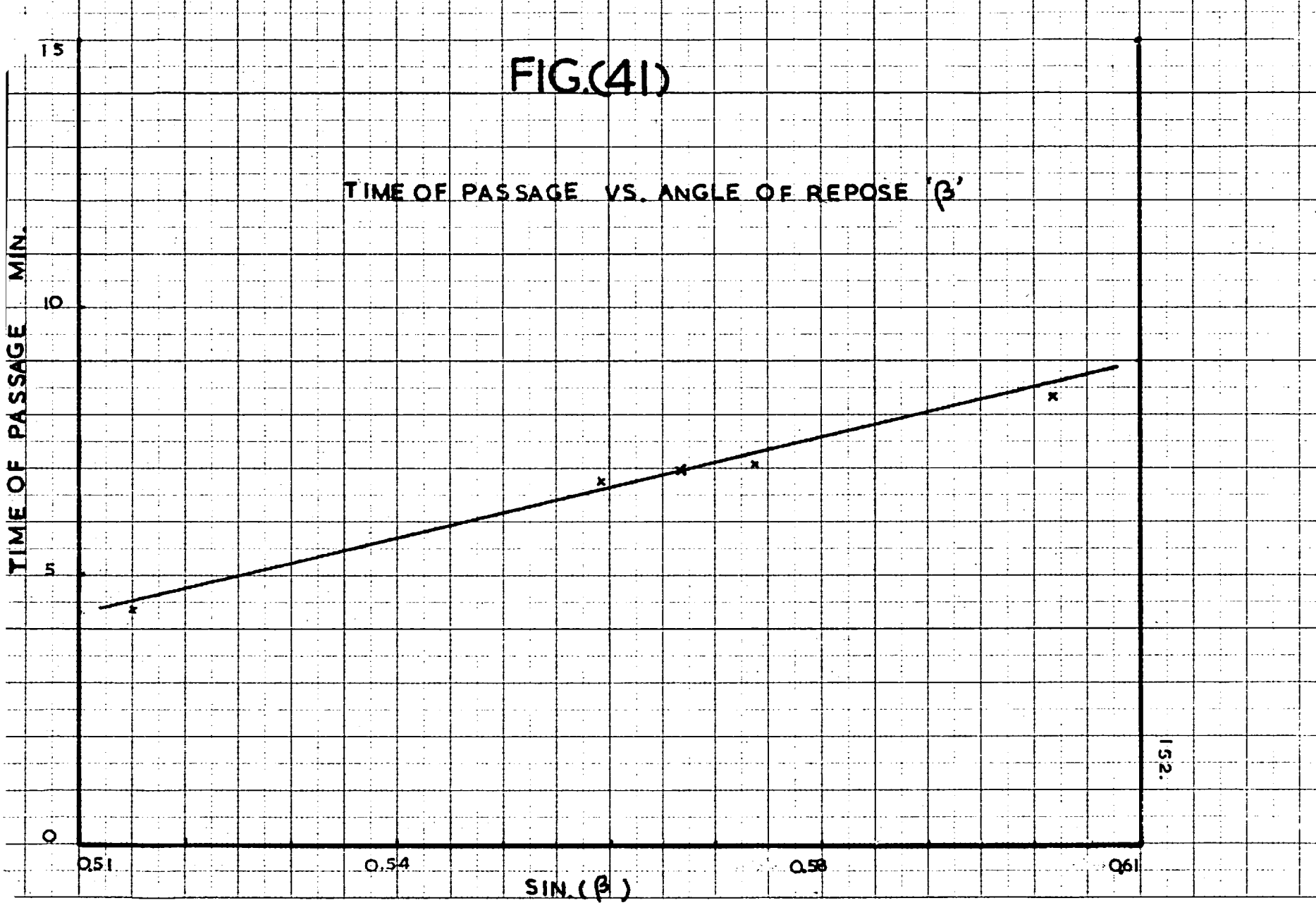
Table (18).

Effect of Dyn. angle of Repose on the Time of Passage.

R.P.M. = 2 and 10; Slope 4°

No.	Material.	Dyn. angle of Repose Degrees.	Sin	Time of Passage. Minutes. Cascading (R.P.M=2)	Sliding (R.P.M.=10).
1.	Haematite.	37	0·6018	8·32	1·22
2.	Felspar.	35·5	0·5807	(4·920)	(0·722)
3.	Starch.	35	0·5736	7·07	0·933
4.	Coal.	34·5	0·5664	6·92	0·872
5.	Sand.	34	0·5592	6·06	0·552
6.	Gravel.	31	0·5150	4·34	-

FIG.(41)


TIME OF PASSAGE VS. ANGLE OF REPOSE 'β'
TIME OF PASSAGE MIN.
15
10
5
0
0.51
0.54
0.58
0.61
SIN.(β)

5. Empirical Equations.

The experiment results just described have shown that the time of passage t, is related to the cylinder variables as follows:

$t \propto L$ (for sliding).

$L^{1.5}$ (For cascading).

$1/D$ "

$1/N$ "

$1/\text{Sin}\,\phi$ "

Thus for cascading we may write that:

$$t = k_c \frac{L^{1.5}}{D\ N\ \text{Sin}} \qquad (86)$$

In equation (86), k_c will partly depend on the dynamic angle of repose β of the material. Thus when the value of k_c for different materials as indicated in Table (18) are plotted against Sin β (see Fig. 42), we get a straight line relationship expressed by the equation:

$$k_c = 1.181\ (\text{Sin}\ \beta - 0.434) \qquad (87)$$

The value of k_c when substituted in equation (86) gives a correlation of the type:

$$t = \frac{1.181\ (\text{Sin}\ \beta - 0.434)\ L^{1.5}}{D\ N\ \text{Sin}\ \phi} \qquad (88)$$

Similarly, for sliding, the average time of passage is given (based on Tables 18 and 19) by the following equation:

$$t = \frac{2.57\ (\text{Sin}\ \beta - 0.517)\ L}{D\ N\ \text{Sin}\ \phi\ (= \alpha)} \qquad (89)$$

where

t = Time of passage in mts.

β = Dyn. angle of repose Degrees.

L = Length of the cylinder Ft.

D = Diameter of the cylinder Ft.

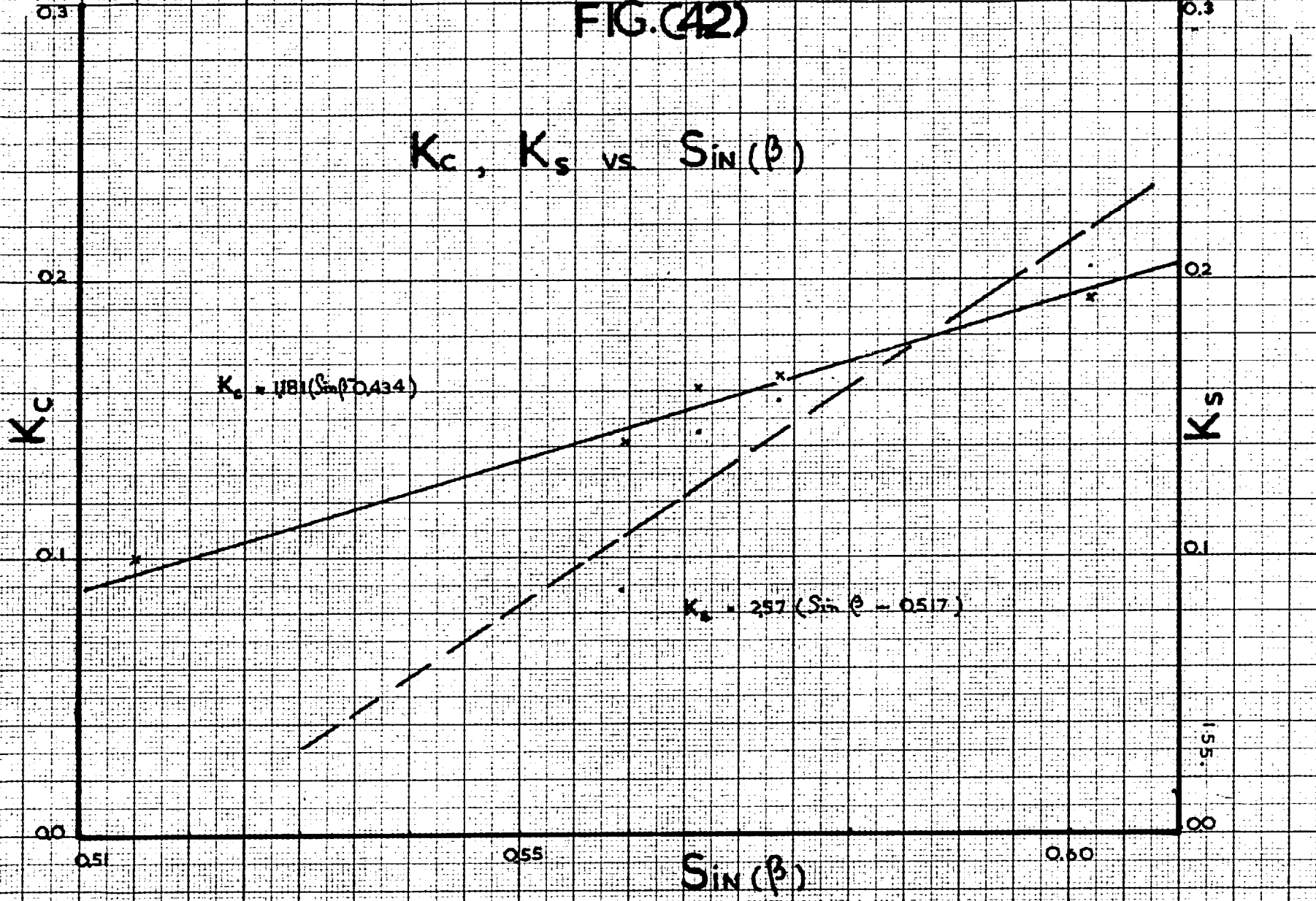
ϕ = Slope " " BED. Degrees.

Table (19).

k_c and k_S as function of Sin β .

No.	Material.	Sin β	k_c (Cascading)	k_S (Sliding)
1.	Haematite.	0·6018	0·194	0·206
2.	Felspar.	0·5807	(0·115)	(0·122)
3.	Starch.	0·5736	0·165	0·157
4.	Coal.	0·5664	0·161	0·147
5.	Sand.	0·5592	0·141	0·088
6.	Gravel.	0·5150	0·101	-

FIG.(42)


K_c , K_s vs $Sin(\beta)$
$K_c = 1.81(Sin\beta - 0.434)$
$K_s = 2.57(Sin\beta - 0.517)$
K_c
K_s
0.3
0.2
0.1
0.0
0.51
0.55
0.60
$Sin(\beta)$

6. Effect of Feed Rate on Hold-up, the Bed-Depth and the Time of Passage.

(1) The effect of the feed-rate on the hold-up or the bed-depth was experimentally studied for coal of particle size distribution (- 18 + 22) Mesh B.S.S. The results appear in Table 23 (a), (b) and (c) (see Appendix) and plotted in Fig. (43) which shows that the profile of the beds does not change and that in all cases the depth of the bed (or the hold-up) diminishes rapidly near the discharge-end. The 'end-effect' is related to the hold-up and for large values of hold-up may extend to one third or even one half of the length of the cylinder.

It should be noted that this end-effect is not related to the onset of sliding but is associated with the bed that is cascading throughout the whole length. From Fig. (43), it will also be seen that for a given cylinder slope and rate of rotation, as the feed-rate increases, the hold-up also increases from 15% to 28% of the cylinder volume (see also Table 24 in Appendix).

(2) The effect of feed-rate on the time of passage were studied for coal and sand, at different

cylinder speeds and inclinations. The results which appear in Tables (25) and (26) (see Appendix) and graphically presented in Figs. (44) and (45). Both these figures indicate that $F \propto X$, where F is the feed-rate in lbs/min and X, the hold-up in lbs. A further examination of Table (25) and (26) will also indicate that the time of passage is independent of the feed-rate (and consequently the hold-up).

Referring to Fig. (45), it may be seen that for 2 R.P.M., if the slope is increased from 2 to 4 degrees, the hold-up will fall from 2·4 lbs to 1·7 lbs when the feed-rate is 1·5 lbs/10 minutes i.e. for a given feed-rate, increase in cylinder slope will diminish the time of passage.

FIG.(43)

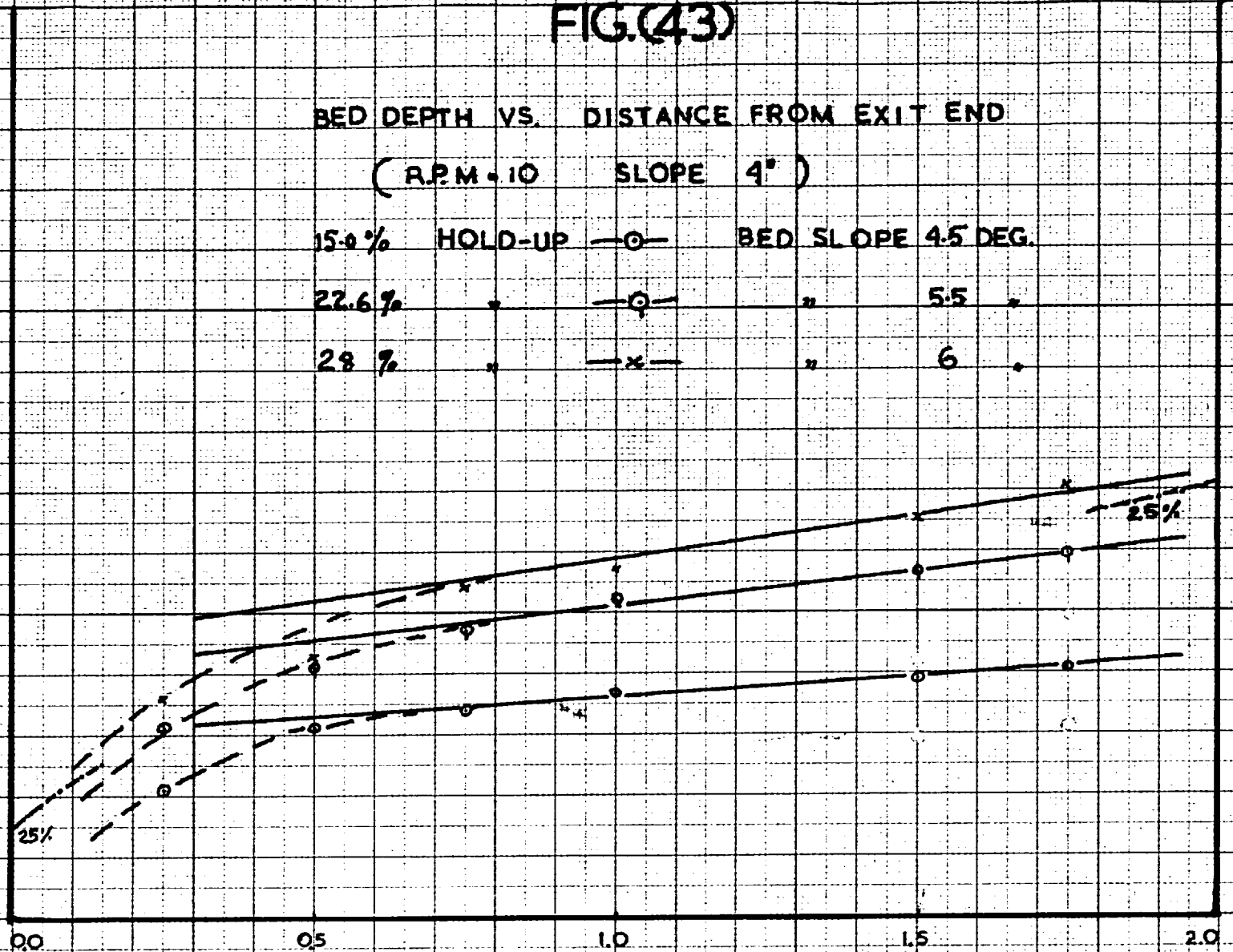

BED DEPTH VS. DISTANCE FROM EXIT END
(R.P.M = 10 SLOPE 4°)
15.0 % HOLD-UP —o— BED SLOPE 4.5 DEG.
22.6 % " —o— " 5.5 "
28 % " —x— " 6 "
BED DEPTH FT.
0.2
0.1
0.0
25%
2.5%
0.0
0.5
1.0
1.5
2.0
DISTANCE FROM EXIT END FT.

FIG.(44)

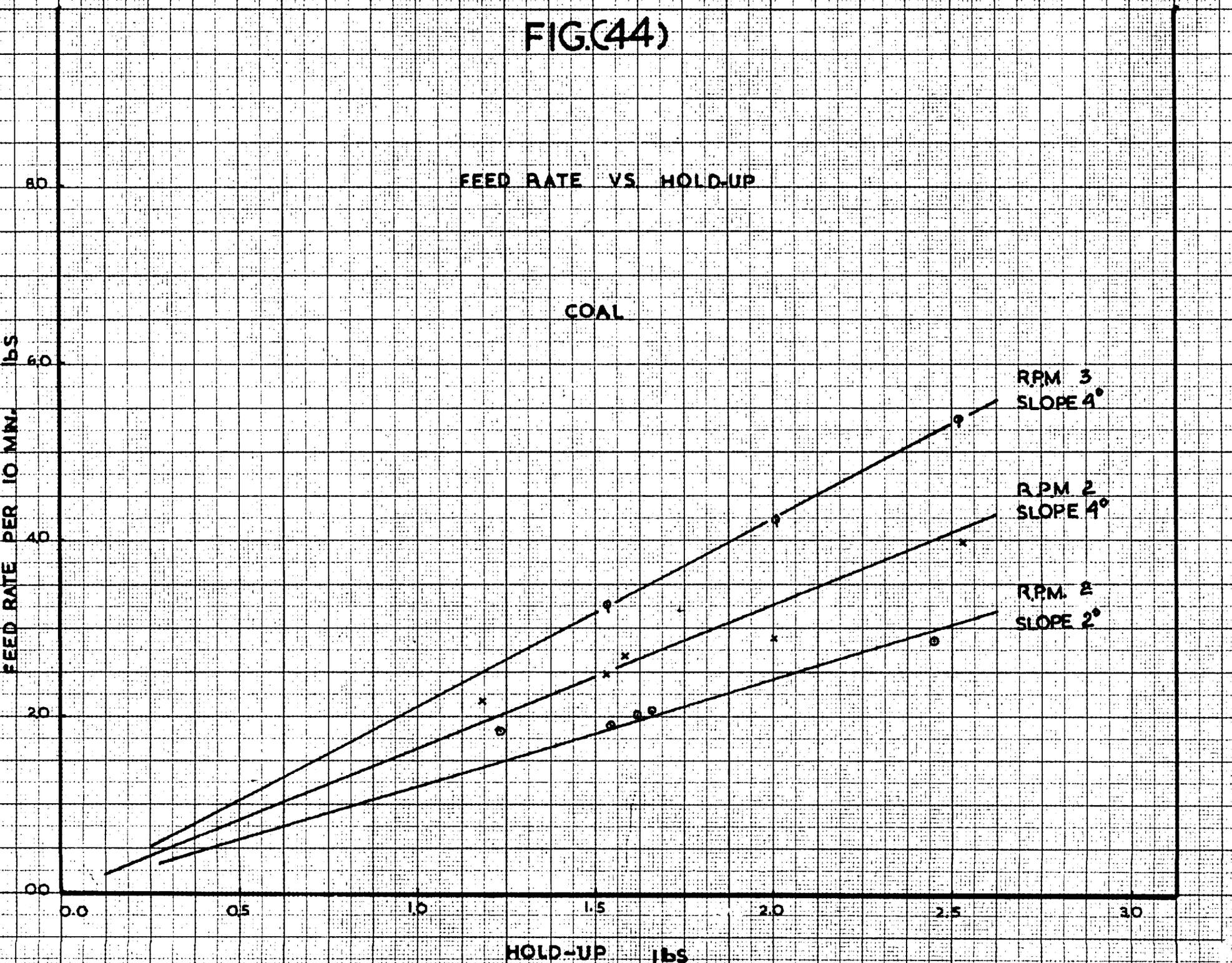
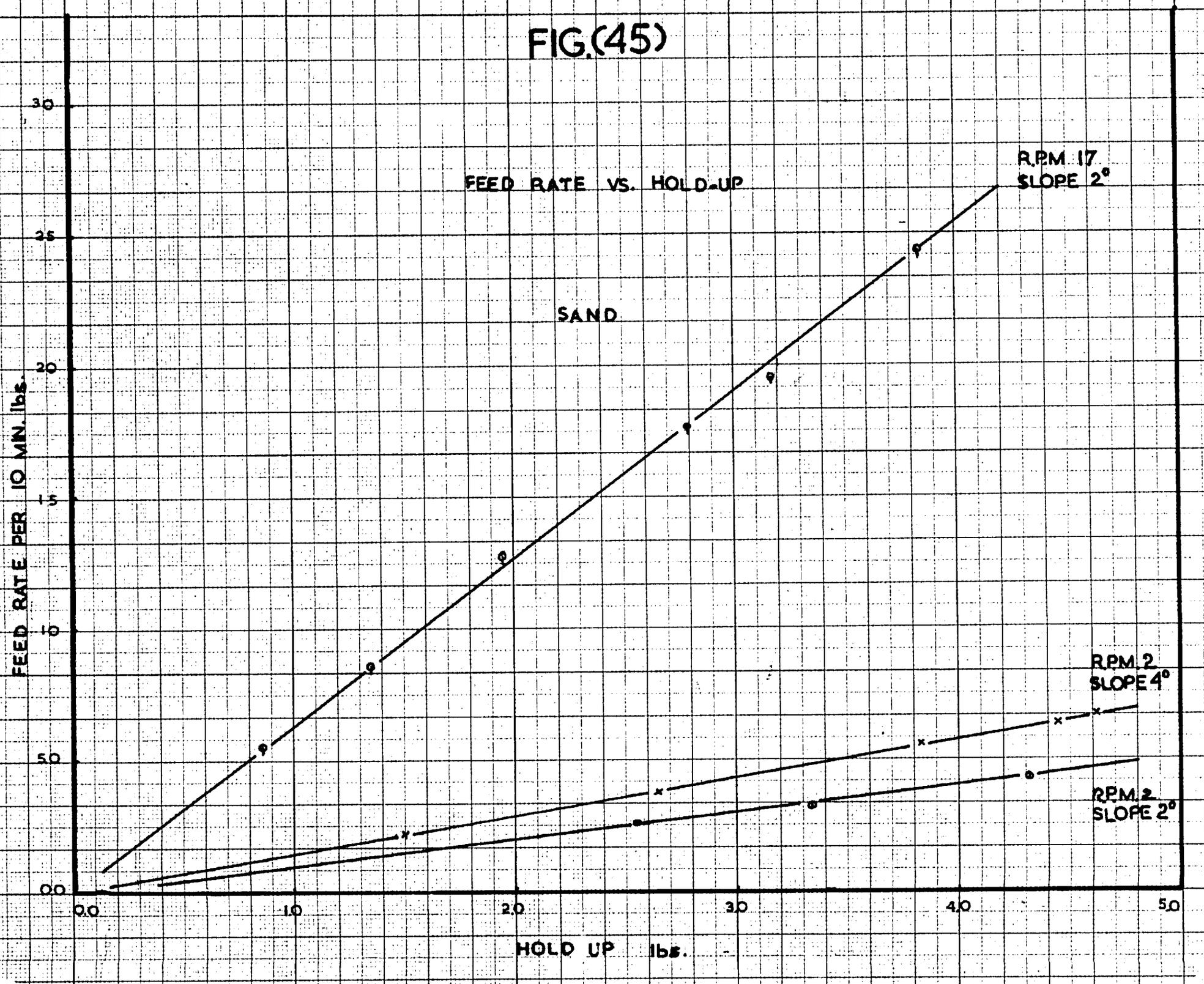

FEED RATE VS. HOLD-UP
COAL
FEED RATE PER 10 MIN. lbs
80
60
40
20
00
0.0
0.5
1.0
1.5
2.0
2.5
3.0
HOLD-UP lbs
R.P.M. 3
SLOPE 9°
R.P.M. 2
SLOPE 9°
R.P.M. 2
SLOPE 2°

FIG.(45)


FEED RATE VS. HOLD-UP
SAND
R.P.M. 17
SLOPE 2°
R.P.M. 2
SLOPE 4°
R.P.M. 2
SLOPE 2°
FEED RATE PER 10 MN. lbs.
HOLD UP lbs.
0.0
1.0
2.0
3.0
4.0
5.0
0.0
5.0
10
15
20
25
30

7. Bed Slope vs Cylinder Slope.

The effect of the feed-rate on the slope of the bed is evident from the previous experiments i.e. as the feed-rate increases, the bed slope will also increase.

When the cylinder is rotating at a given speed, with a hold-up amounting to 25% of the cylinder volume, it has been observed that over a cylinder inclination range of 1 to 10 degrees, the difference between the slope of the bed ϕ and the cylinder slope S, remains practically constant. (see Tables 20 (a) and (b)).

On the basis of these results, the relationship between ϕ and S for a 25% hold-up can be expressed as:

$$\phi = S + 2 \qquad (90)$$

where

ϕ = Slope of the bed Degrees.

S = " " " cylinder Degrees.

Table (20).

Cylinder Slope vs Bed Slope.

(a)

Coal (- 18 + 22) Mesh. B.S.S. R.P.M. = 10.

No.	Feed Rate. lbs/min.	Cylinder Slope S Deg.	Bed Slope Deg.
1.	0·303	0	2
2.	0·332	1	3
3.	0·806	2	4·5
4.	0·906	3	5
5.	1·330	4	6
6.	1·425	5	6·5
7.	1·425	6	7·5
8.	1·475	8	10
9.	2·345	10	11·75
10.	2·210	12	14
11.	3·985	15	17

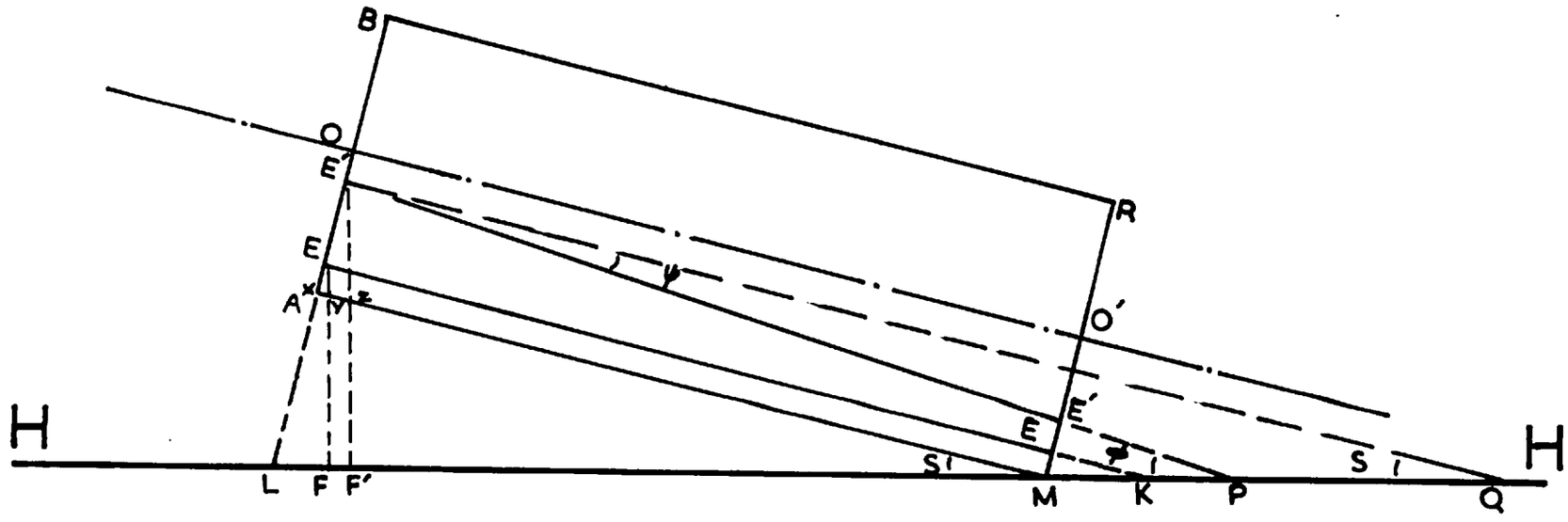
(b)

Gravel (+ 18) Mesh B.S.S. R.P.M. = 10.

1.	2·400	0	2
2.	2·830	1	3
3.	2·175	2	4
4.	3·620	3	5
5.	4·660	4	6
6.	3·445	5	7
7.	3·770	6	8
8.	3·175	8	9·5
9.	8·790	10	12
10.	15·850	12	14

FIG. (46)

ANGLE OF SLIDE VS. CYLINDER INCLINATION



CHAPTER 7.

Theory.

1. Angle of Slide (or Descent) vs Angle of Inclination of Cylinder. (A geometric analysis).

Referring to Fig. (46), BRAM is a cylinder rotating at a speed of N R.P.M. and inclined at angle S to the horizontal.

Two situations may arise, in one case the surface of the hold-up material, is parallel to the cylinder and in the second case it is inclined to the horizontal HH at an angle ϕ . The former situation is less common while the latter corresponds to usual kiln-practice. It will now be shown geometrically, that the angle of slide (to be defined later) in each case is equal to the slope of the cylinder S and not the slope of bed ϕ . It will also be explained why the slope of the bed ϕ rather than the slope of the cylinder S, has been incorporated in the proposed theoretical analysis.

For ordinary hold-ups it will be noted that the surface indicated by the line EE is parallel to the cylinder wall AM. EE when produced back meets the horizontal line HH in K, giving an angle EKH equal to angle AMH, the slope of the cylinder S. Produce BA to

meet the line HH in L and from E drop a perpendicular on the line HH at F. Since triangles LEF and LEK are both right angled, it can easily be shown:

Angle LEF = Angle EKL = Angle S (91)

where the angle LEF may be called the angle of Slide or Descent of Particles or Granules.

Thus it is easy to visualise that for small hold-ups i.e. where the hold-up surface is parallel to the cylinder wall, the angle of slide or descent is equal to the slope of the cylinder.

In the second case, let EE' represent the inclined surface of the bed which when produced back, meets the line HH in P, to give an angle $E'PH$ ($= \phi$). Again from E' drop perpendicular $E'F'$ on HH at F'. The triangles $LE'F'$ and $LE'P$ are not equiangular, and consequently the angle $LE'F'$, the angle of slide, is not equal to the angle LPE' ($= \phi$). But the triangles LEF and $LE'F'$ are equiangular and hence the angle of descent, in the second case also is equal to the slope of the cylinder S.

Thus it may be concluded that whatever be the hold-up, the angle of descent is always equal to the

slope of the cylinder.

Taking this argument further, it is possible to show that there exists a relationship between the angles ϕ and S such as:

$$\phi = S + \psi \qquad (92)$$

where ψ = Angle between the slope of the bed and that of the cylinder. Degrees.

ϕ and S are as already defined.

It has been shown experimentally (see Chapter VI) that for hold-ups 25% of the cylinder volume, the value of the angle ψ is approximately 2 degrees. Hence

$$\phi = S + 2 \qquad (93)$$

How the hold-up effects the number of cycles of a granule over the cylinder length, may be seen from the triangle XEY and XE'Z. In these triangles XY represents the advancement per cycle when the hold-up corresponds to EE and XZ shows the advancement per cycle when the hold-up rises to E'E'. Thus it will be seen that for large hold-ups, the advancement per cycle is greater than for low hold-ups i.e. XZ > XY, at the feed-end of the cylinder. This means that the number of cycles diminish with increase of hold-up.

From the foregoing discussion, it may therefore be concluded that:

(1) The angle of descent is equal to the slope of the cylinder, whatever the hold-up may be.

(2) For a given hold-up the angle ϕ is related to the angle S, by the expression $\phi = S + \psi$, the value of ψ for hold-ups 25% (approx.) being nearly equal to 2 degrees.

(3) The number of cycles made by a granule traversing the cylinder depends on the hold-up or the angle ϕ.

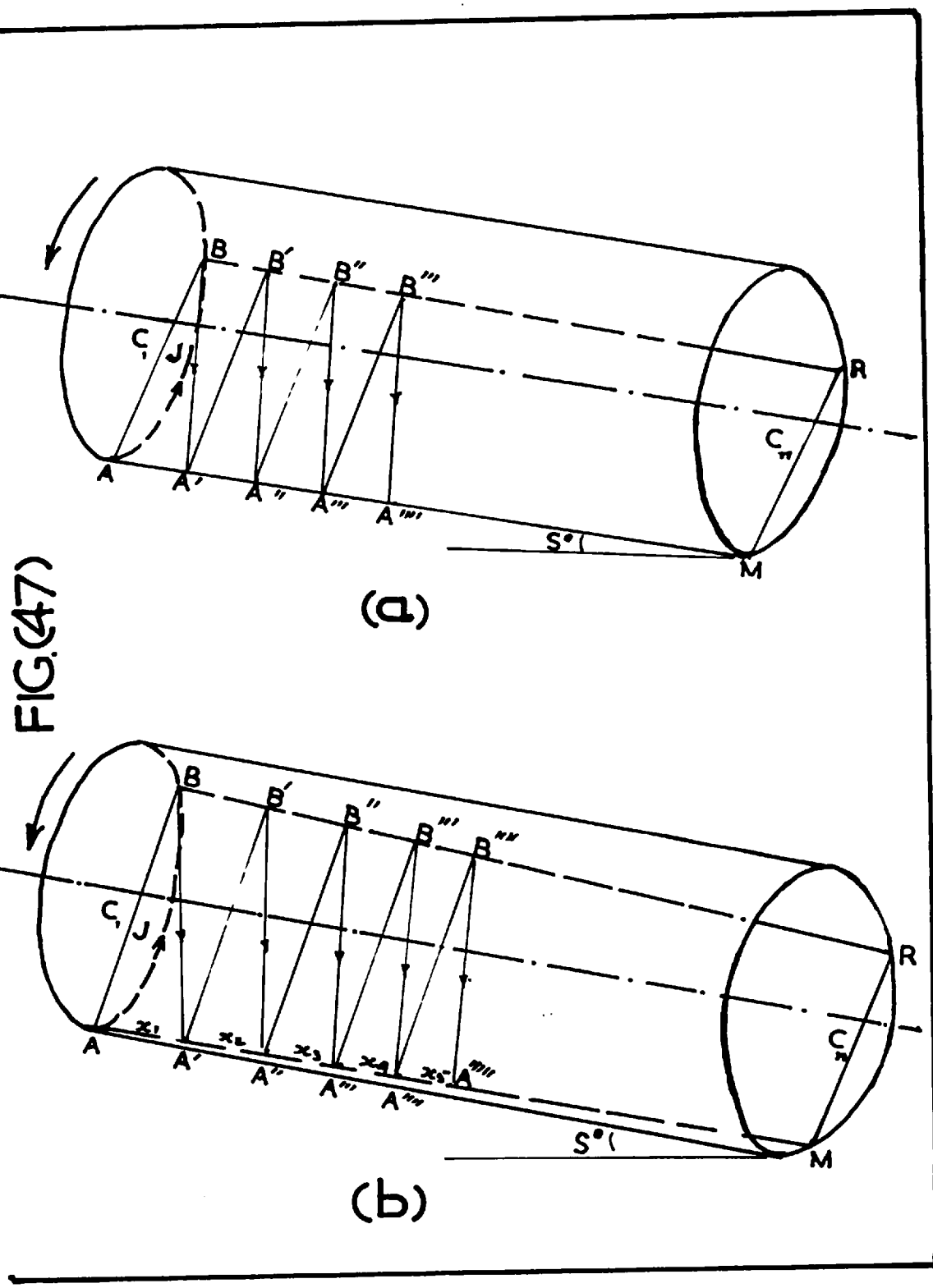
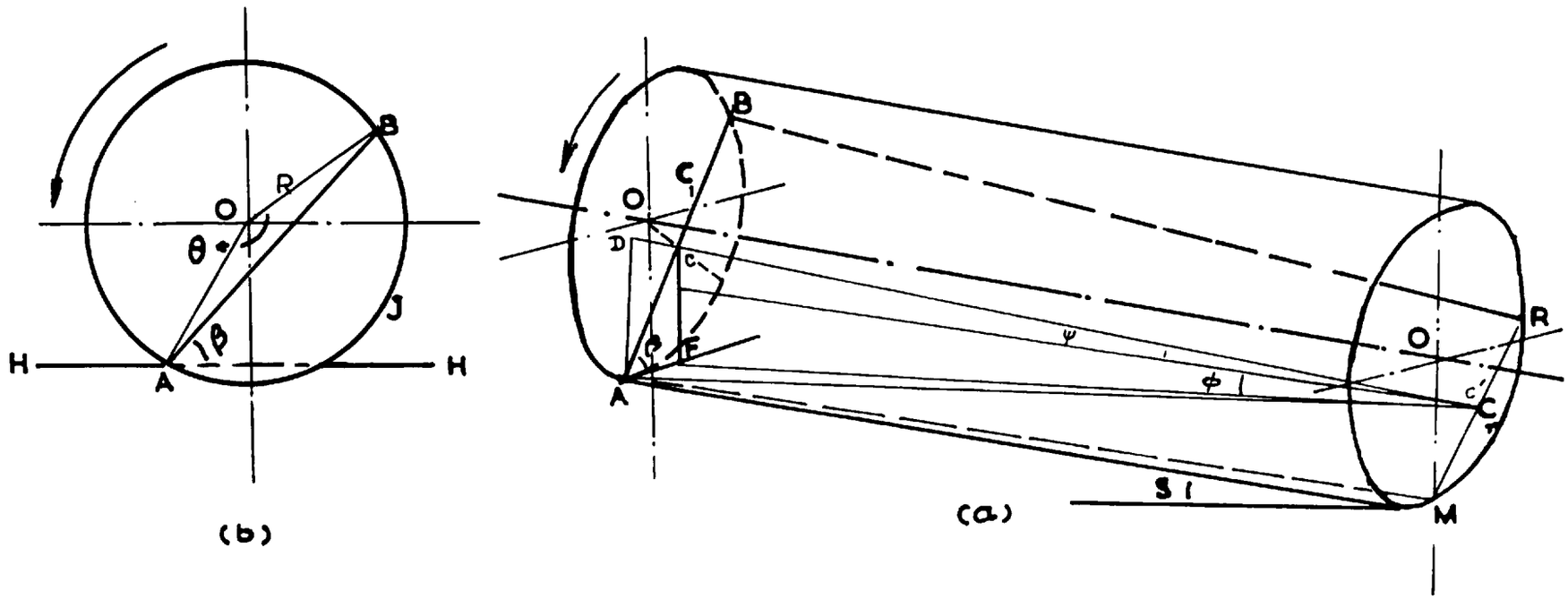
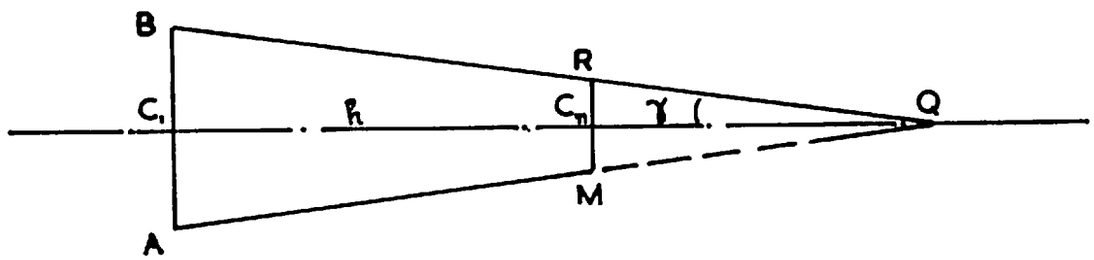


FIG.(47)

FIG(48)





Theory.

The theoretical treatments so far proposed, have already been discussed in brief. It will be noted that practically all the correlations (excepting Saeman's) are based on the assumption that the slope of the bed is equal to the slope of the cylinder. This assumption no doubt simplifies the solution but appears to be contrary to the usual kiln practices where the bed is inclined at an angle greater than the slope of the cylinder.

2. Number of Cycles over Cylinder Length.

When the slope of the hold-up is equal to that of the cylinder, it is relatively simple to find the number of cycles per unit length of cylinder, because the 'advancement' of the granule along the foot of the charge per cycle remains unaltered (Fig. 47a). When the slope of the bed is greater than the slope of the cylinder, this 'advancement' per cycle diminishes as the granule progresses towards the exit-end of the cylinder (see Fig. 47b).

Let us now consider Fig. 48 (a) where a cylinder of length L and diameter D, inclined at angle S

with the horizontal, is shown rotating on its axis OO', in the direction indicated by the arrow. ABRM represents the inclined surface of the hold-up material and the location of the points OO' is such that they lie in a plane at right angles to the axis of the cylinder. From O and O' drop perpendiculars to meet AB and RM in C and C'. Join C and C'. Again drop perpendicular from C to meet the horizontal line AF in F. The angle BAF will then indicate the dyn. angle of repose of the material. Join F and A with C and assume that both the lines $C'F$ and $C'A$ lie in the same horizontal plan.

From the right angled triangles CFC' and CFA, it is evident that

$$CF = CC' \text{ Sin } \phi = L \text{ Sin } \phi \qquad (94)$$

and $$CF = CA \text{ Sin } \beta = C1/_2 \text{ Sin } \beta \qquad (95)$$

Eliminating CF from equations (94) and (95), we get:

$$CC' = C1/_2 \cdot \frac{\text{Sin } \beta}{\text{Sin } \phi} \qquad (96)$$

DA shows half the path of the granule sliding down the inclined surface. Since $C'A$ is horizontal, the angle DAC will be a right angle, CD, which is obtained by producing $C'C$ to join AD in D, shows half the advancement of the granule per cycle along the foot

of the charge. Thus from the right angled triangles DAC and ACC',

$$CD = \frac{(CA)^2}{CC'} \qquad (97)$$

Since $2CA = C_1 = AB$ and $CC' = C1/_2 . \frac{\text{Sin } \beta}{\text{Sin } \phi}$, these values when substituted in equation (97) give:

$$2CD\ (= AA') = C_1 . \frac{\text{Sin } \phi}{\text{Sin } \beta} \qquad (98)$$

where AA' = Advancement per cycle, along the foot of the charge. (Fig. 9b).

ϕ = Slope of the bed. Degrees.

β = Dyn. angle of repose. Degrees.

C_1 = Length of the chord AB.

Referring to Fig. 47 (b), it may be recalled that as the granule progresses through the rotary-cylinder, the distance AA' moved per cycle, diminishes along the foot of the charge in a manner such that $AA' > A'A'' > A''A''' >$ ------ and so on. Fig. 48(c) indicates that the free surface of the bed ABRM resembles a trapezium, whose sides BR and AM, when produced back meet at Q where the angle AQB is equal to 2δ. IF AB is denoted by C_1 and RM by C_n and the height of the trapezium be h, then we may write:

$$\tan \gamma = \frac{C_1 - C_n}{2h} = \frac{C_1 - C_n}{2L'} \qquad (99)$$

where $L' = L \text{ Sec.} \psi$

and the other variables have the same significance as explained before.

Let the increments AA', $A'A''$, $A''A'''$, ------ be denoted by x_1, x_2, x_3, ------- x_n ; equation (98) can be rew ritten in the form:

$$x_1 = C_1 \cdot \frac{\text{Sin } \phi}{\text{Sin } \beta}$$

$$x_2 = C_2 \cdot \frac{\text{Sin } \phi}{\text{Sin } \beta}$$

$$x_3 = C_3 \cdot \frac{\text{Sin } \phi}{\text{Sin } \beta}$$

$$x_4 = C_4 \cdot \frac{\text{Sin } \phi}{\text{Sin } \beta}$$

$$x_n = C_n \cdot \frac{\text{Sin } \phi}{\text{Sin } \beta} \qquad (100)$$

In equation (99), it has been shown that $\tan \gamma = \frac{C_1 = C_n}{2 L'}$, whence it is possible to develope the following series:

$$C_1 = (C_n + 2L \tan \gamma)$$

$$C_2 = C_n + 2 \tan \gamma \ (L - x_1)$$

$$= (C_n + 2L \tan \gamma)(1 - 2 \tan \gamma \cdot \frac{\sin \phi}{\sin \beta})$$

$$= C_1 \cdot (1 - 2 \tan \gamma \cdot \frac{\sin \phi}{\sin \beta}).$$

$$C_3 = C_1 \cdot (1 - 2 \tan \gamma \cdot \frac{\sin \phi}{\sin \beta})^2$$

$$C_4 = C_1 \cdot (1 - 2 \tan \gamma \cdot \frac{\sin \phi}{\sin \beta})^3$$

$$C_n = C_1 \cdot (1 - 2 \tan \gamma \cdot \frac{\sin \phi}{\sin \beta})^{n-1} \quad (101)$$

Substituting the values of C_1, C_2, C_3 ------ and C_n in series (100), we get:

$$x_1 = C_1 \cdot \frac{\sin \phi}{\sin \beta}$$

$$x_2 = C_1 \cdot \frac{\sin \phi}{\sin \beta} \ (1 - 2 \tan \gamma \cdot \frac{\sin \phi}{\sin \beta})$$

$$x_3 = C_1 \cdot \frac{\sin \phi}{\sin \beta} \ (1 - 2 \tan \gamma \cdot \frac{\sin \phi}{\sin \beta})^2$$

$$x_n = C_1 \cdot \frac{\sin \phi}{\sin \beta} \ (1 - 2 \tan \gamma \cdot \frac{\sin \phi}{\sin \beta})^{n-1} \quad (102)$$

Series (102) is obviously a converging Geometric-Series, with a common-ratio r equal to:

$$r = 1 - 2 \tan \gamma \quad \frac{\text{Sin } \phi}{\text{Sin } \beta}$$

$$= 1 - \frac{C_1 - C_n}{L} \cdot \quad \frac{\text{Sin } \phi}{\text{Sin } \beta} \qquad (103)$$

In the light of the foregoing analysis it is now possible, to determine the number of cycles N', the granule will complete before dropping out of cylinder. In a converging geometric-series, the number of the terms N', constituting the series, is given by the expression:

$$N' = \frac{\log (l) - \log (a)}{\log (r)} + 1 \qquad (104)$$

where

N = Number of the terms in the series.

l = Last term in the series.

a = First term.

r = Common Ratio.

Example.

A glass cylinder 2·1 feet in length and 0·3386 feet in diameter, is rotating at 2 R.P.M. The slope of the bed is 6 while that of the cylinder is 4 degrees. If the bed-depth at the feed and discharge-end, is 0·144 ft. and 0·04 feet respectively, how many times would a

granule cascade before falling out of the free-end? The dyn. angle of repose of the material being 34 Degrees.

Solution:

C_1 and C_n, the chord-lengths at both the ends of the cylinder can be worked out with the help of formula:

$$C_1 = 2\sqrt{Dh_1 - h_1^2} = 0{\cdot}336 \text{ ft.}$$

$$C_2 = 2\sqrt{Dh_2 - h_2^2} = 0{\cdot}218 \text{ ft.}$$

Since the number of the cycles or cascades is given by the expression:

$$N' = \frac{\log (l) - \log (a)}{\log (r)} + 1 \qquad (104)$$

where $a = C_1 \cdot \frac{\text{Sin } \phi}{\text{Sin } \beta} = 0{\cdot}0627$ ft.

$l = C_n \cdot \frac{\text{Sin } \phi}{\text{Sin } \beta} = 0{\cdot}0407$ ft.

and $r = 1 - \frac{C_1 - C_n}{L} \cdot \frac{\text{Sin } \phi}{\text{Sin } \beta} = 0{\cdot}9895$

Substituting these values in the above equation, we get:

$$N' = \frac{\log (0{\cdot}0407) - \log (0{\cdot}0627)}{\log (0{\cdot}9895)} + 1$$

$$= \frac{\bar{2}{\cdot}60959 - \bar{2}{\cdot}79787}{\bar{1}{\cdot}99542} + 1$$

$$= 42$$

Thus a granule moving in contact with the cylinder wall, under the above conditions, will cascade 42 times before falling out of the free-end.

3. Time of Passage through Rotary Cylinder.

The preceding analysis can now be utilised to find the average time of passage of a granular material through an inclined rotary-cylinder. We know that each cycle of granular movement, consists of an arc S and chord C (fig.48 (b)) and that the time spent by the granule in moving down the inclined plan (along the chord C), is negligible as compared with the time spent on the arc S. Thus if we sum up all such 'arcs', the analytical expression for the time of passage can be worked out in the following manner.

From elementary geometry, the length of the arc S, can be expressed as:

$$S = D \cdot \theta/_2$$

$$= D \, \mathrm{Sin}^{-1} \, C_1/_D \qquad (105)$$

where

θ = The angle subtended by the arc S or chord C_1 at the centre of the circle of reference. (Radians.)

Assuming * that the convergency ratio r, of the 'arcs' is the same as that of the granular 'advancements' along the foot of the charge, the 'arcs' may be summed up with the help of the following expression, generally used for summing up convergent geometric series:

$$S_m = \frac{a}{1 - r}\ (1 - r^{N'}) \qquad (106)$$

where S_m = Sum of N terms.

a = First term.

r = Convergency ratio.

N' = Number of terms.

But $a = S = D \sin^{-1} C_1/_D$

$$r = 1 - 2 \tan \gamma \cdot \frac{\sin \phi}{\sin \beta} = 1 - \left(\frac{C_1 - C_n}{L}\right)\left(\frac{\sin \phi}{\sin \beta}\right)$$

N = Number of cycles.

= 42.

These values when substituted in equation (106), we get:

$$S_m = \frac{D.\ \sin^{-1} C_1/_D}{\frac{C_1 - C_n}{L'} \cdot \frac{\sin \phi}{\sin \beta}}\ (1 - r^{N'}) \qquad (107)$$

In equation (107), $\sin^{-1} C_1/_D$ may be expanded into the following series:

---

* For explanation, please see discussion.

$$\text{Sin}^{-1}\ C_1/_D = \left(\frac{C_1}{D}\right) + \frac{(C_1/_D)^3}{6} + \frac{3(C_1/_D)^5}{40} \text{-------}$$

$$\text{when } -1 < C_1/_D < +1$$

Assuming $\text{Sin}^{-1}\ C_1/_D$ * is equal to $C_1/_D$ we get:

$$S_m = \frac{L' \text{Sin}\ \beta}{\text{Sin}\ \phi} \cdot \frac{C_1}{C_1 - C_n} \cdot [\ 1 - r^{N'}] \qquad (108)$$

When the above equation is divided by (π D), the number of 'circumferences' can be expressed as:

$$\text{Number of circumferences} = \frac{L' \text{Sin}\ \beta}{\pi D\ \text{Sin}\ \phi} \cdot \frac{C_1}{C_1 - C_n} [.1 - r^{N'}] \qquad (109)$$

If N is the number of revolutions per minute of the rotary-cylinder, then the time of passage is given by the following equation:

$$\text{Time of passage } t = \frac{L' \text{Sin}\ \beta}{\pi\ DN \text{Sin}\ \phi} \cdot \frac{C_1}{C_1 - C_n} \cdot [\ 1 - r^{N'}] \qquad (110)$$

Since it is difficult to measure C_1 and C_n the chord lengths at the feed and the discharge ends, they can be expressed in terms of bed-depths h_1 and h_2 and the above equation may be re-written to show:

---

* See discussion.

$$t = \frac{L' \sin \beta}{\pi DN . \sin \phi} \cdot \frac{\sqrt{Dh_1 - h_1^2}}{\sqrt{Dh_1 - h_1^2} - \sqrt{Dh_2 - h_2^2}} \cdot (1 - r^{N'}) \qquad (111)$$

where t = Average time of passage. mts.

β = Dyn. angle of repose. Degrees.

ϕ = Slope of the bed. Degrees.

L' = L Sin ψ , where L is the length of the cylinder. Ft.

D = Diameter of the cylinder. Ft.

h_1 = Bed-depth at feed-end. Ft.

h_2 = Bed-depth " Discharge end. Ft.

r = Convergency ratio.

N' = Number of cycles.

For 25% hold-up when h_1 = 0·144 ft. and h_2 = 0·04 ft., the above relationship is simplified to the form:

$$t = \frac{0.326 \, L \sin \beta}{D \, N \sin \phi} \qquad (112)$$

4. Discussion.

The theoretical approach to find out the time of passage of free flowing granular materials through

inclined rotary kilns/dryers, is based upon the geometrical movement of the granules lying in immediate contact with the shell.

Pickering, Feakes etc. etc. (44) gave an analysis based on the assumption that the slope of the bed is equal to the slope of the cylinder, which is contrary to usual kiln-practice.

Seaman's analysis is rigid and takes into account the difference in slope between the bed and cylinder.

The present analysis differs from the previous ones in that it takes into account not only the slope of the bed ϕ , but also the number of the cycles N' and the bed depths h_1 and h_2 over the cylinder ends. It has been assumed that the arcs S_1, S_2, S_3, ------ S_n belong to a convergent geometric series and that the convergency ratio S_2/S_1 of the arcs is the same as that of 'the advancements', x_2/x_1 along the foot of the charge. This assumption has been made owing to the lack of an analytical expression for the convergency ratio of the following series:

$$S_1 = D \sin^{-1} \left(C_1/_D\right)$$

$$S_2 = D \sin^{-1} \left(C_2/_D\right) = D \sin^{-1}\left[C_1/_D\left(1 - 2 \tan\gamma \frac{\sin\phi}{\sin\beta}\right)\right]$$

$$S_3 = D \sin^{-1}\left(C_3/_D\right) = D \sin^{-1}\left[C_1/_D\left(1 - 2 \tan\gamma \frac{\sin\phi}{\sin\beta}\right)^2\right]$$

$$S_4 = D \sin^{-1}\left(C_4/_D\right) = D \sin^{-1}\left[C_1/_D\left(1 - 2 \tan\gamma \frac{\sin\phi}{\sin\beta}\right)^3\right]$$

$$S_n = D \sin^{-1}\left(\frac{C_n}{D}\right) = D \sin^{-1}\left[C_1/_D\left(1 - 2 \tan\gamma \frac{\sin\phi}{\sin\beta}\right)^{n-1}\right] \quad (113)$$

The convergency ratio 'r' may be expressed as:

$$r = S_2/_{S_1} = \frac{\sin^{-1}\left[C_1/_D \left(1 - 2 \tan\gamma . \frac{\sin\phi}{\sin\beta}\right)\right]}{\sin^{-1}\left(C_1/_D \right)} \quad (114)$$

Though with the help of equation (114), it is possible to find out the numerical value of the ratio r it seems difficult to obtain any analytical expression which could be used in subsequent analysis. Thus there is no way out except to assume that the series S_1, S_2, S_3, -------- S_n is a convergent geometric series and that its convergency ratio is the same as that of the 'advancements' along the foot of the charge.

Again in course of summation of the arcs S_1, S_2, S_3 -------- S_n, the first term of the series namely

D. $\mathrm{Sin}^{-1}\left(\frac{C}{D}\right)$ has been simplified to D $\left(\frac{C}{D}\right)$. Since the angle $\mathrm{Sin}^{-1}\left(\frac{C}{D}\right)$ is about 160 degrees, this simplification introduces an error of about 15%. The overall deviation between the observed and the theoretical values is about $\pm$ 25%.

A P P E N D I X

Table (1)

Bulk-density as function of Particle-Size

No.	Material	Particle Size (d_a)	$\log(d_a)$	Bulk-Density (ρ_a)	$\log(\rho_a)$
		19.666×10^{-4}	$\bar{3}.2936$	55.2	1.7259
		15.125x	$\bar{3}.1796$	49.8	1.6972
1.	Coal	11.758x	$\bar{3}.0700$	46.0	1.6628
		8.980x	$\bar{4}.9523$	44.6	1.6493
		7.042x	$\bar{4}.8477$	41.8	1.6212
		20.917x	$\bar{3}.3204$	78.9	1.8971
		11.042x	$\bar{3}.0429$	72.9	1.8627
2.	Felspar	7.042x	$\bar{4}.8477$	68.8	1.8248
		5.250x	$\bar{4}.7202$	-	-
				104.5	2.0191
				91.1	1.9595
3.	Sand	--do--	--do--	79.0	1.8977
				72.0	1.8574
				81.3	1.9101
4.	Limestone	--do--	--do--	78.2	1.8932
				73.6	1.8669
				70	1.8451
				106.2	2.0261
				90.2	1.9552
5.	Magnesite	--do--	--do--	86.8	1.9386
				84.2	1.9354

TABLE (2)

COAL

VARIATION WITH SPEED OF THE SURFACE DYNAMIC ANGLE OF REPOSE 'β'

NO	CYLINDER SPEED (R.P.M) N	RATIO OF CYLINDER SPEED TO CRITICAL SPEED. N/Nc	(18–30) MESH		(30–36) MESH		(36–52) MESH		(52–60) MESH		(60–85) MESH	
			β° DEG.	1/β	β°	1/β	β°	1/β	β°	1/β	β°	1/β
1.	0	—	34	—	34	—	34	—	33.5	—	33.5	—
2.	2	0.015	34.5	0.02899	34.5	0.02899	34.5	0.02899	34	0.02941	34	0.02941
3.	5	0.0374	34	0.02941	34	0.02991	34	0.02941	33	0.03030	32	0.03125
4.	10	0.0748	33	0.03030	32.5	0.03060	32	0.03125	32	0.03125	31	0.03225
5.	20	0.15	31.5	0.03175	31	0.03225	30	0.03333	29	0.03448	28	0.03571
6.	30	0.2243	29.5	0.03391	29	0.03448	28	0.03571	27.5	0.03637	25	0.04
7.	40	0.2990	28	0.03571	27	0.03703	26	0.03846	25	0.04	23	0.04348
8.	50	0.3738	26.5	0.03775	26	0.03846	25	0.04	23.5	0.042	22	0.04545
9.	60	0.4486	25.5	0.03923	25	0.040	24	0.04166	22.5	0.0446	20	0.05
10.	70	0.5233	24.5	0.04083	23.5	0.042	23	0.04348	21.5	0.04653	19	0.05263

TABLE (3)

FELSPAR VARIATION WITH SPEED OF THE SURFACE DYN. ANGLE OF REPOSE 'β'

NO.	CYLINDER SPEED (R.P.M.) N	RATIO OF CYLINDER SPEED TO CRITICAL SPEED N/N_c	(18–36) MESH		(36–60) MESH		(60–85) MESH		(85–100) MESH	
			β° Deg.	1/β	β°	1/β	β	1/β	β	1/β
1.	0	—	35	—	35	—	34.5	—		
2.	2	0.015	35.5	0.0282	—	—	—	—		
3.	5	0.0374	35	0.02857	—	—	33	0.0303		
4.	10	0.0748	34	0.02941	33.5	0.0297	31	0.03225		
5.	20	0.15	33	0.3030	32	0.03125	29	0.03448	— NIL —.	
6.	30	0.2243	32	0.03125	30	0.0333	27	0.03704		
7.	40	0.2990	30	0.03333	28.5	0.03510	25	0.04		
8.	50	0.3738	29	0.03448	26.5	0.03775	23	0.04348		
9.	60	0.4486	28	0.03571	25	0.040	22	0.04545		
10.	70	0.5233	27	0.03704	24	0.0416	21	0.04762		

TABLE (4)

SAND

VARIATION WITH SPEED OF THE SURFACE DYN. ANGLE OF REPOSE 'β'

NO.	CYLINDER SPEED (R.P.M) N	RATIO OF CYLINDER SPEED TO CRITICAL SPEED N/Nc	(18-36) MESH		(36-60) MESH		(60-85) MESH		(85-100) MESH	
			β° Deg.	1/β	β°	1/β	β	1/β	β	1/β
1.	0	—	34	—	34	—	33.5	—	33	—
2.	2	0.015	34	0.02899	34	0.02941	34.5	0.02899	33.5	0.0297
3.	5	0.0374	34	0.02899	33	0.03030	33	0.0303	32	0.03125
4.	10	0.0748	32.5	0.0306	31	0.03226	30	0.0333	29.5	0.03391
5.	20	0.15	30	0.0333	27	0.03704	26	0.03846	25	0.04
6.	30	0.2243	28	0.03571	25.5	0.03923	24	0.04167	23	0.04348
7.	40	0.2990	26	0.03846	24.5	0.04083	21.5	0.04653	20.5	0.04881
8.	50	0.3738	24.5	0.04083	22.5	0.04446	20	0.05	18	0.05555
9.	60	0.4486	23.5	0.042	21	0.04762	18.5	0.05409	16	0.0625
10	70	0.5233	22.5	0.0446	20	0.05	17	0.05882	14.5	0.06905

TABLE (5)

LIMESTONE

VARIATION WITH SPEED OF THE SURFACE DYN. ANGLE OF REPOSE 'β'

NO	CYLINDER SPEED (R.P.M) N	RATIO OF CYLINDER SPEED TO CRITICAL SPEED N/Nc	(18-36) MESH		(36-60) MESH		(60-85) MESH		(85-100) MESH	
			β° Deg.	1/β	β°	1/β	β°	1/β	β°	1/β
1.	0	—	37	—	36.5	—	36	—	35	—
2.	2	0.015	37.5	0.02667	37	0.02702	36	0.02778	36	0.02778
3.	5	0.0374	36	0.02778	36	0.02778	35.5	0.02817	35	0.02857
4.	10	0.0748	35	0.02857	35	0.02857	34	0.02941	33	0.03030
5.	20	0.150	34	0.02941	33.5	0.0297	32	0.03125	31	0.03226
6.	30	0.2243	32.5	0.0306	31	0.03225	29.5	0.03391	27	0.03704
7.	40	0.2990	30.5	0.03279	28	0.03571	27	0.03704	25	0.04
8.	50	0.3738	29	0.03448	27	0.03704	25	0.04	23	0.04348
9.	60	0.4486	28	0.03571	25.5	0.03923	23.5	0.042	22	0.04545
10	70	0.5233	26.5	0.03775	24	0.04167	22.5	0.04446	20	0.05

TABLE(6)

MAGNESITE

VARIATION WITH SPEED OF THE SURFACE DYN. ANGLE OF REPOSE 'β'

NO	CYLINDER SPEED (R.P.M) N	RATIO OF CYLIN-DER SPEED To CRITICAL SPEED N/Nc	(18-36) MESH		(36-60) MESH		(60-85) MESH		(85-100) MESH	
			β° Deg.	1/β	β°	1/β	β	1/β	β	1/β
1.	0	—	35.5	—	35	—	34.5	—	34.5	—
2.	2	0.015	36	0.02767	35.5	0.02817	35	0.02857	35	0.02899
3.	5	0.0374	35.5	0.02817	35	0.02857	34.5	0.02899	34	0.02941
4.	10	0.0748	34.5	0.02899	34	0.02941	33	0.03030	32	0.03125
5.	20	0.150	33	0.03030	32	0.03125	31	0.03125	29	0.03448
6.	30	0.2243	30.5	0.03279	29.5	0.03391	29	0.03448	25.5	0.03923
7.	40	0.2990	29.5	0.03391	28	0.03571	26	0.03846	23.5	0.042
8.	50	0.3738	28	0.03571	26	0.03846	24	0.04167	21.5	0.04654
9.	60	0.4486	26.5	0.03775	24.5	0.04083	22	0.04545	19.5	0.05138
10.	70	0.5233	25	0.04	23.5	0.0420	21	0.04762	18.5	0.05409

Table(7)

B'' as function of a) Particle-Size(d_a) and b) the ratio of Bulk-Density to True-Density.

No.	Material	B''	Particle Size. Ft.	Bulk-Density / True-Density
		42.055	19.666×10^{-4}	0.601
		35.942	15.125x	0.562
		34.259	11.758x	0.519
1.	Coal	29.073	8.980x	0.503
		21.805	7.042x	0.472
		53.400	20.917x	0.610
		40.050	11.042x	0.564
2.	Felspar	27.185	7.042x	0.532
		---	5.252x	---
		32.224		0.631
		23.787	--do--	0.544
3.	Sand	17.430		0.471
		13.364		0.428
		49.840		0.489
		34.772		0.471
4.	Limestone	29.904	--do--	0.443
		22.885		0.421
		43.610		0.509
		36.712		0.433
5.	Magnesite	26.116	--do--	0.411
		19.673		0.404

Table(8)

Parabolic Theory of Free - Flight.

Coal(-18+36) Mesh B.S.S.

(a)

R.P.M= 20 (=10.5 Cm/Sec.): Angle θ=77 Deg.

$y = 4.3315x - 87.4\ x^2$

No.	x	y
1.	0.0	0.0
2.	0.1	-0.437
3.	0.2	-2.625
4.	0.3	-6.567
5.	0.4	-12.254

(b)

R.P.M.= 30(=15.75 Cm/Sec.) ; Angle θ= 76 Deg.

$y = 4.011x - 34\ x^2$

No.	x	y
1.	0.0	0.0
2.	0.1	+0.064
3.	0.2	-0.558
4.	0.3	-1.857
5.	0.4	-3.836
6.	0.5	-6.495
7.	0.6	-9.814
8.	1.0	-29.989

(c)

R.P.M.=40(=21 Cm/Sec.) ; Angle θ = 75 Deg.

$$y = 5.732\,x - 16.6\,x^2$$

No.	x	y
1.	0.0	0.0
2.	0.1	+0.021
3.	0.2	+0.082
4.	0.3	-0.374
5.	0.4	-1.165
6.	0.5	-2.284
7.	0.6	-4.114
8.	0.8	-7.634
9.	1.0	-12.868

(d)

R.P.M = 50(= 26.25 Cm/Sec.) ; Angle θ = 72 Deg.

$$y = 3.077\,x - 7.46\,x^2$$

No.	x	y
1.	0.0	0.0
2.	0.1	+0.233
3.	0.2	+0.317
4.	0.3	+0.242
5.	0.4	+0.372
6.	0.5	-0.212
7.	0.6	-0.844
8.	0.8	-2.318
9.	1.0	-4.383
10.	1.5	-12.2

(e)

R.P.M. = 60(=31.5 Cm/Sec.) ; Angle θ = 68 Deg.

$$y = 2.475\ x - 3.53\ x^2$$

No.	x	y	$\frac{*}{y}$
1.	0.0	0.0	0.0
2.	0.1	+0.212	+0.179
3.	0.2	+0.354	+0.313
4.	0.3	+0.425	+0.429
5.	0.4	+0.425	+0.502
6.	0.5	+0.356	+0.538
7.	0.6	+0.213	+0.540
8.	0.8	-0.28	+0.448
9.	1.0	-1.055	+0.193
10.	1.2	-	+0.197
11.	1.5	-3.237	-1.038
12.	2.0	-9.169	-3.055
13.	3.0	-24.345	-10.042

(f)

R.P.M.= 70(=56.7 Cm/Sec.) ; Angle θ = 63 Deg.

$$y = 1.963\ x - 1.77\ x^2$$

For different values of x and y, see Table(8) e under column y^*.

Table(9)

Gow's Theory.

Coal (-18+36) Mesh B.S.S.

(a)

R.P.M. =30 (=1575 Cm/Sec.) ; Angle θ = 76 Deg.

$$y = 0.584\left[\log_{10}\ \frac{\cos(\theta - 226\ x)}{\cos\theta}\right]$$

No.	x	y	y^*
1.	0.0	0.0	0.0
2.	0.1	+0.228	+0.265
3.	0.2	+0.321	+0.413
4.	0.3	+0.351	-
5.	0.4	-	+0.566
6.	0.6	-	+0.606

(b)

R .P.M.= 40(=21 Cm/Sec.) ; Angle θ = 75 Deg.

$$y = 1.035\left[\mathrm{Log}_{10}\ \frac{\cos(\theta - 127.5x)}{\cos\theta}\right]$$

For given values of x, the calculated values of y are tabulated in the above table(a) under the column y^* .

(c)

R.P.M. =50 (=26.25 Cm/Sec.) ; Angle θ = 72 Deg.

$$y = 1.62\left[\mathrm{Log}_{10}\ \frac{\cos(\theta - 81.6x)}{\cos\theta}\right]$$

No.	x	y	y^*
1.	0.0	0.0	0.0
2.	0.1	+0.303	+0.266
3.	0.2	+0.426	+0.387
4.	0.4	+0.645	+0.635
5.	0.6	+0.766	+0.796
6.	0.8	+0.82	+0.913
7.	1.0	-	+0.960

(d)

R.P.M.= 60(=31.5 Cm/Sec.) ; Angle θ = 68 Deg.

$$y = 2.328 \ \text{Log}_{10} \ \frac{\text{Cos}(\theta - 56.6x)}{\text{Cos}\ \theta}$$

The values of the co-ordinate y calculated with the help of the above equation are tabulated in Table 9 (c), under column y^{*}.

--

(e)

R.P.M.= 70 (=36.7 Cm/Sec.) ; Angle θ = 63Deg.

$$y = 3.18 \left[\text{Log}_{10} \ \frac{\text{Cos}(\theta - 41.7x)}{\text{Cos}\ \theta} \right]$$

No.	x	y
1.	0.0	0.0
2.	0.1	+0.181
3.	0.2	+0.337
4.	0.4	+0.575
5.	0.6	+0.764
6.	0.8	+0.902
7.	1.0	+0.993
8.	1.5	+1.010
9.	1.75	+1.075

--

Table(10)

Modified Gow's Equation

Coal (-18+36) Mesh B.S.S.

(a)

R.P.M.= 40(=21 Cm/Sec.) ; Angle θ = 75 Deg.

Co-efficient of friction= 0.8391; K= 2.27

$$y = 0.457 \left[\text{Log}_{10} \frac{\text{Cos}(\theta - 289x)}{\text{Cos}\ \theta} \right]$$

No.	x	y	y*
1.	0.0	0	0
2.	0.1	0.196	0.21
3.	0.2	0.259	0.317
4.	0.3	-	0.374
5.	0.4	-	0.397

(b)

R.P.M.= 50 (=26.25 Cm/Sec.) ; Angle θ = 72 Deg.
K= 2.05

$$y = 0.79 \left[\text{Log}_{10} \frac{\text{Cos}(\theta - 72.5x)}{\text{Cos}\ \theta} \right]$$

The values of the co-ordinate 'y' for given values of 'x' may be seen in Table 10 (a) under the column y^*.

(c)

R.P.M.=60 (=31.5 Cm/Sec.) ; Angle θ = 68 Deg.
K = 2.03.

$$y = 1.148 \left[\text{Log}_{D} \frac{\text{Cos}(\theta - 115x)}{\text{Cos}\ \theta} \right]$$

No.	x	y	y^*
1.	0.0	0.0	0.0
2.	0.1	0.192	0.169
3.	0.2	0.276	0.296
4.	0.3	0.4	0.394
5.	0.4	0.451	0.467
6.	0.5	0.482	0.522
7.	0.6	-	0.557
8.	0.8	-	0.597

(d)

R.P.M.= 70 (=36.7 Cm/Sec.); Angle θ = 63 Deg.

K = 1.673.

$$y = 1.74 \ \text{Log}_{10} \ \frac{\text{Cos}(\theta - 75.7x)}{\text{Cos}\ \theta}$$

The values of y calculated with the help of this equation are given in Table 10(c) under column y*.

Table (11)

Discharge- Rate Q Vs. Head

(Orifice Diameter= 0.25 in.)

(b)

Coal (-18+22) Mesh B.S.S.

No.	Head Ft.	Time of Discharge of 5oo cc.(≡0.914 Ibs.)	Discharge Rate Ibs/Sec.
1.	0.916	4 Minutes 40 Secs.	0.00327
2.	0.844	4 30	338
3.	0.760	4 45	320
4.	0.656	4 50	315
5.	0.552	4 55	310
6.	0.438	4 55	310
7.	0.344	4 55	310
8.	0.250	4 45	320
9.	0.157	4 " 50 " .	315

(c)

Sand (-18+22) Mesh B.S.S.

No.	Head Ft.	Time of Discharge of 500 CCs(=1.775Ibs.)	Discharge Rate Ibs/Sec.
1.	0.907	4 Minutes 50 Secs.	0.00612
2.	0.803	4 48	616
3.	0.708	4 50	612
4.	0.604	4 50	612
5.	0.511	4 50	612
6.	0.396	4 48	616
7.	0.302	4 50	612
8.	0.208	4 48	616
9.	0.094	4 48	616
10.	0.021	4 " 50 "	612

(d)

Haematite* (-18+22) Mesh B.S.S.

1.	0.913	2 " 43	0.00997
2.	0.840	2 43	997
3.	0.755	2 43	"
4.	0.657	2 43	"
5.	0.552	2 43	"
6.	0.439	2 43	"
7.	0.343	2 43	"
8.	0.248	2 43	"

---

* 500 CC's ≡ 1.625 Ibs.

Table (12)

Discharge Rate Q VS. Head

(Orifice Diameter=0.375in.)

(a)

Rapeseed (+18) Mesh B.S.S.

No.	Head Ft.	Time of Discharge of 500 CC'S(≡0.713 Ibs)	Discharge Rate Ibs/Sec.
1.	0.896	1 Minute 21 Secs.	0.00881
2.	0.790	1 20	893
3.	0.697	1 20	893
4.	0.625	1 21	881
5.	0.521	1 20	893
6.	0.457	1 20	893
7.	0.365	1 21	881
8.	0.250	1 20	893
9.	0.136	1 20	893
10.	0.073	1 20	893

(b)

Coal* (-18+22) Mesh B.S.S.

1.	0.905	60 Secs.	0.0152
2.	0.813	60	152
3.	0.710	58	158
4.	0.583	58	158
5.	0.500	58	158
6.	0.396	59	155
7.	0.281	58	158
8.	0.208	60	152
9.	0.104	60	152
10.	0.021	55	156

* 500 CC's ≡0.914 Ibs.

(c)

Sand (-18+22) Mesh B.S.S.

No.	Head Ft.	Time of Discharge of 500 CC's(≡1.775Ibs)	Discharge Rate Ibs/Sec.
1.	0.905	1 Minute 5Secs.	0.0273
2.	0.803	0 55	323
3.	0.710	1 0	296
4.	0.604	1 3	281
5.	0.521	1 2	286
6.	0.406	1 5	273
7.	0.302	1 4	277
8.	0.208	1 3	281
9.	0.094	1 5	273
10.	0.021	1 5	273

(d)

Haematite* (-18+22) Mesh B.S.S.

1.	0.906	45.5	0.0357
2.	0.804	46	353
3.	0.707	45	361
4.	0.603	45	361
5.	0.512	46	353
6.	0.396	46	353
7.	0.300	45	361
8.	0.209	46	353

---

* 500 CC's ≡ 1.625 Ibs.

Table (13)

Discharge Rate Vs. Head

(Orifice Dia.=0.5 in.)

(a)

Rapeseed +18 Mesh B.S.S.

No.	Head Ft.	Time of Discharge of 500 CC's(≡ 0.713 Ibs)	Discharge Rate Ibs/Sec.
1.	0.916	25 Seconds	0.0285
2.	0.833	25	0.0285
3.	0.750	23	310
4.	0.656	25	285
5.	0.587	26	274
6.	0.490	26	274
7.	0.396	26	274
8.	0.292	25	285
9.	0.166	26	274
10.	0.092	26	274

(b)

Coal* (-18+22) Mesh B.S.S.

1.	0.907	20 Seconds	0.0456
2.	0.833	19	481
3.	0.740	20	456
4.	0.595	20	456
5.	0.5	19	481
6.	0.407	20	456
7.	0.324	19	481
8.	0.250	20	456
9.	0.146	19	481
10.	0.052	20	456

---

* 500 CC's = 0.914Ibs.

(c)

Sand (-18+22) Mesh B.S.S.

No.	Head Ft.	Time of Discharge of 500 CC's(≡1.775 Ibs.)	Discharge Rate Ibs/Sec.
1.	0.976	21.5 Seconds	0.0826
2.	0.792	21	846
3.	0.740	21	846
4.	0.604	21.5	826
5.	0.5	21.5	826
6.	0.407	21	846
7.	0.29	21	846
8.	0.198	21	846
9.	0.094	21.5	826

(d)

Haematite* (-18+22) Mesh B.S.S.

1.	0.897	15 Seconds	0.108
2.	0.792	14.5	112
3.	0.696	15	108
4.	0.623	15.5	105
5.	0.520	15	108
6.	0.456	15	108
7.	0.360	14.5	112
8.	0.254	15.5	105

* 500 CC's ≡ 1.625 Ibs.

Table (14)

Physical Properties of the Granular Materials

No.	Material	Mean Sieve Dia. Ft.	True-Density Ibs/ C.FT	Bulk Density Ibs/C.Ft.	Angle of Repose (Dyn.)
1.	Starch	2.541×10^{-3}	71.17	50.3	35 Deg.
2.	Coal	"	88.651	51.4	34.5
3.	Felspar	"	129.651	86.4	35.5
4.	Sand	"	165.127	100.7	34
5.	Haematite	"	242.728	91.6*	37

* Haematite appears to be porous. To obtain cascading it was washed and dried.

Table (15)

Effect of Cylinder Inclination on the Average Time of Passage

(R.P.M.= 2)

(a)

Granular- Starch

No.	Slope S Deg.	$\frac{1}{\sin(S+2)}$	Feed Rate Ibs/Min.	Hold Up Ibs.	Time of Passage Minutes.	$t_{emp.}$	$t_{theo.}$
(a)	(b)	(c)	(d)	(e)	(f)	(g)	(h)
1.	1	19.120	0.157	2.876	13.350		11.2
2.	2	14.326	0.316	3.016	9.560		8.35
3.	3	11.467	0.316	2.219	7.01		6.7
4.	4	9.570	0.381	2.219	5.82		5.53
5.	5	8.203	0.447	3.328	5.22		4.78
6.	6	7.183	0.508	2.266	4.47	----	4.48
7.	7	6.393	0.572	2.344	4.11		3.72
8.	8	5.666	0,678	2.674	3.95		3.5
9.	9	5.241	0.631	2.297	3.64		3.1.
10.	10	4.810	0.797	2.266	2.85		2.8

(b)

Coal

1.	1.	"	0.181	2.375	13.10	13.9	10.9
2,	2	"	0.265	2.485	9.36	10.5	8.2
3.	3	"	0.332	2.578	7.77	8.33	6.6
4.	4	"	0.423	2.687	6.34	6.9	5.5
5.	5	"	0.443	2.437	5.51	5.8	4.7
6.	6	"	0.372	1.876	5.04	5.2	4.1
7.	7	"	0.443	"	4.23	4.6	3.7
8.	8	"	0.664	2.688	4.05	4.1	3.3
9.	9	"	0.712	"	3.78	3.8	3.0
10.	10	"	0.766	2.437	3.18	3.5	2.8

(c)

Felspar

(a)	(b)	(c)	(d)	(e)	(f)	(h)
1.	1	19.120	0.312	2.937	10.730	11.1
2.	2	14.326	0.329	3.000	9.120	8.42
3.	3	11.467	0.426	3.256	7.630	6.73
4.	4	9.57	0.475	2.844	5.875	5.63
5.	5	8.203	0.607	3.187	5.250	4.82
6.	6	7.183	0.656	2.5	3.810	4.18
7.	7	6.393	0.713	2.25	3.160	3.75
8.	8	5.666	0.965	2.175	2.250	3.32
9.	9	5.241	1.091	2.25	2.060	3.08
10.	10.	4.810	1.171	2.125	1.810	2.82

(d)

Sand

1.	1		0.288	3.312	11.50	10.8
2.	2		0.386	3.718	9.65	8.1
3.	3		0.378	3.078	8.14	6.5
4.	4		0.618	3.892	6.30	5.4
5.	5	--do--	0.618	3.468	5.62	4.6
6.	6		0.599	2.625	4.39	4.1
7.	7		0.722	2.500	3.47	3.6
8.	8		1.298	4	3.08	3.2
9.	9		1.390	4	2.88	2.96
10.	10		1.495	3.25	2.17	2.71

(e)

Haematite

(a)	(b)	(c)	(d)	(e)	(f)	(h)
1.			0.261	4.062	15.60	11.6
2.			0.335	3.782	11.31	8.6
3.			0.439	4.312	9.78	6.87
4.			0.552	4.250	7.71	5.8
5.	----do----		0.586	3.766	6.44	4.98
6.			0.764	4.625	6.03	4.35
7.			0.882	4.125	5.26	3.88
8.			0.837	4.000	4.77	3.44
9.			0.837	3.625	4.33	3.18
10.			1.173	5.000	4.27	2.92

Table (16)

Effect of Cylinder Inclination on the Average Time Of Passage.

(R.P.M. = 10)

(b)

Coal

(a) No.	(b) Slope Deg.	(c) $S\ \frac{1}{\sin(S+2)}$	(d) Feed Rate lbs/Min.	(e) Hold Up lbs.	(f) Time of Passage Min.	t	(h) $t_{theo.}$
1.	1	19.120	0.415	1.297	3.220		
			0.587	2.063	3.520		
			0.664	2.047	3.080		
			0.687	2.187	3.185		
			0.486	1.453	2.985		
				Av.	3.198		2.18

(a)	(b)	(c)	(d)	(e)	(f)	(h)
2.	2	14.326	0.867	2.203	2.545	
			0.737	2.000	2.710	
			0.623	1.516	2.440	
			0.832	2.078	2.5	
			0.815	2.063	2.54	
				Av:	2.546	1.64
3.	3	11.467	1.105	2.359	2.130	
			1.075	2.313	2.140	
			1.105	2.344	2.120	
			1.022	2.109	2.065	
			1.048	2.297	2.190	
				Av:	2.129	1.31
4.	4	9.570	1.172	2.297	1.960	
			1.328	2.547	1.920	
			1.328	2.453	1.845	
			1.423	2.797	1.965	
			1.423	2.828	1.985	
				Av:	1.935	1.09
5.	5	8.203	1.533	2.656	1.735	
			1.475	2.516	1.715	
			1.475	3.000	2.030	
			1.423	2.141	1.505	
			1.285	1.995	1.520	
				Av:	1.70	0.94
6.	6	7.183	1.735	2.562	1.480	
			1.993	3.094	1.555	
			1.895	2.875	1.515	
			1.895	2.484	1.310	
			1.895	3.031	1.595	
				Av:	1.491	0.82

(a)	(b)	(c)	(d)	(e)	(f)	(h)
7.	7	6.393	1.993	2.344	1.175	
			2.095	2.687	1.287	
			2.095	2.891	1.378	
			2.095	3.031	1.445	
			2.210	2.953	1.334	
				Av:	1.323	0.73
8.	8	5.666	2.490	3.000	1.205	
			2.348	3.063	1.305	
			2.210	3.000	1.355	
			2.348	2.797	1.192	
			2.348	3.000	1.280	
				Av:	1.267	0.65
9.	9	5.241	3.070	3.562	1.163	
			2.850	3.031	1.065	
			2.345	2.500	1.055	
			3.070	3.531	1.152	
			2.345	2.500	1.055	
				Av:	1.098	0.60
10.	10	4.810	3.790	3.031	0.800	
			3.990	3.000	0.753	
			3.630	3.125	0.853	
			3.990	3.031	0.762	
			3.990	3.093	0.776	
			---	Av:	0.788	0.55

(c)

Felspar.

(a)	(b)	(c)	(d)	(e)	(f)	(h)
1.	1	19.120	1.094	3.469	3.170	
			1.111	3.406	3.060	
			0.937	2.750	3.010	
			1.094	3.562	3.200	
			1.132	3.235	3.150	
				Av:	3.118	2.24
2.	2	14.326	0.528	1.423	2.690	
			1.094	2.923	2.680	
			0.937	2.703	2.890	
			1.490	3.694	2.480	
			1.490	3.219	2.160	
				Av:	2.58	1.70
3.	3	11.467	0.468	0.891	1.900	
			1.425	2.720	1.905	
			1.642	2.750	1.680	
			1.642	3.047	1.860	
			1.823	3.391	1.860	
				Av:	1.841	1.34
4.	4	9.570	1.310	1.859	1.415	
			1.823	2.562	1.401	
			1.931	3.141	1.630	
			2.048	3,203	1.562	
			2.983	4.391	1.462	
				Av:	1.494	1.12
5.	5	8.203	1.213	1.454	1.200	
			1.262	1.500	1.190	
			2.185	2.735	1.250	
			2.345	3.266	1.390	
			2 .52	3.485	1.380	
				Av:	1.282	0.96

(a)	(b)	(c)	(d)	(e)	(f)	(h)
6.	6	7.183	1.638	1.797	1.095	
			2.520	2.970	1.175	
			2.618	2.932	1.114	
			2.980	3.500	1.175	
			3.280	3.625	1.105	
				Av:	1.132	0.84
7.	7	6.393	1.770	1.422	0.815	
			2.425	2.187	0.902	
			3.280	3.078	0.937	
			2.980	2.923	0.982	
			3.640	3.016	0.827	
				Av:	0.892	0.75
8.	8	5.666	1.630	1.410	0.697	
			2.110	1.892	0.895	
			2.850	2.484	0.870	
			3.855	3.375	0.877	
			6.560	5.187	0.793	
				Av:	0.824	0.66
9.	9	5.241	2.185	1.693	0.774	
			2.730	2.073	0.760	
			5.470	4.468	0.816	
			3.280	2.266	0.692	
			4.680	3.422	0.732	
				Av:	0.754	0.61
10.	10	4.810	2.520	1.828	0.725	
			2.980	1.937	0.650	
			4.090	2.923	0.715	
			6.560	4.250	0.693	
			6.560	4.531	0.691	
				Av:	0.694	0.56

Sand (a)	(b)	(c)	(d)	(e)	(f)	(h)
1.	1	19.120	0.865	3.031	3.510	
			1.128	3.562	3.170	
			1.555	4.875	3.140	
				Av:	3.273	2.16
2.	2	14.326	0.865	2.250	2.610	
			1.555	4.281	2.760	
			1.996	5.078	2.550	
				Av:	2.64	1.62
3.	3	11.467	0.885	1.875	2.12	
			1.855	3.781	2.05	
			2.593	5.203	2.05	
				Av:	2.073	1.30
4.	4	9.570	1.555	2.562	1.645	
			2.358	3.973	1.670	
			3.250	5.437	1.645	
				Av:	1.653	1.08
5.	5	8.203	1.298	1.641	1.265	
			1.946	2.641	1.360	
			2.780	3.750	1.350	
				Av:	1.321	0.92
6.	6	7.183	1.342	1.703	1.270	
			2.593	3.094	1.192	
			3.535	4.500	1.275	
				Av:	1.242	0.81
7.	7	6.393	1.298	1.641	1.265	
			1.946	2.641	1.360	
			2.780	3.750	1.350	
				Av:	1.321	0.72

(d)

Sand

(a)	(b)	(c)	(d)	(e)	(f)	(h)
8.	8	5.666	3.540	2.969	0.842	
			4.330	3.782	0.778	
			5.560	4.719	0.849	
				Av:	0.823	0.64
9.	9	5.241	3.110	2.406	0.774	
			5.560	4.454	0.801	
			6.484	5.357	0.827	
				Av:	0.800	0.59
10.	10	4.811	5.560	4.422	0.795	
			6.484	5.375	0.829	
			8.650	6.219	0.720	
				Av:	0.781	0.54

(e)

Haematite

1.		0.837	3.187	3.815	2.32
2.		1.172	3.520	3.000	1.72
3.		2.190	4.687	2.138	1.37
4.		2.190	4.187	1.920	1.16
5.	----do----	2.190	3.782	1.724	0.99
6.		2.190	3.078	1.390	0.87
7.		2.190	2.516	1.145	0.77
8.		2.710	2.156	0.927	0.68
9.		2.710	2.156	0.794	0.63
10.		2.710	2.000	0.737	0.58

Table (17)

Effect of Cylinder Slope on the Average Time of Passage.(Sliding Motion)

R.P.M. 10

(a)

Felspar No.	Slope S DEG.	$\frac{1}{Sin(S)}$	Feed Rate Ibs/Min.	Hold-Up Ibs.	Time Of Passage. Min.
(a)	(b)	(c)	(d)	(e)	(f)
1.	1	57.30	0.844	1.828	2.170
2.	2	28.6	0.858	1.468	1.710
3.	3	19.1	1.610	1.892	1.175
4.	4	14.35	1.156	0.923	0.800
5.	5	11.5	1.818	1.422	0.784
6.	6	9.57	1.818	1.250	0.624
7.	7	8.23	1.894	1.078	0.555
8.	8	7.17	2.070	1.000	0.483
9.	9	6.4	2.330	0.891	0.421
10.	10	5.76	2.140	0.827	0.385

(b)

Sand					
1.	1		0.985	2.000	2.030
2.	2		0.797	1.375	1.730
3.	3		1.346	1.516	1.125
4.	4		1.780	1.563	0.880
5.	5	---do---	1.780	1.312	0.738
6.	6		2.657	1.523	0.575
7.	7		2.657	1.422	0.536
8.	8		3.500	1.500	0.428
9.	9		3.500	1.344	0.385
10.	10		3.500	1.281	0.366

Table (18)

Effect of Cylinder Length on the Average Time of Passage. (Cascading Motion)

(a)

Starch R.P.M.= 2 Slope= 4 Deg.

No.	Length Ft.	Feed Rate Ibs/Min.	Hold Up Ibs.	Time of Passage Min.	$t_{emp.}$	$t_{theo.}$
(a)	(b)	(c)	(d)	(e)	(f)	(g)
1.	0.167	0.305	0.039	0.128		(0.126)
2.	0.333	"	0.125	0.410		(0.85)
3.	0.499	"	0.226	0.742		(1.275)
4.	0.664	"	0.344	1.128		1.695
5.	0.833	"	0.5	1.640		2.130
6.	1	"	0.641	2.102	----	2.56
7.	1.167	"	0.828	2.710		2.98
8.	1.333	"	1.031	3.380		3.41
9.	1.499	"	1.281	4.190		3.82
10.	1.666	"	1.561	4.970		4.26
11.	1.833	"	1.844	6.050		4.68

(b)

Coal R.P.M.= 2 Slope= 4 Deg.

1.	--do--	0.289	0.039	0.135	0.149	0.434
2.		"	0.117	0.405	0.432	0.870
3.		"	0.203	0.703	0.778	1.300
4.		"	0.344	1.192	1.190	1.740
5.		"	0.500	1.730	1.675	2.170
6.		"	0.633	2.190	2.200	2.610
7.		"	0.797	2.760	2.770	3.040
8.		"	0.985	3.410	3.390	3.480
9.		"	1.125	3.990	4.040	3.910
10.		"	1.391	4.810	4.720	4.330
11.		"	1.594	5.510	5.510	4.780

(c)

Felspar R.P.M. = 2 Slope = 4 Deg.

(a)	(b)	(c)	(d)	(e)	(f)	(g)
1.	0.167	0.586	0.070	0.120		(0.465)
2.	0.333	"	0.157	0.268		(0.932)
3.	0.499	"	0.266	0.453		(1.400)
4.	0.666	"	0.406	0.693		1.865
5.	0.833	"	0.547	0.934		2.34
6.	1	"	0.750	1.278		2.80
7.	1.167	"	1.000	1.703	----	3.26
8.	1.333	"	1.327	2.250		3.74
9.	1.499	"	1.683	2.860		4.20
10.	1.666	"	2.149	3.640		4.66
11.	1.833	"	2.563	4.360		5.14

(d)

Sand R.P.M. =2 Slope = 4 Deg.

1.		0.598	0.078	0.131		(0.428)
2.		"	0.196	0.327		(0.856)
3.		"	0.344	0.575		(1.280)
4.		"	0.547	0.913		1.71
5.	---do---	"	0.782	1.308	----	2.14
6.		"	1.094	1.821		2.57
7.		"	1.422	2.365		3.00
8.		"	1.783	2.962		3.43
9.		"	2.196	3.650		3.85
10.		"	2.640	4.380		4.28
11.		"	3.047	5.070		4.72

(e)

Haematite R.P.M. = 2 Slope = 4 Deg.

(a)	(b)	(c)	(d)	(e)	(f)	(g)
1.		0.586	0.094	0.165		(0.461)
2.		"	0.281	0.494		(0.921)
3.		"	0.516	0.907		(1.380)
4.		"	0.782	1.335		1.835
5.	---do---	"	1.156	2.035	----	2.310
6.		"	1.532	2.695		2.77
7.		"	1.985	3.490		3.22
8.		"	2.468	4.340		3.69
9.		"	2.938	5.170		4.14
10.		"	3.469	6.100		4.60
11.		"	3.876	6.820		5.07

Table (19)

Effect of Cylinder Length on the Average Time of Passage.(Cascading Motion)

R.P.M. = 10 Slope = 4 Deg.

(a)

Starch

1.		1.927	0.047	0.029		0.085
2.		"	0.156	0.099		0.178
3.		"	0.297	0.188		0.255
4.		"	0.468	0.296		0.339
5.	---do---	"	0.625	0.395	----	0.426
6.		"	0.781	0.493		0.512
7.		"	0.784	0.621		0.596
8.		"	1.219	0.770		0.682
9.		"	1.532	0.967		0.764
10.		"	1.782	1.124		0.852
11.		"	2.000	1.263		0.936

(b)

Coal

(a)	(b)	(c)	(d)	(e)	(f)	(g)
1.		1.328	0.039	0.029		0.087
2.		"	0.129	0.097		0.174
3.		"	0.258	0.194		0.260
4.		"	0.426	0.321		0.348
5.		"	0.613	0.462		0.432
6.	--do--	"	0.754	0.568	----	0.522
7.		"	0.943	0.710		0.608
8.		"	1.172	0.833		0.696
9.		"	1.375	1.037		0.782
10.		"	1.595	1.200		0.860
11.		"	1.860	1.400		0.956

(c)

Felspar

1.		1.930	0.047.	0.243		0.093
2.		"	0.203	0.105		0.196
3.		"	0.336	0.174		0.280
4.		"	0.570	0.295		0.373
5.		"	0.782	0.405		0.446
6.	--do--	"	1.031	0.535	----	0.560
7.		"	1.281	0.655		0.652
8.		"	1.578	0.817		0.748
9.		"	1.782	0.923		0.840
10.		"	2.234	1.158		0.932
11.		"	2.641	1.370		1.030

(d)

Sand

(a)	(b)	(c)	(d)	(e)	(f)	(g)
1.		2.595	0.094	0.036		0.085
2.		"	0.250	0.096		0.171
3.		"	0.453	0.175		0.256
4.		"	0.609	0.235		0.342
5.		"	0.923	0.356		0.428
6.	---do---	"	1.266	0.488	-----	0.514
7.		"	1.516	0.585		0.600
8.		"	1.875	0.756		0.686
9.		"	2.297	0.886		0.770
10.		"	2.593	0.996		0.856
11.		"	3.125	1.201		0.944

(e)

Hamatite

1.		2.530	0.063	0.038		0.092
2.		"	0.219	0.084		0.184
3.		"	0.423	0.165		0.276
4.		"	0.687	0.264		0.367
5.	---do---	"	1.047	0.402	----	0.462
6.		"	1.423	0.546		0.554
7.		"	1.797	0.689		0.644
8.		"	2.250	0.864		0.738
9.		"	2.797	1.074		0.828
10.		"	3.281	1.260		0.920
11.		"	3.827	1.470		1.014

Table (20)

Effect of Cylinder Length On the average Time of Passage. (STEEL CYLINDER)

Cyl inder length = 5.5 Ft.
" Diameter = 1.08Ft.
R.P.M.= 3.25

(a)

CASCA DING MOTION

Sand (18+22) Mesh B.S.S.

No.	Slope S Deg.	Cylinder Length Ft.	Feed Rate Ibs/Min.	Hold Up Ibs.	Time of Passage Min.
1.	2	1	2	1.5	0.750
2.	"	2	"	3.75	1.875
3.	"	3	"	6.25	3.125
4.	"	4	"	9.5	4.750
5.	"	5	"	14	7,000
1.	3	1	2.5	1.5	0.600
2.	"	2	"	4.25	1.700
3.	"	3	"	6.75	2.7o0
4.	"	4	"	10	4
5.	"	5	"	14.25	5.700

Sand (Zircon)

(b)

SLIDING MOTION

1.	2	1	2	1.75	0.875
2.	"	2	"	4.0	1.875
3.	"	3	"	6.5	3.250
4.	"	4	"	9	4.5
5.	"	5	"	11.25	5.625
1.	3	1	3.7	2.5	0.667
2.	"	2	"	5.25	1.4
3.	"	3	"	8.5	2.27
4.	"	4	"	12.25	3.27
5.	"	5	"	15.50	4.12

Table (21)

Effect of Cylinder Diameter on the Average Time of Passage.

R.P.M.= 10 Slope = 4 Deg.

No.	Diameter D Ft.	I/D	Feed Rate Ibs/10 Min.	Hold Up Ibs.	Time of Passage Min.	t_{exp}	$t_{theo.}$
Starch							
1.	0.167	6.000	1.354	0.568	4.20		3.22
2.	0.25	4.000	5.720	1.375	2.39	--	1.50
3.	0.339	2.952	10.7	1.400	1.31		1.11
Coal							
1.			2.15	0.718	3.340	2.87	2.22
2.	--do--	--do--	5.86	1.406	2.400	1.85	1.48
3.			11.73	2.297	1.900	1.37	1.09
Felspar							
1.			2.75	1.094	3.975		2.39
2.	--do--	--do--	6.930	1.578	2.270		1.59
3.			29.850	4.391	1.462		1.17
Sand							
1.			3.650	1.281	3.515		2.20
2.	--do--	--do--	5.960	1.484	2.493		1.47
3.			15.58	2.562	1.645		1.10
Haematite							
1.			2.830	1.313	4.475		2.37
2.	--do--	--do--	10.050	2.849	2.655	--	1.58
3.			21.920	4.187	1.920		1.16

Table (22)

Effect of Cylinder Speed on the Average Time of Passage.

Cylinder Slope = 4 Deg.

(a)

Starch

(a) No.	(b) R.P.M. (N)	(c) I/N	(d) Feed Rate Ibs/ Min.	(e) Hold Up Ibs.	(f) Time of Passage Min.	(g) $t_{emp.}$	(h) $t_{theo.}$
1.	1	1	0.200	2.850	14.25		11.10
2.	1.5	o.667	0.241	2.297	9.53		7.40
3.	2	0.5	0.316	2.234	7.07		5.55
4.	2.5	0.4	0.350	1.958	5.60		4.43
5.	8	0.125	0.732	1.391	1.902	---	1.39
6.	15	0.067	0.763	0.907	1.185		0.74
7.	20	0.050	1.220	0.938	0.769		0.55
8.	25	0.040	1.143	0.625	0.547		0.44
9.	30	0.033	2.033	1.047	0.515		0.37
10.	35	0.029	1.926	0.828	0.431		0.32

(b)

Coal

1.	1	1	0.221	2.907	13.130	13.63	11.2
2.	1.5	0.667	0.205	2.141	8.880	9.10	7.47
3.	2	0.5	0.327	2.260	6.920	6.82	5.60
4.	2.5	0.4	0.319	1.700	5.330	5.45	4.47
5.	7	0.143	1.208	2.655	2.200	1.95	1.60
6.	10	0.010	1.735	2.580	1.490	1.36	1.12
7.	15	0.066	1.899	1.953	1.030	0.91	0.747
8.	20	0.050	2.210	1.640	0.743	0.68	0.560
9.	25	0.040	2.345	1.328	0.567	0.55	0.447

(a)	(b)	(c)	(d)	(e)	(f)	(g)	(h)
10.	30	o.033	3.320	1.578	0.475	0.454	0.373
11.	35	0.029	3.620	1.266	0.349	0.389	0.320
12.	40	0.025	5.680	1.828	0.321	0.341	0.280
13.	45	0.022	4.975	1.328	0.267	0.303	0.250
14.	50	0.020	4.975	1.156	0.232	0.273	0.224
15.	55	0.018	9.970	1.891	0.190	0.247	0.204
16.	60	0.017	9.970	1.547	0.155	0.227	0.187
			(c)				

Felspar

1.	1	1	0.290	2.85	9.850		11.20
2.	1.5	0.667	0.410	2.8	6.820		7.48
3.	2	0.5	0.394	1.953	4.920		5.61
4.	2.5	0.4	0.358	2.437	4.080		4.48
5.	7.75	0.129	2.5	4.047	1.620		1.45
6.	10	0.1	2.5	3.25	1.300		1.12
7.	15	0.067	1.933	2.187	1.131		0.749
8.	20	0.05	1.725	1.562	0.905	---do--	0.561
9.	25	0.04	2.980	2.156	0.723		0.448
10.	30	0.033	2.730	1.507	0.560		0.374
11.	35	0.029	3.282	1.657	0.505		0.320
12.	40	0.025	4.675	2.281	0,487		0.280
13.	45	0.022	4.675	2.0	0.427		0.250
14.	50	0.020	4,675	1.782	0.380		0.224
15.	55	0.018	6.570	2.437	0.370		0.204
16.	60	0.017	6.570	2.25	0.343		0.187

(d)

Sand

(a)	(b)	(c)	(d)	(e)	(f)	(g)	(h)
1.	1	1	0.371	4.468	12.05		10.8
2.	1.5	0.667	0.519	4.347	8.35		7.2
3.	2.	0.5	0.487	2.95	6.06		5.4
4.	2.5	0.4	0.599	3.037	5.06		4.32
5.	8.8	0.113	2.430	4.437	1.825		1.23
6.	10	0.1	2.598	3.625	1.4		1.08
7.	15	0.067	2.360	2.375	1.010		0.72
8.	20	0.05	2.240	1.970	0.892		0.54
9.	25	0.04	2.430	1.656	0.682	-----	0.43
10.	30	0.033	3.385	1.891	0.561		0.36
11.	35	0.029	3.540	1.693	0.478		0.31
12.	40	0.025	5.650	2.5	0.450		0.27
13.	45	0.022	5.650	2.219	0.399		0.24
14.	50	0.020	5.650	1.860	0.335		0.216
15.	55	0.018	5.650	1.693	0.305		0.197
16.	60	0.017	5.650	1.562	0.281		0.18

(e)

Haematite

1.	1	1	0.273	4.594	16.95		11.62
2.	1.5	0.667	0.414	4.625	11.15		7.76
3.	2	0.5	0.542	4.516	8.32		5.81
4.	2.5	0.4	0.735	4.641	6.33		4.65
5.	8	0.125	1.774	3.656	2.075		1.45
6.	10	0.1	1.774	2.578	1.460	----	1.16
7.	15	0.067	1.774	2.047	1.163		0.776

(e)

(a)	(b)	(c)	(d)	(e)	(f)	(g)	(h)
8.	20	0.05	1.774	1.516	0.861		0.581
9.	25	0.04	2.430	1.673	0.688		0.465
10.	30	0.035	2.430	1.406	0.578		0.387
11.	35	0.029	2.348	1.094	0.450	-----	0.333
12.	40	0.025	3.520	1.532	0.434		0.291
13.	45	0.022	3.520	1.344	0.381		0.259
14.	50	0.020	3.520	1.141	0.324		0.232
15.	55	—	--	--	--		--
16.	60	0.018	3 .520	0.937	0.265		0.194

Table (23)

Hold Up Vs. bed-Depth

Coal

R.P.M. = 10 Slope = 4 Deg.

(a)

No.	Percent Hold-Up	Bed Slope Deg.	Cylinder Length.Ft.	Bed-Depth Ft.
(a)	(b)	(c)	(d)	(e)
1.	15%	5	0.25	0.042
2.	"	"	0.5	0.063
3.	"	"	0.75	0.067
4.	"	"	1.00	0.073
5.	"	"	1.5	0.078
6.	"	"	1.75	0.083

(a)	(b)	(b) (c)	(d)	(e)
1.	22.6%	5.75		0.063
2.	"	"		0.083
3.	"	"	--do---	0.094
4.	"	"		0.104
5.	"	"		0.114
6.	"	"		0.119
		(c)		
1.	28%	6		0.073
2.	"	"		0.084
3.	"	"	--do---	0.109
4.	"	"		0.114
5.	"	"		0.131
6.	"	"		0 .141

Table (24)

Feed Rate Vs. Hold-Up & Bed Depth.

(a)

Coal (-18+22) Mesh , R.P.M.=10 , Slope= 4 Deg.

No.	Feed Rate Ibs/Min.	Bed Slope Deg.	Hold-Up Ibs.	% Hold Up	Time of Passage
(a)	(b)	(c)	(d)	(e)	(f)
1.	0.332	4	0.316	4.047	0.995
2.	0.797	4.5	0.766	9.776	0.963
3.	0.948	5	0.907	11.561	0.956
4.	1.172	5.5	1.094	13.945	0.936
5.	1.328	5.5	1.269	16.177	0.955

(a)	(b)	(c)	(d)	(e)	(f)
6.	1.553	5.75	1.407	17.934	0.913
7.	1.809	6	1.786	22.766	0.983
8.	1.992	6	1.812	23.098	0.912

(b)

Sand (-18+22) Mesh B.S.S.

1.	0.708	3.75	0.906	5.874	1.28
2.	1.287	4.5	1.675	10.840	1.30
3.	1.556	4.75	1.892	12.265	1.22
4.	2.290	4.75	2.782	18.036	1.22
5.	2.995	5.75	3.812	24.721	1.27

Table (25)

Effect of Feed Rate on the Hold-Up and the Time of Passage.

COAL

(a)

R.P.M.= 2 Slope = 2Deg.

No.	Feed Rate per 10 Minutes. Ibs.	Hold Up Ibs.	Time of passage. Min.
1.	1.812	1.468	8.11
2.	1.897	1.578	8.32
3.	2.035	1.719	8.46
4.	2.066	1.782	8.32
5.	2.850	2.406	8.42

(b)

R.P.M.=2 Slope= 4 Deg.

1.	2.215	1.375	6.22
2.	2.490	1.578	6.32
3.	2.655	1.657	6.24
4.	2.850	2	6.58
5.	3.980	2.562	6.44

(c)

R.P.M.=3 Slope= 4Deg.

1.	3.270	1.567	4.78
2.	4.240	2.016	4.75
3.	5.380	2.531	4.70

Table (26)

Effect of Feed Rate on Hold Up and the Time of Passage.

SAND

(a)

R.P.M.= 2 Slope= 2Deg.

No.	Feed per 10 Minutes. Ibs.	Hold Up IBs.	Time of Passage. Min.
1.	2.590	2.532	9.77
2.	3.540	3,344	9 .46
3.	4.575	4.312	9.42

(b)

R.P.M.=2 Slope= 4 Deg.

1.	2.225	1.5	6.75
2.	3.890	2.657	6.82
3.	5.560	3.813	6.87
4.	6.484	4.453	6.88
5.	6.710	4.718	7.02

(c)

R.P.M.= 17 Slope= 2Deg.

1.	5.560	0.860	1.550
2.	8.650	1.344	1.556
3.	12.970	1.953	1.510
4.	16.6	2.782	1.678
5.	19.490	3.172	1.630

BIBLIOGRAPHY.

(1) Davis, E.W. — Trans. Amer. Instn. Min. (Metall.) Engrs. 61, 250 (1919).

(2) Von-Steiger, R. — Zement, 18, 1106, (1929).

(3) Gow, A.M., Campbell, A.B., and Coghill. — Amer. Instn. of Min. & Metallurgical Engrs. Tech. Puh. No. 326, March 1930.

(4) White, H.A. — J. Chem. Soc. South Africa, 31, 1, (1930).

(5) Conner, J.M. — Ph.D. Thesis, University of London (1936).

(6) Rose, H.E., and Sullivan, R.M.E. — Internal Mechanics of the Ball, Tube and Rod Mills. London. (1958)

(7) Wilson, G. — Proc. Instn. of Civil Engrs., 149, 210 (1902)

(8) Crosswaite, P.M. — Prac. Instn. of Civil Engrs., 203, 124, (1916)

(9) Cain, W. — Trans. Amer. Soc. Civil Engrs., 72, 403, (1911)

(10) Rankine, W.J.H. — Trans of the Royal Society (London) 9 - 27 (1856-57)

(11) Richter, D.W. — Agric. Engr. 35, 411, (1954)

(12) Holbrook and Fraser. — Bull. U.S. Bur. of Mines No. 234 (1925)

(13) Fowler, R.T., and, Chodziesner, W.B. — Chem. Eng. Sci. 10, No.3, 157-63 (1959)

(14) Denning, W.W., and Mehring, A.L. — Ind. Engng. Chem. 21, 661, (1929)

(15) Neuman. — Flow Properties of Dispersed systems. Editor Herman North, Holland Park Co., Amsterdam, Chapter X (1953)

(16) Craik, J.D. J. Pharm. Pharmacul. 10, 73, Fch. (1958)

(17) Takahashi, H. Sci. Paper, Inst. Phys. Chem. Res. Tokyo, No.540, 26, 11 (1934)

(18) Rose, H.E. and Sullivan, R.M.E. Loc. Cit. P.54 (1958)

(19) Nekon. J.Amer.Phar. Ass. Sci. Ed., 44, 435 (1955)

(20) Sullivan, J.D., Maier, G.G., and Ralston, O.C. U.S. Bur. of Mines, Dept. of Commerce, Tech. Papers No.384 (1927)

(21) Franklin, F.C?and Johnson, L.N. Chem. Eng. Sci. 4, 121-22 (1955)

(22) Train, D. J. Pharm. and Parmacul. 10, 127T-135T Supp. (1958)

(23) British Standard Specification No. 410 (1943)

(24) Dallavalle, J.M. Micromeritic. (1948)

(25) Herden. Small Particle Statistics 0.(1953)

(26) Cocking, T.T. Pharm. Journal 107, 226-7 (1921)

(27) Raller, P.S. I.E.C. 22, 1206-8 (1930)

(28) Heywood, H. Symposium on Particle Size Analysis.Instn. of Chem. Engrs. (London)Feb. 4 (1947)

(29) " " J.Imp. College, Chem. Engg.Soc. 8, 25-33 (1954)

(30) Timoshenko, S and Young, D.H. Engineering Mechanics (1949).

(31) Ketchum, M.S. Walls, Bins and Grain Elevators, McGraw Hill, New York (1911)

(32) Takahashi, H. Bull. Inst. Phys. Chem. Res. Tokyo, 12, 984 (1933)

(33)	Newton, R.H. Dunham, G.S. and Simpson, T.D.	Trans. Instn. of Chem. Engrs. 41, 218 (1945)
(34)	Ransch, J.M.	Ph.D. Thesis, Princeton University, U.S.A. (1948)
(35)	Shirai, T.	Chem. Engg. (Japan) 16, 86, (1952)
(36)	Brown, R.L. and Hawkesley, P.G.W.	Fuel, 26, 159, (1953)
(37)	Fowler, R.T. and Glastonbury, J.R.	Chem. Eng. Sci., 10, 150-56, (1959)
(38)	Brown, R.L. and Richards, J.C.	Trans. Instn. Chem. Engrs. (London) 37, 108-16, (1959)
(39)	Ginstling, A.M., Zilberman, D.M. & Gvozdev, N.V.	Khim Mashionostroenie No. 8, 8, (1939)
(40)	Smith, B.A.	Trans. of Amer. Instn. Chem. Engrs. 38, 251, (1942)
(41)	Prutton, C.F., Miller, C.O. and Schutte, W.H.	Trans. Amer. Instn. Chem. Engrs., 38, 123, (1942)
(42)	Bayard, R.A.	Chem. E. Met, Engng. 52, 100 (1945)
(43)	Friedman, S.J., & Marshall, W.R.	Chem. Engng. Prag. 45, (1949)
(44)	Pickering, R.W., Feakes, F, and Fitzgerald, M.L.	J. Applied Chem., 1, 13-19, (1951)
(45)	Saeman, W.C.	Chem. Engng. Progress, 47, 508, (1951)
(46)	Davis, A.E.	Portland Cement, (1943)
(47)	Parry, J.	Handbook of Chem. Engrs. 832 (1950)
(48)	Bogus Lavskii, N.H.	Khim. Prom. 2, 89-97, (1956).